Peripheral Nerve Injury:

Primary Sensory Neuronal Death

&

Regeneration After Chronic Nerve Injury

Thesis Submitted for Doctor of Medicine

University of Glasgow

June 2001

Mr. Andrew M^{c}Kay Hart

BSc. M.R.C.S. A.F.R.C.S.

Blond-M^{c}Indoe Centre, Royal Free University College Medical School, London, U.K.

Department of Surgical & Perioperative Science, Section for Hand & Plastic Surgery, Umea University, Sweden

Abstract

Peripheral nerve trauma remains a major cause of morbidity, healthcare expenditure, and social disruption, largely because the death of up to 50% of primary sensory neurons ensures that sensory outcome remains overwhelmingly poor despite major advances in surgical technique. Hence the principal aim of this project was to identify novel, clinically applicable strategies for the prevention of sensory neuronal death after peripheral nerve injury.

After a defined unilateral sciatic nerve transection in the rat, a novel triple staining technique was employed in order to enable the detection of neuronal death in L4 & L5 dorsal root ganglia by light microscopic morphology, and TdT Uptake Nick-End Labelling (TUNEL). Optical disection was then used to quantify neuronal loss from statistically unbiased estimates of the number of surviving neurons.

Neuronal death was demonstrated to begin within 24 hours of injury and to peak 2 weeks later, while neuronal loss plateaued 2 months after axotomy, and 39.2% of neurons died overall. Thus the most relevent experimental timepoints at which to examine the effects of putative neuroprotective strategies are 2 weeks and 2 months after axotomy, until which time a window of opportunity exists for therapeutic intervention.

The principal that sensory outcome might be related to the delay between injury and nerve repair was confirmed by the fact that although surgical nerve repair reduced neuronal death 2 weeks after axotomy, the neuroprotective benefit depended upon how soon after injury the nerve was repaired. Even immediate repair did not entirely eliminate neuronal loss, confirming the need for an adjuvant therapy. Hence the effect of two promising agents with established clinical safety records was examined. N-acetyl-cysteine (NAC) is a clinically proven glutathione substrate with antioxidant, and anti-mitotic properties. Systemic treatment caused a dose-dependent improvement in neuronal morphology, a significant reduction in the number of TUNEL positive neurons 2 weeks after axotomy ($p<0.05$), and 2 months after axotomy it was found to have reduced neuronal loss from 35% to only 3% ($p<0.001$). L-acetyl-carnitine (LAC) is a physiological peptide integral to mitochondrial aerobic glycolysis that was found to be even more neuroprotective than NAC, since after LAC treatment no neuronal loss was detected 2 months after axotomy (no treatment 35% loss; high-dose LAC -4% loss, $p<0.001$).

LAC was also found to promote peripheral nerve regeneration ($p<0.05$) independently of its effect upon neuronal survival, suggesting an additional role in the treatment of chronic peripheral nerve pathologies. This was confirmed by a small clinical trial using immunohistochemical quantification of cutaneous innervation in nucleoside analogue related distal symmetrical polyneuropathy (DSP) in HIV disease. Innervation was found to be reduced in established DSP, but after 6 months of oral LAC treatment (1500mg b.d.) substantial increases were found (up to 599% for some fibre types). Small sensory (C, Aδ) fibres showed the greatest response to treatment, and innervation with some fibre types returned to the same level as that found in asymptomatic HIV negative controls.

Given its demonstrated neuroprotective potential, and ability to promote peripheral nerve regeneration in both experimental and clinical settings, LAC is proposed as the first agent clinically suitable for the adjuvant pharmacotherapy of peripheral nerve trauma. If current clinical trials are successful, then LAC may also have potential in spinal cord and traumatic brain injury, and in a wider range of neurodegenerative disorders with dysfunctional mitochondrial bioenergetic aetiologies.

Table of Contents

List of Figures

List of Tables

Acknowledgements

Many shall run to and fro, and take paines in finding out, and knowledge shall be increased
Francis Bacon

Science is a conspiracy of brains against ignorance
Freeman Dyson

It is at the moment that they are working the least, that minds achieve the most.
Leonardo da Vinci

All work presented in this thesis was carried out in the Blond-McIndoe Centre and the Centre for HIV Medicine at Royal Free & University College Medical School, London, and in the Departments of Surgical & Perioperative Science (Section for Hand & Plastic Surgery), Medical Biosciences (Pathology), and Integrative Medical Biology (Section for Anatomy) at Umea University, SE - 901 87, Umea, Sweden.

I am grateful for the funding provided by the East Grinstead Medical Research Trust (registered charity number 258154), the Swedish Medical Research Council (grant 02286), the County of Vasterbottens Ane'ers Foundation, and for an unqualified medical grant awarded by Bristol-Myers Squibb U.K. The unqualified donation of anhydrous L-acetyl-carnitine by Sigma Tau Farmacia, Italy is also greatly appreciated.

During the course of this research it has been my great pleasure to share a charmingly "compact & bijou" office space (and a seemingly even more compact & bijou set of hard drives) with Stuart, Ash, Pari, Magda, Richard and Paul. They provided a mixture of enthusiasm, discussion, poor chat, good humour, friendship, and dodgy French & excellent Persian food that has helped in no small part to the completion of this research project. Mike Youle enthusiastically enabled the work in HIV neuropathy, and the patients involved in the study should be thanked for their enthusiasm. I am also grateful to have had the benefit of two bosses, Giorgio Terenghi and Mikael Wiberg, who have provided good humoured encouragement and tempered restraint at appropriate times. Their friendly approach, trust and flexibility enabled me to work effectively, despite carrying my work back and forth across the Baltic.

Thanks also to all the folks in Umea who did so much to facilitate my work there, and who made Sweden a second home for me. Without Thomas Brannström's guidance, and selfless technical support, I couldn't have put out the technical bush-fires that occasionally threatened my work. Lev & Ludmilla, Gunnel, and Prof. Jan-Olaf Kellerth never failed to provide help and friendship even at inconvenient times for them, welcomed me into University life, and did the electron microscopy. In particular I should also thank Mikael's family for being so welcoming and kind in opening up their home to me, and to Kina & Johan for doing all of the above.

Lastly I wish to thank my parents, family and friends for their usual encouragement, tolerance and friendly slagging, albeit from more of a distance than usual. From an early age my dad has instilled an interest in research into me, that was confirmed by my time in the Physiology Department of Glasgow University as a BSc student. They've had a lot to answer for during the worries and work of the last two years, although it was clearly worthwhile in the end. During the course of this project I was lucky to marry, and Nicky has provided a background of caring, tolerant reality that gave me the drive to work less and achieve more when it mattered most. Thanks most of all.

Author Declaration

In keeping with the regulations for submission I hereby declare that this thesis was composed by myself, that unless otherwise stated the work presented is my own, and that the books and papers cited were all consulted by me personally.

Signed:..... Date: **20th June 2001**

Chapter 1. Introduction

No adult with a major nerve transection has ever attained normal sensibility.

De Medinacelli & Seaber

1.1 The Clinical Problem: Sensory Outcome After Peripheral Nerve Trauma

In Europe the incidence of peripheral nerve trauma is estimated at 1/1000, although there is considerable local variation depending upon the preponderance of heavy industry and mechanised agriculture. This means that throughout Europe approximately 300,000 peripheral nerve injuries occur each year, of which ~60,000 are in the U.K. Peripheral nerve injuries are typically sustained by adults of working age, many of whom are skilled manual workers, and injuries may vary from the relatively minor (e.g. isolated distal digital nerve in the non-dominant hand) to the functionally devastating (e.g. brachial plexus avulsion in the dominant limb).

Surgical repair remains the definitive treatment, but despite considerable advances in surgical technique [1-7] cutaneous innervation does not return to normal [8], and clinically the sensory outcome remains sufficiently poor [5,6,9] that "despite the application of meticulous techniques to peripheral nerve repair, no adult with a major nerve transection has ever attained normal sensibility" [10] "...and normal restoration of function after significant nerve injury remain unattainable ideals" [7]. This is the case even in the best of scenarios, outcome is even worse in complex nerve injuries [5,11], and in those requiring nerve grafting [2,5,11,12] or a significant delay before repair [4,5,11,13,14]. Sensory outcome also impacts adversely upon motor outcome, particularly in fine manipulative work [15], since adequate proprioceptive feedback is a vital component of normal motor control [16].

Otherwise minor injuries, such as small lacerations, can therefore cause extreme disability if they injure a nerve, and may result in loss of employment and dependence upon others. As a result, peripheral nerve trauma is a significant cause of morbidity, healthcare expenditure, social disruption and lost employment [6]. In order to identify the factors underlying the poor sensory outcome of peripheral nerve injuries, it is necessary to consider the normal structure of the peripheral nervous system, and the ways in which its various components react to injury and repair. Although a variety of factors are implicated [5,17,18], it is likely that the single most important determinant of poor sensory outcome is the extensive primary sensory neuronal death that occurs (cf. *1.4*), since quality of sensation is dependent upon the number of innervating neurons and the size of their receptive fields [17,19].

1.2 Peripheral Nerve Injury, Repair & Regeneration

Most peripheral nerve injuries are caused by direct mechanical trauma, whether by crush injury (causing ischaemia and interruption of axoplasmic flow), transection (partial / complete), traction, or avulsion [20-24]. Other mechanisms include thermal injury, neurotoxins [5,21], metabolic disorders [25], and as a complication of drug therapy [26].

Nerve transection is accompanied by haemorrhage, retraction of the nerve trunk due to its intrinsic elasticity, and mushrooming of neural contents from the cut ends. An inflammatory reaction occurs causing fibrin deposition, scarring, and release of neurotoxic cytokines such as TNFα. Intra-neural fibrosis begins within the endoneurial sheaths of the distal nerve stump 28-35 days after transection [11], reducing their calibre and impeding any subsequent regeneration. Marked fibrosis occurs within 3-6 months of injury, and is complete by 12 months in the rat [27,28]. Endoneurial tube diameter is reduced to 26% of control one year after transection [27], and after 2 years to only 1% in man [11].

Peripheral nerve injuries may be defined as proximal or distal, or by their anatomical site and mechanism. Injuries are clinically graded as "neuropraxia", "axonometsis", or "neurometsis" as progressively more disruption of the normal neural anatomical structure occurs [20], or into Grades 1-5 if more detailed consideration of the fascicular disruption is made [21,29]. Nerve repairs can also be classified by technique and timing, and the temporal classification given by Green [11] has been adopted in this thesis. Primary repairs are those performed within 48 hours of injury, early secondary repairs between 2 days and 6 weeks after injury, and late secondary repairs between 6 weeks and 6 months after injury.

Current clinical management of peripheral nerve injuries remains based upon direct microsurgical nerve repair by either epineurial or fascicular suture, with autologous nerve grafting reserved for those injuries that cannot be repaired without undue tension [5,6]. Axons begin to sprout [17] after a delay of around 3-14 days [5,11] after peripheral nerve injury and repair, during which time the perikaryal injury response occurs [30,31] (*cf. 1.3*). Nerve fibres grow by sprouting ~50-100 neurites that advance through the repair site only to be pruned down to around 5 neurites per parent axon when the endoneurial tubes of the distal stump are reached [17]. Neurite growth is facilitated by contact guidance from matrix proteins [32] and cellular adhesion molecules, such as those found upon Schwann cells [33]. Neurotropic guidance up the concentration gradients of nerve growth factor (NGF), leukaemia inhibitory factor (LIF), glial derived neurotrophic factor (GDNF), and other diffusible molecules also causes preferential neurite growth into the distal stump [34,35]. Axons regenerate at around 0.25mm/day when crossing the repair site, and then at 1-8.5mm/day

in distal stump. The rate of regeneration is inversely proportional to distance from the cell body [11], but an overall figure of 1mm/day is widely accepted in clinical practice [5].

Target organs atrophy during the period of denervation, but the sensory organs fare somewhat better than muscle [11]. In the skin Merkel's discs disappear by 35 days in the cat [36], Meissner's corpuscles persist for 6 months before degenerating [22], and although Pacinian corpuscles atrophy, they survive for at least 10 months in the rat [37]. The extent of target sensory organ reinnervation after peripheral regeneration is difficult to quantify and few studies exist, however clinically it is clear that after any nerve repair the functional outcome is markedly worse than normal, and that outcome is even worse after chronic injuries. These injuries correspond to those which require a diagnostic delay [6] or which cannot be repaired early due to co-morbidity [11], and to nerve repairs which fail, in which case the need for re-operation is often not discovered for many months [5,6]. There is also some correlation with proximal injuries in long nerves undergoing primary repair, since there is a considerable delay until regenerating axons reach the periphery and the distal segment therefore remains chronically denervated [17]. This is also the scenario in chronic die-back neuropathies such as those found in diabetes and in nucleoside analogue reverse transcriptase therapy (NRTI) associated distal symmetrical polyneuropathy (DSP), which is the commonest form of neuropathy in HIV disease [26].

Outcome is even worse in chronic nerve injuries, not only as a result of denervation atrophy but also because, after eventual repair, axonal regeneration to the target organs is impaired. In clinical practice it has long been recognised that, when compared to primary repair, the outcome is markedly worse if nerve repair is significantly delayed [5,11,17], particularly with delays of 6-12 months or more [17,38,39]. Fibrosis and narrowing in the endoneurial sheath [40,41] were cited as the cause of poor regeneration [5,11,28] since it was assumed that "that the regenerative capacity...[of individual neurons]...is maintained as long as cell death does not occur" [42]. However this assumption may be false, given the changes in neurotrophin secretion and receptor profiles of neurons and Schwann cells [40,43], and experimental evidence exists for such a loss of regenerative capacity in the rat [13] and rabbit [41].

Despite occasional reports of the return of some function after delays of up to 22 years [3,11,21] it is now clear that primary repair gives the best outcome [44,45], and the general consensus is that the timing of nerve repair should be as follows [6,11]. Nerves are repaired primarily where possible, however early secondary repair may be more appropriate when tissues are significantly devitalised, contused, or contaminated, and in the case of a complex wound requiring other bony or soft tissue repair. Late secondary repair after a

delay of up to 4 months is appropriate for certain wounds caused by high velocity projectiles. Also, it may be appropriate to wait up to 3 months in closed injuries where it is uncertain whether neurometsis has occurred, in order to exclude a more simple injury not requiring surgery.

In the rat, complete loss of regenerative capacity has been demonstrated through denatured muscle grafts after more than 56 days delay, and any delay impaired myelination [13]. In the distal stump conditions for regeneration begin to deteriorate after 10 weeks, Schwann cells begin to atrophy after 20 weeks, to disappear after 30 weeks, and by 50 weeks there is severe Schwann cell atrophy, and endoneurial fibrosis [28]. Mean fascicular area falls by 39% after 3 months, 64% after 6 months, and 79% after 12 months, with comparable reductions in endoneurial tube diameter [27]. Glial Growth Factor (GGF) [46] is the principal neuregulin controlling the interaction between Schwann cells and ingrowing axons [17,47,48], and after delays of more than 2 months distal stump Schwann cells begin to lose expression of c-erbB2&4 [43] making them unresponsive to GGF [43]. Neurons also lose expression of the regenerative neuropeptide GAP-43, and if repair is delayed by 2 months or more then the amount of axonal ingrowth into the distal stump found 28 days later is approximately half that found after an immediate repair [43].

It is evident that in the rat, with delays of greater than 2 months before nerve repair, regenerative capacity diminishes coincident with increased endoneurial fibrosis and a decrease in Schwann cell numbers and neurotrophin responsiveness. Similar changes within the endoneurium, and in the number and morphology of distal stump Schwann cells have been documented in human nerves 8-53 months after injury [40].

1.3 Cellular Events After Nerve Injury

Axonal injury briefly exposes the intracellular compartment to the extracellular milieu [49], until calcium dependent restoration of axolemmal continuity occurs [50] and the axon retracts proximally, to the next node of Ranvier in myelinated nerves [11,28,47], as part of the process of somatofugal axonal atrophy [35]. Distal to the injury axons undergo Wallerian degeneration [5,11,47], detach from their myelin sheath [47], and are phagocytosed by macrophages and activated Schwann cells [27,47,48,51]. The Schwann cells recycle myelin proteins and cholesterol under the influence of Apolipoprotein E from activated invading macrophages [51], and in the rat sciatic nerve the whole process is completed within one month [27].

The axotomised neurons display a stereotyped perikaryal injury response pattern, termed chromatolysis [52], which involves Nissl body displacement [5,11,30,31,47], nuclear

condensation and peripheralisation [30,31,53], and perikaryal swelling that first occurs after 1 day, and then recurs after 8-11 days [31]. Metabolically active mitochondria accumulate within the cell body [53], central processes retract [54], and by 4 days after axotomy the cell has shrunk [30,55] to 1/3 of its normal volume [55]. Conversely, some neurons develop a grossly dilated, vacuolated morphology that has been ascribed to a regenerative phenotype [56,57].

Profound changes occur in the DRG neuron phenotype as seen by alterations in mRNA transcription [58-63], protein synthesis [64-69], growth factor and cell receptor profiles [43,47,48,61,70-74], the secretion of neuropeptides and neurotrophic factors [47,67,68,70,72,75,76], and in the cells' electrophysiological properties [77,78]. Axonal transport of neuropeptides [61] and structural proteins [69,79] is altered, more so by a transection than a crush injury [80]. Given the important role of target-derived neurotrophic factors in neuronal survival and regeneration [7,17,47,81,82] it is of note that after injury NGF, GDNF, neurotrophin-3 (NT-3), and BDNF are retrogradely transported to subpopulations of cells with differing mean diameters [47,83,84]. The receptor-mediated uptake and retrograde transport of LIF by a separate subpopulation of small diameter neurons [47,85,86] increases [84,87], and an increased range of DRG neurons markedly increase their uptake and retrograde transport of ciliary neurotrophic factor (CNTF) [84,88].

Similarly, glial cells are also affected by a peripheral nerve injury. NGF, LIF, GDNF, and GGF receptor (p185erbB2/neu) mRNA is upregulated in the nerve trunk [48,58,69,87,89], while glial cells in the DRG also upregulate GDNF mRNA after chronic nerve transection [89]. Schwann cells increase NGF, BDNF, NT4 and LIF secretion [47,48,51,69,87], and damaged ones are an important source of CNTF [48,69,88]. Intimately related to the axons in normal peripheral nerves, Schwann cells are essential for the guidance and support of regenerating axons after injury [17,48,90,91], and following axotomy those in the distal stump shrink away from the endoneurium to form solid columns, the "Bands of Bungner" [27,40]. Some will also die [27] by apoptosis [92], particularly if denervation is prolonged [27]. After an initial period of proliferation, and upregulation of c-erbB2&4 (parts of the GGF receptor complex) [43] under the influence of macrophage derived IL-1 [47,51,69], Schwann cells begin to atrophy, and become unresponsive to GGF due to loss of c-erbB2&4 expression after 2-6 months of denervation [43]. Schwann cells appear to require axonal contact for prolonged survival [27,40], and profound atrophy and cell death occurs 20-50 weeks after denervation [28].

Secretion of IL-1 by both resident and invading macrophages is vital for Schwann cell activation and proliferation [69], and macrophage invasion appears to be essential for Wallerian degeneration [51]. Macrophages in the DRG are also activated by peripheral nerve injury [93], and this has been shown to promote nerve regeneration in vivo [94] and vitro [95].

1.4 Axotomy Induced Cell Death Within the Dorsal Root Ganglia

It has been recognised since the early 1900's that experimental nerve injuries lead to primary sensory neuronal death [57,96,97], and more recently this has been confirmed by the demonstration of DNA fragmentation within individual neurons in vivo [92,98-102]. It is now apparent that a considerable proportion of all neurons in the sensory pool will die [17,47,103], with estimates ranging from 7 to 50% [55,57,98,102,104-110] depending upon the exact nature of the experimental model. A similar magnitude of sensory neuronal loss has also been found to occur in higher mammals [111,112], for example neuronal loss after permanent division of the radial nerve was ~40% in the cat [113], and 27% in the macaque monkey [114]. A similar loss has also been demonstrated clinically in post-mortem studies [115], and sensory neuronal death does appear to correlate with loss of sensory function since a significant loss of functioning sensory units has been demonstrated electrophysiologically [19].

Neuronal loss appears to be less after crush injuries or when the transected nerve is immediately co-apted [116,117]. However these findings may merely represent an effect upon horseradish peroxidase transport rather than cell death [117], and the effect of the timing of nerve repair upon neuronal death has not been fully investigated despite its obvious clinical significance.

It has been proposed that proximal injuries are more likely to induce neuronal death than distal ones. This certainly seems to be the case for motorneurones, which die only after very proximal lesions [17], but the evidence is less clear for sensory neurons which are far more sensitive to the effects of peripheral axotomy [47]. Ygge did demonstrate a 27% loss of L4-6 DRG neurons after sciatic nerve transection in the thigh, as opposed to 7% loss after a lesion in the calf [118], however the sciatic nerve contains afferent fibres from approximately 19,000 neurons in the thigh [119], but from only ~5,000 in the calf [116]. Since neuronal loss is calculated as a percentage of the total number of neurons in the ganglia, the fourfold difference in loss may largely be due to the distal lesion having axotomised only a quarter of the number of neurons injured by the proximal lesion. This would imply that a substantial proportion of the primary sensory neurons whose axons project to the level of even a very distal injury might die after axotomy, suggesting that sensory neuronal death might be critical to the clinical sensory outcome of injuries even as distal as digital nerve transections.

Although sensory neuronal death has been clearly demonstrated to occur, its timecourse has not been fully described, and yet the timecourse is of crucial clinical importance since it would allow a therapeutic window to be defined during which attempts could be made to reduce neuronal death. Using in-situ end labelling (ISEL) Groves et al [98]

did demonstrate the presence of dying neurons 7 days after sciatic nerve division in the rat, but there are no studies using earlier timepoints in the adult. Similarly, despite most authors having failed to demonstrate any neuronal loss until 7 days after axotomy, Vestergaard et al did find a 6% loss at 4 days, rising to 19% after 8 days [55] so it remains uncertain exactly how soon after peripheral nerve injury neurons begin to die. Nor is it clear how long the period of cell death lasts. Although the only studies that employed sufficiently long timepoints have not shown any significant difference between the loss found 1-2 months after injury and that found after 6-12 months [98,107,108], they either lacked sufficient timepoints for an accurate determination of when neuronal death ends [107], or used small groups [98,108], and non-stereological counting techniques [108].

In determining the timecourse of neuronal death it is important to understand the ways in which cell death can be detected and quantified, and what aspect of neuronal death each marker demonstrates (*Figure 1.1*). Although the calculation of neuronal loss quantifies the number of neurons that have died up until that timepoint, complete involution does not occur for some hours in vitro [120-122] and an unspecified time in vivo [123] after the start of the cell death cycle. Evidence of individual cell death, whether morphological or DNA fragmentation, is therefore more appropriate for determining the onset of cell death after axotomy, as well as being more sensitive for detecting low rates of cell death, since the normal biological variation in neuronal numbers may also mask very small losses.

Until recently the interpretation of neuron counts was further complicated by the use of assumption based counting techniques that are "statistically biased", meaning that the mean of all possible estimates will tend away from the true value [124]. Although serial reconstruction counts are the gold standard technique, they are impractical in ganglia which contain tens of thousands of neurons, and so methods for estimating the number of neurons have been developed instead. The simplest of these is profile counting, whereby one counts the number of neurons ("profiles") present in a sample of sections from the ganglion, and multiplies the mean value by the total number of sections. Since large neurons have profiles in more sections than small neurons, they are more likely to be counted, and so the count is likely to be a biased [125] overestimate [126]. To combat this problem various systems were developed, such as those of Abercrombie [127] and Konigsmark [128], that involve measuring the size distribution of a sample of neurons in order to obtain a correction factor. However these factors do not fully take account of the non-spherical shape of cells or their anisotropic orientation and distribution within the ganglia [129], and so the only way to obtain a truly accurate correction factor would be to

measure every neuron in the ganglion [129], yet that would be a serial reconstruction. Estimates obtained using profile counts and correction factors must therefore involve assumptions about the shape of cells, and the homogeneity of their distribution throughout the ganglia. Since these assumptions have now been demonstrated to be untrue [126,129], the counts are "biased" in the statistical sense that the mean of all possible estimates tends away from the true value [130]. The techniques are also imprecise, since variations of over 40% [125] have been found in the counts obtained from individual ganglia using these techniques [131], and authors using these techniques have quoted figures for the number of neurons in normal rat L5 DRG's that range from 2,000 to 15,000 [132]. They are also inaccurate since they reliably gave an incorrect estimate of the number of neurons in a known population of neurons [126].

In order to overcome these problems, design-based stereological techniques have been developed [129]. These are time-efficient [130], do not require any assumptions about the tissue being quantified, and are rapidly becoming the standard tools for quantitative morphological study of biological systems, although this has recently been questioned on the grounds that the anisotropic arrangement of neurons within the nervous system, and the effects of section shrinkage may result in inaccuracies [133]. However when the technique is correctly applied, with adequate, systematic random sampling, it is efficient, theoretically sound, and has been empirically validated against serial reconstruction counts of DRG neurons [125,134,134]. The correct use of systematic random sampling obviates any bias arising due to the non-homogenous distribution of cells within the tissue [124], and the rules used with the counting systems ensure that counting is performed within three dimensions [124]. Hence every cell has an equal chance of being counted irrespective of its size, shape, or orientation [124,129]. Stereological counting techniques, such as the physical and optical disector [125], therefore permit "statistically unbiased" counting, whereby the mean of all possible estimates will tend infinitely toward the true value [130]. Counts are therefore accurate [129], as long as certain rules are adhered to [129,135]. The optical disector technique ought to be superior to the physical, since it is more time-efficient [136] and avoids underestimates due to tissue sectioning artefacts and lost caps [124,131,136]. Although precision is proportional to the amount of sampling performed, biological variation rapidly outweighs the benefit of increased sampling, and so counting remains time-efficient [129].

As a marker of DNA fragmentation, terminal deoxyribonucleotidyl transferase (TdT) uptake nick-end labelling (TUNEL) is a reliable marker of neuronal death [92,99,100], particularly when combined with Hoechst 33342 counterstaining [137,138] and microwave tissue permeabilisation [139]. Although TUNEL was initially proposed as a specific marker

Figure 1.1 Detecting Primary Sensory Neuronal Death After Peripheral Axotomy

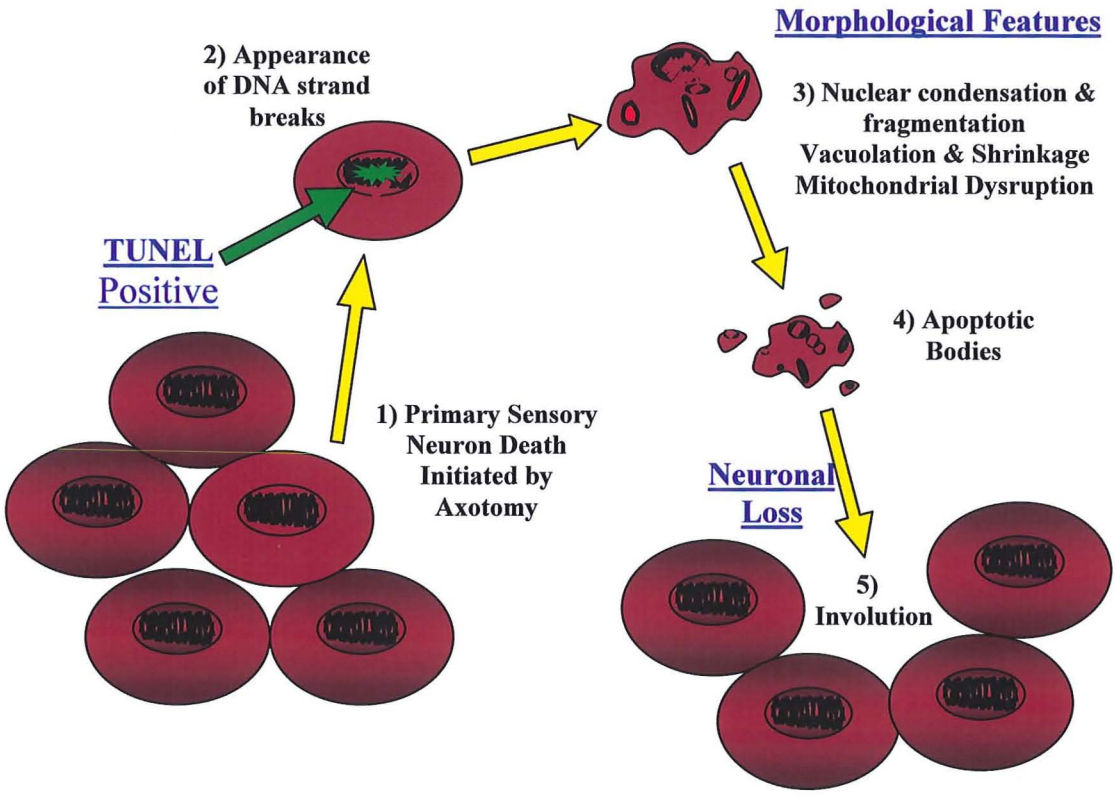

The cell death cycle is shown schematically for axotomised primary sensory neurons. Neuronal death within dorsal root ganglia can be detected by 3 main ways. DNA fragmentation is the earliest sign of a cell's irreversible commitment to die, and can be detected by techniques such as TUNEL. Morphological evidence of neuronal death can then be sought at the light, or electron microscopic level, using the features described above. Finally, by subtracting the number of neurons present in an axotomised ganglion from that in normal control ganglia, the total number of neurons that have died and involuted completely can be quantified. This is termed the "neuronal loss."

for apoptosis [140], positive staining has subsequently been found in necrosis [141,142], and in the S-Phase of mitosis [143], hence morphological confirmation of the mode of cell death is also required [141].

The term apoptosis comes from the Greek "αποπτωσιο", meaning the falling of petals from a flower, and was coined by Kerr, Wyllie & Currie in 1972 to describe an active physiological cell death process with a morphological pattern (*Figure 1.1*) that contrasted with that found in necrosis [144]. Subsequently the term has been widely applied [145] and has wrongly become synonymous with programmed cell death [146], which is in fact the embryological process whereby numbers of cells are pruned during development [147]. Apoptosis has also been widely applied to neuronal death throughout the nervous system, although subsequent critical appraisal has not confirmed this assumption to be true for many forms of neuronal death that actually exhibit mixed features of necrosis and apoptosis [146].

Some axotomised primary sensory neurons display apoptotic morphological features at both the light [98] and electron microscopic level [148], and are positively labelled by TUNEL or ISEL [92,98,99,102]. However the number of apoptotic neurons is small compared to the massive cell death which occurs [98], and neurons are also present that display other morphological features [56,57,96] now known to be potentially compatible with neuronal death [146]. Finally, although neuronal death is reduced by inhibition of protein synthesis [92], a feature of apoptosis, this may merely be due to shunting of amino acids into glutathione synthesis [149], and so it may be that cell death actually occurs by an active process which is not strictly apoptotic.

After peripheral nerve transection glial cells in the DRG also die [92,98], and although the significance of this is uncertain in the spinal cord [150] it has been suggested to compound the effects of the initial injury [138]. In neonates glial death occurs with a slower time course to that of neuronal death [100], but the timecourse in adults has not been described.

1.5 Mechanism of DRG Neuronal Death

Very few studies have directly investigated the mechanism of primary sensory neuronal death after peripheral axotomy, and so one must infer from other models. The normal developmental apoptosis in sympathetic ganglia and DRG's that occurs at embryonic stages E15-18 in the rat [151] has been extensively investigated [17,151-155], as has cell death initiated in neuronal cell lines by neurotrophin withdrawal [120,154,156-160], axotomy [153,158], and other in vitro stimuli [161]. The caenorhabditis elegans nematode [162,163], aplysia californica mollusc [17], and various transgenic mouse models have proved informative

[154,164,165], and since active cell death (e.g. apoptosis) is by definition an ordered process, it is reasonable to assume that a similar final pathway exists irrespective of the initiating cause [166].

Within the injured neurons pathways for cell death and for regeneration are triggered in response to antidromic electrical activity and neurotoxic cytokines from the site of axotomy [103,104], although the principal determinant of the proportion of neurons that subsequently die appears to be the loss of target derived neurotrophic support [17,103] that arises secondary to interruption of retrograde axonal transport. Evidence of this comes from the protective effects of exogenous neurotrophic factor administration after experimental nerve injuries in adults [47]. For example primary sensory neuronal loss was prevented by NGF delivered either intrathecally [109], or locally in a silicon tube [105,167], and when delivered by a fibronectin mat used for gap repair loss of 40-50μm diameter CGRP positive neurons was reduced in the monkey [168]. LIF is also protective after peripheral axotomy [87,106], but the effects of GDNF [169], NT-3 [109,148], CNTF [83,148,158], and BDNF seem to depend upon the route of administration [83,109] and the subpopulation of DRG neurons under consideration [164,169].

Signalling is effected principally through the mitogen activated protein kinase (MAPK), c-Jun kinase (JNK), and PI3 kinase pathways [82,103,170], which lead to transcription of both cell death (via JNK,PI3K) [65] and regenerative (via MAPK) [170] genes. These pathways increase c-Jun cell protein activity. A member of the AP-1 superfamily, c-Jun is a gene transcription regulator whose levels/activity increase after trophin withdrawal [65,171,172], axotomy [64,66,173,174] or oxidative stress [65], and which is appears to be essential for apoptosis [65,172,175]. However, c-Jun level is not specific for apoptosis [64,172] since it is also increased in actively regenerating neurons [174,176] and those protected from apoptosis [177], so it may merely have a role in initiating homeostatic and regenerative responses [178]. In contrast, another immediate early gene, c-fos, does appear to be specific for apoptosis [172] since its induction coincides with the appearance of apoptotic morphology and the irreversible stages of the cell death cycle [65].

Cell death proteins have been well characterised in lower order species, and much of our knowledge of the mammalian system comes from the identification of homologous proteins, or cDNA sequences. In the nematode caenorhabditis elegans the protein ced-3 is pro-apoptotic [162] and has structural homology with the cysteine protease interleukin-1β-converting enzyme (ICE) in mammals [162], whilst ced-9 is known to be anti-apoptotic [179] and to have structural homology with proteins of the mammalian Bcl family [179,180]. Although Bcl-xs can be pro-apoptotic [179-181], Bcl-2, and Bcl-xl are said to be anti-apoptotic,

indeed "the prototypic regulator of mammalian cell death is the proto-oncogene bcl-2" [154]. Although their mechanism of action remains uncertain, they act downstream of c-Jun [65,177] and may have antioxidant activity [179] or reverse the effects of trophin withdrawal [182,183]. Bcl-2 is known to arrest the cell cycle [161] at G0/1 [184], and to inhibit caspase activation [170] primarily by an effect to limit mitochondrial calcium flux and the release of pro-apoptotic molecules [161,179,185].

Bax is an AP-1 cell death protein that reverses the arrest of the cell cycling caused by Bcl [184], and has been proposed as part of the trophin withdrawal apoptotic pathway [152,163,171]. Although Bax-mRNA levels do not alter significantly after axotomy when the DRG is considered as a whole [186], Bax levels do increase in small DRG neurons [64]. The Bax:Bcl ratio is predictive of entry into the irreversible stages of apoptosis [64,147,187], although the exact mechanism for this remains uncertain since unlike intracellular calcium, isolated Bcl, or Bax levels are not predictive of apoptosis [157,188]. Bax associated events occur downstream of c-Jun activity, but upstream of the ICE/caspase dependent steps, and may include c-fos induction [177]. One way in which the Bcl:Bax ratio may determine the cell's fate is by an effect upon the abortive entry into the cell cycle that has been implicated in the mechanism of post-axotomy neuronal death [184,189,190], although it is more likely that the protective role of Bcl is due to mitochondrial protection [185].

In a range of conditions mitochondria play a central role in neuronal death [53,185,191,192] through the failure of oxidative metabolism, the generation of reactive oxygen species, and the release of pro-apoptotic molecules that trigger the caspase cascade [185]. Furthermore, axotomy induced retrograde degeneration occurs in association with perikaryal accumulation of mitochondria and oxidative stress [53,193], an effect which may be mediated by increased nitric oxide synthase NOS activity [194,195] and mitochondrial NO levels [196-198]. In normal neurons transient increases in NO reversibly inhibit complex IV activity in the mitochondrial electron transport chain as part of the physiological respiratory regulation of ATP production [199]. However sustained pathological increases after axotomy may cause permanent inhibition of cytochrome C (complex I), thereby disrupting the electron transport chain [199] and causing the generation of reactive oxygen species (ROS) [197]. It is postulated that as the bioenergetic dysfunction worsens dysregulation of mitochondrial membrane potential (MMP) [185,196,200] and calcium levels may occur [191], further increasing the production of ROS [191]. Mitochondrial protophores may then open, directly triggering neuronal death by the release of cytochrome-C (which activates caspase-9), and other apoptosis inducing factors (AIF's) that act downstream of the caspases [185,197,201]. Mitochondrial bioenergetic dysfunction is also implicated as the

cause of NRTI associated DSP in HIV disease, this time secondary to iatrogenic inhibition of DNA polymerase-γ [202]. It is postulated that the resulting inhibition of mitochondrial replication leads to an overall reduction in neuronal oxidative metabolic capacity, leaving the cells unable to meet the metabolic demands of maintaining (and regenerating) long peripheral axons [203]. Hence a chronic glove and stocking pattern of neuropathy develops [204].

Considerable evidence exists for the role of reactive oxygen species (ROS) such as peroxynitrite ($ONOO^-$), lipid peroxidation, and oxidative stress as mediators of neuronal death [147,166,193,197,198], although direct evidence from primary sensory neurons in vivo remains rare. Mn-superoxide dismutase activity increases 30% in the DRG after axotomy, suggesting an attempted homeostatic response to the generation of ROS [205] that may be cytoprotective since ROS are generated early in the cell death pathway, rather than being the final effector mechanism [120]. Although some antioxidant agents, such as SOD, Bcl, and N-acetylcysteine, are protective against ROS [120,160,179,206], others are not [160], and it is not generally concluded that the successful agents act purely by a direct antioxidant mechanism [160,179,206].

Another interesting feature of active neuronal death is that many of its stimuli may involve attempted entry into the cell cycle [190]. For example NT-3 withdrawal and Bax both promote entry into the cell cycle [184,207], and IL-1β and induces apoptosis in neurons arrested at the growth phase G1/S [189]. The anti-apoptotic agent Bcl arrests cell cycling [161] at G0/1 [184], and other anti-apoptotic agents such as acetylcysteine and protein synthesis inhibitors also inhibit entry into the cell cycle [159,160]. Thus axotomy may cause abortive entry into the cell cycle, at a time at which this cannot be sustained [207], with the result that neurons apoptose.

The ced-3 homologue ICE, which converts prointerleukin-1β into interleukin-1β (IL-1β) in mammals [189], also plays a role in neuronal death since trophin withdrawal apoptosis of DRG neurons is almost eliminated by expression of the ICE-inhibitory viral gene crmA [145,162]. In keeping with the cell-cycle theory of neuronal death, IL-1β induces apoptosis in neurons arrested at the growth phase G1/S, and antibodies against it, or its type 1 receptor, limit apoptosis [189]. Eleven other ICE-like proteases, or "caspases" have now been identified [208,209], and they may be activated by a range of mechanisms such as trophin withdrawal, axotomy, Fas ligand or p75 activation [82], and mitochondrial disruption [185]. The caspases, particularly caspases-3 & 9 [156,210-212], are intrinsic to active neuronal death [156,177,209,213], appearing in the pathway downstream of Bax activation and c-fos

induction [177], and leading to DNA fragmentation by activated α-spectrin proteases such as DNAse-1 [147,185].

Thus the mechanism by which peripheral axotomy brings about the death of some DRG neurons may proceed as portrayed in *Figure 1.2.*

1.6 Potential Interventions to Reduce Primary Sensory Neuronal Death

The poor sensory outcome found after peripheral nerve injury, particularly chronic injuries, would therefore seem to be due to a variety of causes. Schwann cell atrophy and loss of GGF responsiveness [27,43] combine with endoneurial fibrosis and other changes in the distal stump to impair peripheral nerve regeneration [17]. The impaired regenerative capacity of individual neurons [17] combines with poor topographical and sensorimotor specificity during regeneration [18] to further reduce the appropriate reinnervation of target sensory organs, which may themselves be severely atrophic. However the single most important determinant of poor sensory outcome is likely to be the death of up to 50% of the entire sensory neuronal pool, since "the first prerequisite for axonal regeneration is the survival of the neuron following injury" [17,17]. Primary sensory neuronal death after peripheral nerve injury is therefore the principal concern of this thesis.

Peripheral nerve repair may reduce neuronal death by reapproximating the axons to the distal nerve stump at a time when synthesis of neurotrophic factors is upregulated, and it may be that by repairing the nerve as early as possible after injury the extent of neuronal death could be limited. However the magnitude of any potential protective benefit is not known, patients frequently do not reach surgical services for many hours after sustaining peripheral nerve injuries, and primary nerve repair is not always clinically feasible (*cf 1.2*). A clear need therefore exists for alternative, adjuvant therapies to reduce neuronal death.

Administration of exogenous neurotrophic (NTF), and other growth factors has been shown to reduce neuronal death after peripheral axotomy [47,105,106,167,214,215] (*cf. 1.5*), and to reverse many of the other deleterious changes [81,164,216-223]. Yet despite over 30 years of research since the discovery of nerve growth factor [224] NTF's have failed to find a mainstream clinical application, and "growth factors have had no real effect on the clinical management of nerve injuries..." [7] for variety of reasons. Firstly, NTF's act on specific subpopulations of neurons [7,47], and so a complex cocktail would be necessary to prevent the death of all subtypes, despite evidence that exogenous NTF's may interact to negate their own efficacy [225]. Furthermore, efficacy may vary unpredictably depending upon the exact timing of administration [226,227], there are concerns over potential carcinogenic actions and toxicity in other cell types [228], and side effects [229-231] and complications at injection

Figure 1.2: Schematic Pathway for Primary Sensory Neuronal Death After Peripheral Axotomy

Peripheral nerve injury causing axotomy

⇩

Cellular disruption & antidromic electrical activity

Neurotoxic cytokine release

Interruption of retrograde axonal transport causing loss of distal neurotrophic support

⇩

Activation of MAPK, JNK,PI3-K & other signalling pathways

Mitochondrial bioenergetic dysfunction (possibly mediated by increased $[NO]_{i.m.}$)

Generation of reactive oxygen species & altered cellular & mitochondrial redox level

⇩

Phosphorylation of c-Jun

⇩

Induction of c-Jun target genes (c-Jun, Bcl, cell death genes, cell regeneration genes)

Decreased transduction of protective genes

⇩

Possible attempted entry into the cell cycle

Ratio of Bcl:Bax determines whether cell enters irreversible stage of cell death process

⇩

Activation of ICE-like proteases

Caspase activation

c-fos induction

⇩

Calpain activation

DNA fragmentation by alpha-spectrin proteases

Morphological changes of apoptosis develop

sites [229] have limited the use of systemic administration. As a result, most experimental studies have used local delivery by continuous intra-thecal administration [214], even though this may not be clinically applicable [232]. There is therefore a pressing need for an alternative approach using an easily administered, clinically safe therapy, which will prevent neuronal death in a range of subpopulations, and in response to a variety of insults.

In contrast to the specificity of neurotrophic factors [47], there appears to be relative homogeneity between neuronal subpopulations in the way that the initiation of neuronal death is signalled and then effected [103,166]. The preservation of these mechanisms within different neuronal subpopulations means that a therapeutic agent acting at the signalling, or effector level of the cell death process ought to be protective for a wide range of neuronal subtypes after injury. Mitochondrial bioenergetic dysfunction, which may be mediated by increased NO synthesis [196-198], and the ensuing generation of reactive oxygen species and release of pro-apotoptic molecules [185] are particularly attractive targets given their potential role in neuronal death in a range of neurodegenerative and traumatic pathologies [166,185,198,206,233-238].

Various other agents have been used experimentally to reduce neuronal death, but their clinical applicability is uncertain. For example the cytokine regulator linomide was associated with a 60-80% reduction in DRG neuronal death [104], and the protein synthesis inhibitor cycloheximide has also been shown to reduce neuronal death [92,239], however both would have significant side effects if used clinically. Two potentially neuroprotective therapies are however available that are safely used for other applications in current clinical practise. N-acetyl cysteine (NAC) is an established glutathione substrate [240,241] which has been shown to be neuroprotective in vitro against a range of stimuli [197,242,243], and may potentially inhibit the effects of reactive oxygen species. The second agent, L-acetyl-carnitine (LAC), is a physiological protein which has neurotrophic effects [244,245], and which plays an essential role in mitochondrial oxidative metabolism, both as an acetyl-group donor [246], and by facilitating the transport of long-chain free fatty acids across the inner mitochondrial membrane [247]. LAC is neuroprotective in vitro [245,248], and is currently showing clinical promise in patients with neuropathy [249]. Both these agents therefore have the potential to address the intermediate events in neuronal death, particularly mitochondrial bioenergetic dysfunction.

1.7 Aims

The overall aim of this project was therefore to identify a clinically applicable therapeutic strategy that might improve the sensory outcome of peripheral nerve injuries by

reducing the death of primary sensory neurons, and facilitating their subsequent regeneration into the target tissues.

The first step in achieving this aim was to describe the timecourse of primary sensory neuronal death after a defined peripheral nerve injury in order to identify experimentally relevant timepoints for the study of potentially neuroprotective strategies, and in order to identify a potential therapeutic window for future clinical interventions. Therapeutic strategies with immediate clinical potential (early nerve repair, NAC & LAC treatment) were then tested for their ability to reduce neuronal death. Finally, the most promising agent was then tested for its ability to enhance the regenerative capacity of surviving neurons in both an animal model of chronic nerve injury, and in the clinical setting of a chronic neuropathy with a predominantly bioenergetic aetiology, namely nucleoside analogue antiretroviral therapy (NRTI) associated distal symmetrical polyneuropathy (DSP) in HIV disease.

Chapter 2. Methods

Systems of statements, in order to be ranked as scientific, must be capable of conflicting with possible, or conceivable, observations.

Karl Popper

A very clever brain can catch a heffalump, if only he knows the right way to go about it.

A.A. Milne

2.1 Pre-Operative Preparation of Materials

Blind ending silicone tubes for the encapsulation of transected sciatic nerve stumps were prepared from high-grade silicone rubber tubing (Philip Harris Scientific Supplies, Product Number T88-5420) of internal diameter 1mm. The tubing was washed and soaked for 24 hours in distilled water, before air drying, cutting the tubes to length (5mm) and sterilising them with gamma-irradiation (3MRad. for 50 hours). At the time of surgery the tubes were soaked in sterile saline, and then doubly ligated with 3/0 Prolene® using a minimum of 5 throws on a surgeon's knot. This created a blind ending tube some 4mm long, with an internal diameter of 1mm, into which the nerve stumps were sutured in order to prevent spontaneous regeneration (*Figure 2.1f*).

L-acetyl-carnitine (LAC, Sigma Tau, Italy) was supplied as an anhydrous powder which was reconstituted in sterile normal saline to give a stock solution of 1g/ml. This solution was stored at 4°C, and was further diluted with sterile normal saline prior to injection in order to give an injection volume of 1ml/animal.

N-acetyl-cysteine (NAC, Evans Medical Ltd., U.K.) was supplied as a sterile 200mg/ml solution ("Parvolex®"), which was stored at 4°C prior to use. Prior to injection this solution was diluted with sterile 5% glucose solution to give an injection volume of 0.3ml/animal for intravenous injections, and 1ml/animal for intraperitoneal injections.

2.2 Operative Procedures:

All work was performed in accordance with the terms of the Animals (Scientific Procedures) Act 1986 (A.S.P.A.), Project License Number PPL70/4210, and Personal Licence Number PIL70/15040. An in-house strain of Sprague-Dawley rats was used for all animal work (Royal Free & University College Medical School Comparative Biology Unit, London, U.K.).

2.2.1 Anaesthesia

Inhalational anaesthesia was employed for all operative procedures involving subsequent recovery, and intraperitoneal sodium pentobarbitone for all terminal procedures

Figure 2.1: Unilateral Sciatic Nerve Division, Ligation & Capping

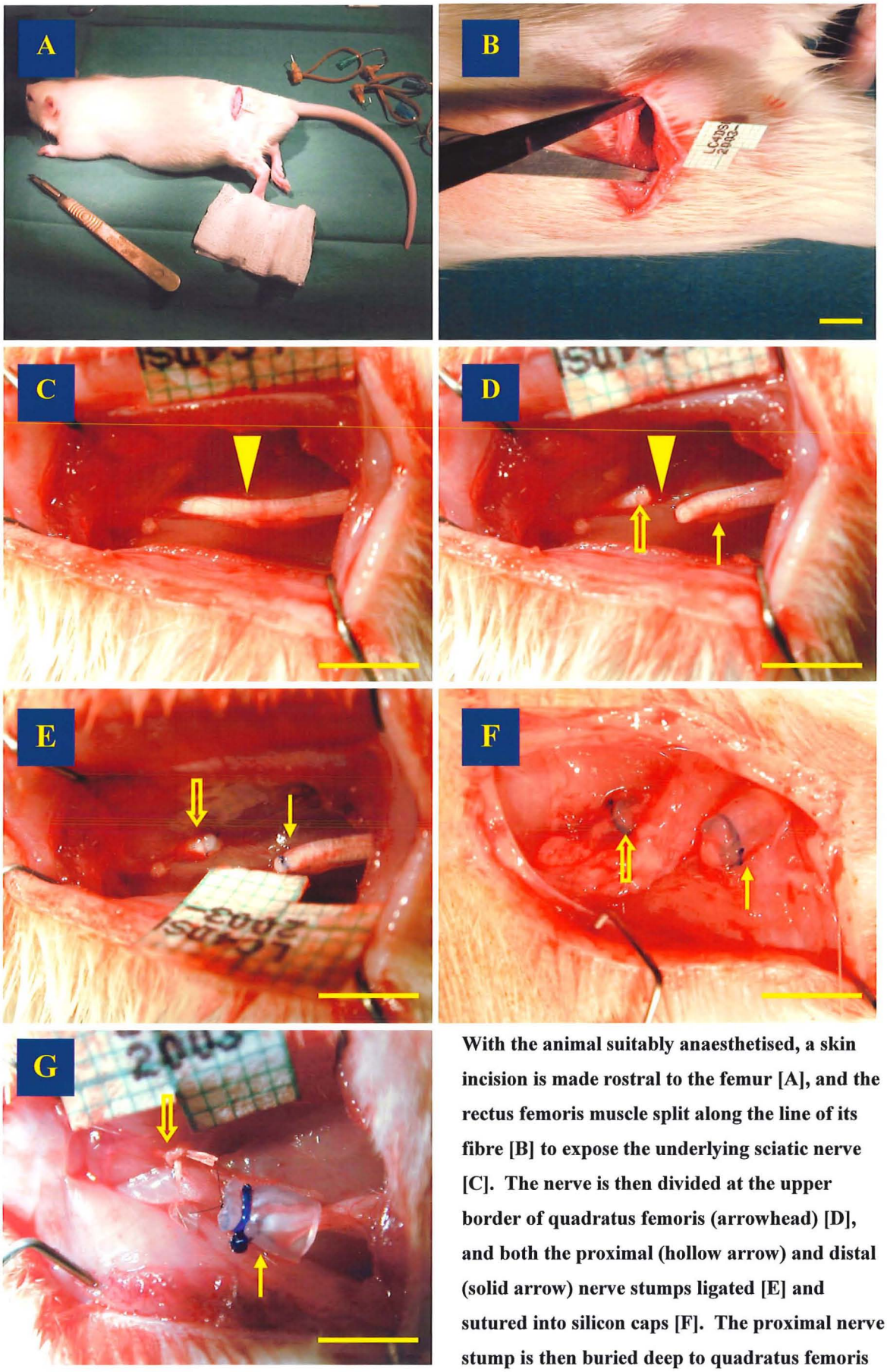

With the animal suitably anaesthetised, a skin incision is made rostral to the femur [A], and the rectus femoris muscle split along the line of its fibre [B] to expose the underlying sciatic nerve [C]. The nerve is then divided at the upper border of quadratus femoris (arrowhead) [D], and both the proximal (hollow arrow) and distal (solid arrow) nerve stumps ligated [E] and sutured into silicon caps [F]. The proximal nerve stump is then buried deep to quadratus femoris [G]. Scale bar 5mm.

involving transcardiac perfusion fixation. For all other tissue harvest procedures CO_2 narcosis was used.

2.2.1a Inhalational Anaesthesia

Anaesthesia was induced by placing the animal into a perspex induction box containing room air. Halothane® (4% in oxygen) was then instilled into the box at 6l/min until anaesthesia was achieved, as determined by loss of the usual righting reflex. The animal was then removed from the induction box, and its hindlimb shaved and prepped with Hydrex® (Adams Healthcare, U.K.), before being transferred to the operating table, where anaesthesia was maintained with halothane (1.5-2.5% in oxygen) delivered by a nose mask (*Figure 2.1a*) at a flow rate of 0.5-1.5l/min. A suction scavenging device was employed to minimise contamination of room air with halothane, and a similar scavenging device used to clean the air of the induction box prior to anaesthetising the next animal.

An adequate depth of surgical anaesthesia was ensured before commencing any operative procedures by demonstrating the abscence of any flexor withdrawal response to paw pinching in both hindlimbs, this was also tested at frequent intervals during the procedure. At the end of each procedure analgesia was administered subcutaneously (10% solution of Temgesic®, 0.1ml/100g body weight), and anaesthesia was then reversed with 100% inhaled oxygen, before placing the animal into a warmed chamber (30°C) for recovery. Animals were inspected frequently, and housed overnight in a warmed recovery room prior to returning to their normal environment within 48 hours.

2.2.1b Terminal Anaesthesia

Terminal anaesthesia was induced by intra-peritoneal injection of a lethal dose (0.5ml/kg body weight) of Sagattal™ (Rhône Mérieux, sodium pentobarbitone 60mg/ml), and death confirmed by exsanguination in keeping with Schedule 1 of the A.S.P.A. 1986.

2.2.1c CO_2 Narcosis

Animals were individually placed into an induction chamber filled with room air, and carbon dioxide (CO_2) narcosis induced by inflow of CO_2 at 4-6l/min, until respiration ceased. Death was confirmed by cervical dislocation in keeping with Schedule 1 of the A.S.P.A 1986.

2.2.2 Sciatic Nerve Division & Capping

Each experimental group consisted of 6 animals, and these were terminated for tissue harvest at 1,4 days, 1, 2 weeks, and 1, 2, 4, 6 months after nerve transection (cf.

2.3.2). Each animal was anaesthetised and prepped (cf. *2.2.1a*) before making a 2cm skin incision parallel to the femur, which began 1cm caudal to the hip (*Figure 2.1a*). The biceps femoris muscle was split along the line of its fibres (*Figure 2.1b*), thereby exposing the underlying sciatic nerve, and the wound was held open by appropriately placed retractors (*Figure 2.1c*). Care was taken at all times to avoid trauma to the nerve.

Under binocular magnification (8x objective lens), and using microsurgical techniques, the sciatic nerve trunk was gently mobilised from below the origin of the muscular branch to the hamstring muscles, to just above its division into the tibial and common peroneal nerves at the lower border of adductor magnus in the peroneal fossa [250]. Using No.5 micro-forceps the nerve was held by the epineurium, divided at the upper border of quadratus femoris with micro-nerve scissors (*Figure 2.1d*), and a 3mm segment was resected from the distal stump.

Both the proximal and distal nerve stumps were ligated with 6/0 Prolene® (*Figure 2.1e*), and then sutured into the silicone caps (cf. *2.1*) with single 9/0 Ethilon® epineurial sutures (*Figure 2.1f*). The capped proximal nerve stump was then buried in a pocket dissected deep to quadratus femoris, and then closed by approximating quadratus femoris to the obturator externus using a 4/0 Vicryl® suture (*Figure 2.1g*). To further reduce any chance of spontaneous regeneration the distal nerve stump was also reflected posteriorly into the cleft between the semimembranosus muscle and the overlying accessory head of the rectus femoris.

The retractors were removed, the rectus femoris edges approximated, and the skin closed with interrupted 4/0 Polydioxanone (PDS®) sutures.

2.2.3 L-Acetyl-Carnitine (LAC) Treatment after Sciatic Nerve Division & Capping

There were 3 treatment groups, each consisting of 6 animals, in which every animal was anaesthetised (cf. *2.2.1a*), and the sciatic nerve divided, ligated and capped as described above (cf. *2.2.2*). Immediately after closing the skin incision, each animal was given a 1ml intraperitoneal (i.p.) injection of L-acetyl-carnitine (LAC) ("low-dose" group: 5mg/kg; "high-dose" groups: 25mg/kg) in sterile normal saline (cf. *2.1*). Subsequently the animals were given LAC by i.p. injection ("low-dose" group: 5mg/kg; "high-dose" groups: 25mg/kg) 12 hourly for 14 days until the animals in the low-dose group, and in one of the two high-dose groups were terminated for tissue harvest (cf. *2.3.2*). Animals in the remaining high-dose treatment group continued to receive 50mg/kg of LAC by once daily i.p. injection (volume of injection=1ml), until being terminated for tissue harvest 2 months after the nerve transection.

There were three control groups. One sham treatment group received injections of sterile saline in an identical pattern to the animals being treated with LAC, and was terminated 2 weeks after nerve transection. Two further groups of animals underwent the same nerve transection procedure, but did not receive any injections ("no treatment"). One of these groups was terminated 2 weeks after nerve transection, and the other group after 2 months. Treatment regimes are summarised in Table 2.1.

2.2.4 N-Acetylcysteine (NAC) Treatment After Sciatic Nerve Division & Capping

There were 3 treatment groups, each consisting of 6 animals. Each animal was anaesthetised (cf. *2.2.1a*), and the procedure for division, ligation and capping of the sciatic nerve was performed as described above (cf. *2.2.2*). Immediately after closing the skin incision, each animal was given a 0.3ml intravenous (i.v.) injection of N-acetyl-cysteine (NAC) (low-dose group: 15mg/kg; high-dose groups: 75mg/kg) in sterile 5% dextrose. Subsequently the animals were given 12 hourly intravenous injections of NAC (low-dose group: 15mg/kg; high-dose groups: 75mg/kg), under halothane general anaesthesia for a total of 5 doses, before switching to i.p. injection. Two weeks after nerve transection the animals in the low-dose group, and in one of the two high-dose groups were terminated for tissue harvest (cf. *2.3.2*). Animals in the remaining high-dose treatment group then continued to receive 150mg/kg NAC by once daily i.p. injection (volume of injection=1ml), until being terminated for tissue harvest 2 months after the nerve transection.

There were three control groups. One sham treatment group received injections of 5% dextrose in an identical pattern to the animals being treated with NAC, and was terminated 2 weeks after nerve transection. The two "no treatment" groups described above (cf. *2.2.3*) were also used as 2 week, and 2 month controls in this study.

Treatment regimes are summarised in Table 2.1.

2.2.5 Sciatic Nerve Division & Primary Repair

This experimental group comprised 6 animals. Each was anaesthetised (cf. *2.2.1a*), and the sciatic nerve was exposed and divided at the upper border of quadratus femoris in the same manner described for sciatic nerve transection experiments (cf. *2.2.2*). The nerve was then immediately repaired using four 9/0 Ethilon® interrupted epineurial sutures, placed at 6, 12, 9, and 3 o'clock, the rectus femoris edges approximated, and the skin closed with interrupted 4/0 PDS® sutures. Animals were terminated for tissue harvesting two weeks later (cf. *2.3.2*).

Table 2.1: L-acetyl-carnitine (LAC) & N-acetyl-cysteine (NAC) Treatment Regimes

Drug:	Intra-Operative Dose	First 2 Weeks Post-Op	From 2 Weeks Post-Op Until Harvest
High-Dose NAC	Dose: 75mg/kg i.v. Total injection volume 0.3ml/dose Made up in sterile 5% Dextrose Give dose after closing the skin	Dose: 75mg/kg b.d. (every 12 hours) First 5 doses given as i.v. injection, total injection volume 0.3ml/dose 6^{th} dose onward given as i.p. injections, total injection volume 1ml/dose Injection made up with sterile 5% Dextrose	Dose: 150mg/kg o.d. (once daily) Give as i.p. injection, total injection volume 1ml/dose Injection made up with sterile 5% Dextrose
High-Dose LAC	Dose: 25mg/kg i.p. Total injection volume 1ml/dose Made up in sterile normal saline Give dose after closing the skin	Dose: 25mg/kg b.d. (every 12 hours) Given as i.p. injections, total injection volume 1ml/dose Injection made up with sterile normal saline	Dose: 50mg/kg o.d. (once a daily) Give as i.p. injection, total injection volume 1ml/dose Injection made up with sterile normal saline
Low-Dose Regimes	Doses: NAC 15mg/kg LAC 5mg/kg Injection schedule & volumes identical to high-dose regime	Doses: NAC 15mg/kg LAC dose 5mg/kg Injection schedule & volumes identical to high-dose regime	

2.2.6 Sciatic Nerve Division & Early Secondary Repair

The animal was anaesthetised (cf. *2.2.1a*), the sciatic nerve was exposed in the same manner described for sciatic nerve transection experiments (cf. *2.2.2*), and then divided at the upper border of quadratus femoris using micro-instruments.

A pocket was then dissected deep to the quadratus femoris muscle, into which the proximal nerve stump was inserted, and held out to its physiological length with a single epineurial 9/0 Ethilon® suture into the muscle. The quadratus femoris was then approximated to the obturator externus with a 4/0 Vicryl® suture, closing the intermusclar pocket.

The distal stump was reflected posteriorly into the cleft between the semimembranosus and the overlying accessory head of the rectus femoris, and held out to length with a single epineurial 9/0 Ethilon® suture into the semimembranosus muscle. The retractors were removed, the rectus femoris edges approximated, and the skin closed with interrupted 4/0 PDS® sutures.

One week later the animals were re-anaesthetised (cf. *2.2.1a*), the original skin wound reopened, and the rectus femoris split as before. The nerve stumps were mobilised after removing the epineurial sutures, and then co-apted using four 9/0 Ethilon® interrupted epineurial sutures placed at 6, 12, 9, and 3 o'clock. The retractors were then removed, the rectus edges reapproximated, and the skin closed with interrupted 4/0 PDS® sutures. Animals were then terminated for tissue harvesting (cf. *2.3.2*) one week later (ie. two weeks after nerve transection).

2.2.7 Sciatic Nerve Division & Late Secondary Nerve Graft Repair

Experimental groups consisted of 5 animals. Each animal was anaesthetised (cf. *2.2.1a*), and the sciatic nerve exposed (cf. *2.2.2*) and divided with micro-instruments at the upper border of quadratus femoris; no segment of distal stump was resected.

In order to prevent spontaneous regeneration, both nerve stumps were ligated with 6/0 Prolene® using a double surgical knot, before being sutured into silicone rubber caps using single 9/0 Ethilon® epineurial sutures (cf. *2.2.2*). The proximal stump was sutured out to its physiological length within the intermuscular cleft deep to the quadratus femoris, using a single 9/0 Ethilon® suture. The pocket over the proximal stump was then closed by approximating the quadratus femoris to the obturator externus with a 4/0 Vicryl® suture.

The distal stump was reflected posteriorly into the cleft between the semimembranosus and the overlying accessory head of the rectus femoris, and held out to

its physiological length with a single 9/0 Ethilon® suture into the muscle. The retractors were removed, the rectus femoris edges approximated, and the skin closed with interrupted 4/0 PDS® sutures.

Two months later the animals were re-anaesthetised (cf. *2.2.1a*), the original skin wound reopened, and the rectus femoris split as before. Using micro-instruments under 8X binocular magnification, the nerve stumps were mobilised, the silicone caps removed, and any remaining adventitial tissue trimmed away. The nerve stumps were then trimmed back to "healthy" nerve (>2mm from the 6/0 Prolene® ligature), leaving a gap of ~1cm between the stumps.

The gap was then repaired using a reversed 1cm long sciatic nerve isograft, freshly harvested from inbred siblings under terminal anaesthesia (cf. *2.2.1b*). The graft was reversed, and anastomosed to both nerve stumps using 10/0 Ethilon® interrupted epineurial sutures placed at 6, 12, 9, and 3 o'clock (*Figure 2.2a*), further sutures were occasionally added if required. The length of the nerve graft was measured under physiological tension, so that there was a 1cm gap between the proximal and distal nerve stumps in the resulting repair (*Figure 2.2b*). The retractors were removed, the rectus femoris edges reapproximated with 4/0 Vicryl® interrupted sutures, and the skin closed with interrupted 4/0 PDS® sutures.

One group of animals was treated with L-acetyl-carnitine (50mg/kg/day) by intraperitoneal injection, with the first dose given immediately the nerve repair was performed and thereafter using the same daily regime as described for the 2 month "high-dose" group in section *2.2.3.* All animals were terminated for tissue harvesting (cf. *2.3.2*) 6 weeks after nerve repair.

2.3 Tissue Harvesting Procedures

2.3.1 Schedule 1 Termination

Animals were terminated in accordances with Schedule 1 of the A.S.P.A 1986, by either terminal anaesthesia (cf. *2.2.1b*), or CO_2 narcosis (cf. *2.2.1c*).

2.3.2 Dorsal Root Ganglia

All perfusion work was carried out in an appropriate fume-cupboard using a Watson-Marlow 505S/RL peristaltic pump set at 25-35rpm, and 5mm internal diameter tubing. An intravenous 18 gauge cannula (Abbocath-T Venisystems™) was attached to the tubing, and the whole system primed with Phosphate Buffered Saline (PBS) chilled to 4°C.

Figure 2.2: Late Secondary Nerve Repair Using Reversed Sciatic Nerve Graft

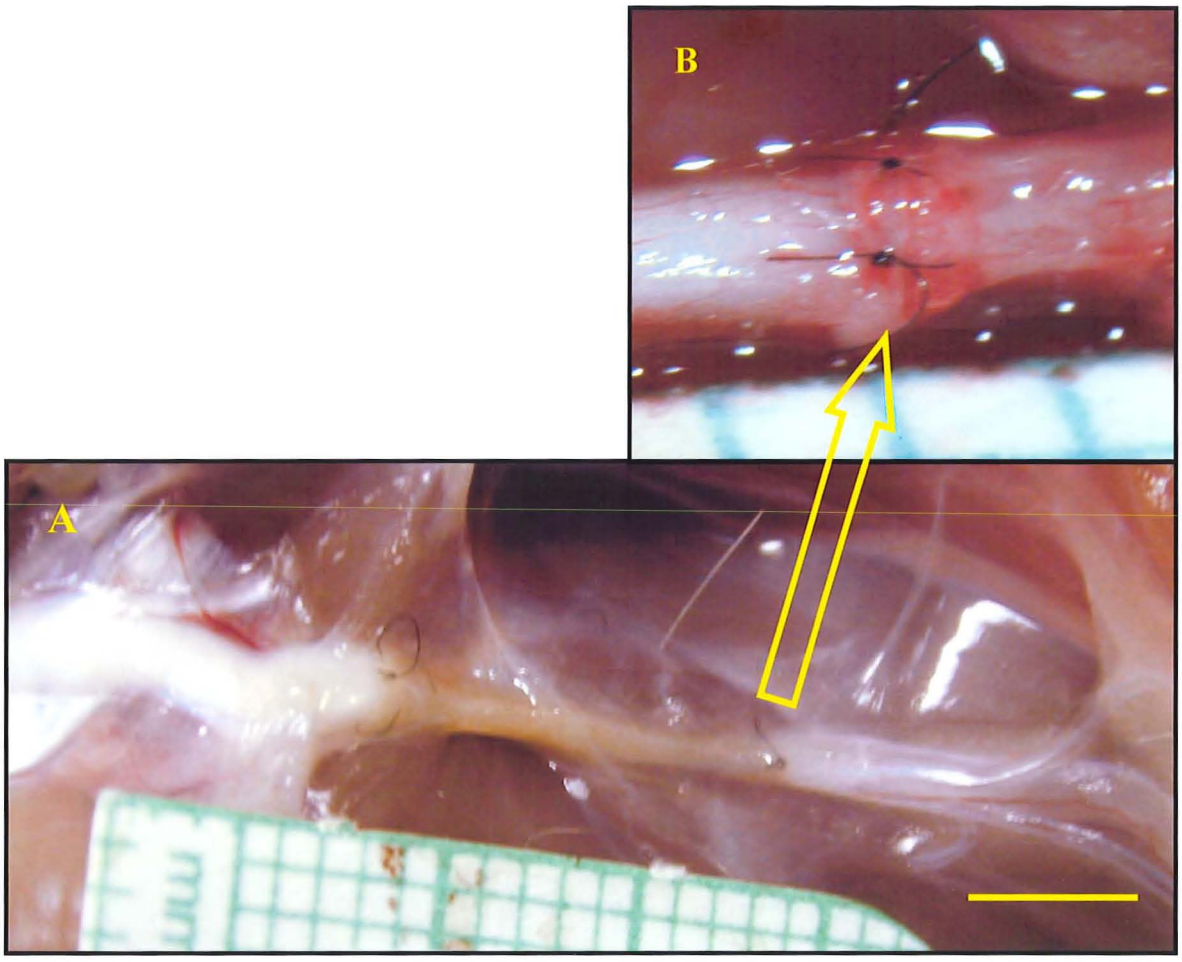

Late secondary nerve graft repair [A]. Two months after transection of the sciatic nerve a 1cm segment of sciatic nerve isograft was harvested from a sibling, reversed and used to perform a 1cm gap repair [A]. After limited trimming of both nerve stumps the graft was inserted, using four 10/0 Ethilon® epineurial sutures [B] placed in order at 6, 12, 3, 9 o'clock for each anastomosis. Scale bar equals 5mm.

With the animal deeply anaesthetised (cf. *2.2.1b*), as shown by absence of both the paw pinch-withdrawal reflex and the corneal reflex, the heart was exposed by a clam-shell incision through the chest wall and the left ventricle cannulated under direct vision with the 18 gauge PTFE cannula. The cannula was advanced into the ascending aorta and secured with a microvascular clamp, and the right atrium incised under direct vision to ensure exsanguination, and to provide an outflow for the perfusing fluids. Perfusion was commenced with 300ml of PBS at a pump rate of 35r.p.m., to flush the vascular system free of blood. The perfusate was then switched to chilled 4% paraformaldehyde (PFA), and the animal perfused with 400ml at a pump rate of 20-30r.p.m.

Immediately after fixation a dorsal skin incision was made along the spine, and the skin and paravertebral musculature reflected laterally. Using 3.5X magnification and micro-rongeurs, the spinal canal was de-roofed, beginning in the sacral region and proceeding rostrally. Taking care to avoid damaging neural structures, the spinal processes, laminae, and pedicles, were removed to expose the spinal cord and lumbar dorsal root ganglia (DRG) up to the level of T8, above the lumbar enlargement. The lumbar DRG's were identified, with the L5 DRG's lying immediately rostral to the L6 vertebra approximately at the level of the iliac crests [250]. The correct vertebral level was confirmed by counting the lumbar vertebrae rostrally from L1, below the last rib, and the L4 and L5 DRG's were carefully dissected out from their intervertebral foramina, taking care to avoid holding the ganglia directly, but rather using the spinal roots or nerves instead. The ganglia were then immediately placed into 4% PFA for 6 hours post-fixation at room temperature, before being removed and placed into a cryoprotectant solution containing 15% sucrose & 0.1% sodium azide in PBS. Three further rinses were then performed over 36 hours, and the samples stored at 4°C prior to the preparation of frozen blocks (cf. *2.4.1a*).

DRG's for electron microscopy were harvested using the same protocol, except that only 50ml of PBS was used, and pre-fixation was achieved with 500ml of a solution of 3% glutaraldehyde & 1% paraformaldehyde in PBS. Ganglia were stored in the same fixative solution at 4°C prior to processing for electron microscopy (cf. 2.4.1b).

2.3.3 Late Secondary Nerve Graft Repairs

Animals were terminated by CO_2 narcosis (cf. *2.2.1c*) in accordance with the terms of the Animals (Scientific Procedures) Act 1986.

The original skin incision was reopened, and extended down to the calcaneum. The rectus femoris was split along the line of its fibres, to expose the underlying conduit repair.

The integrity of the repair was checked, and the sciatic nerve mobilised proximally, and distally down to the gastrocnemius muscle. The sciatic nerve was then pinched proximal to the repair, using Number 5 microforceps, and the gastrocnemius inspected for any visible fibre contraction.

The sciatic nerve was divided 5mm proximal, and 10mm distal to the nerve repair, and the nerve graft removed in continuity, and pinned onto a flat plastic splint using 25 gauge needles through the ends of the sciatic nerve stumps. The specimen was then immediately placed into Zamboni's fluid for post-fixation.

After 12-16 hours post-fixation at 4°C, the nerve repairs were removed from Zamboni's solution and placed into a cryoprotectant solution of 15%Sucrose & 0.1%Sodium Azide in PBS. Three further rinses were then performed over 36 hours, and the samples were stored at 4°C prior to the preparation of frozen blocks (cf. *2.4.1a*).

2.3.4 Human Skin Biopsies

This study was performed in agreement with the terms of the Helsinki Declaration, after appropriate review by the local research ethics committee. Cutaneous excision biopsies were taken from consenting patients with established HIV-associated peripheral neuropathy (DSP) before and then after treatment with LAC, and also from asymptomatic HIV negative controls (cf. *8.2*).

Skin biopsies were excised from a site 1/3 of the way from the lateral malleolus to the head of the fibula, in whichever leg the patient felt to be more symptomatic. Having obtained the patient's consent, 2-5ml of local anaesthetic (1% lignocaine+adrenaline) was instilled subcutaneously into the area of the biopsy. The skin was prepped using aqueous Betadine, and the operative field defined with sterile drapes. Taking care to avoid inducing crush artefacts a 0.5cm x 1cm ellipse of skin was then excised with a scalpel and #15 blade, such that the long axis of the ellipse lay parallel to the tension lines in the skin. The biopsy was pinned onto a flat plastic sheet at its physiological length using 25 gauge needles, and then placed into Zamboni's solution for post-fixation.

The biopsy wound was closed with interrupted 4/0 Surgipro™ sutures and steristrips, and non-adherent gauze was applied (Melolin™) with an adhesive Tegaderm™ dressing. Sutures were removed after 14 days, and steristrips were reapplied for a further 7 days.

After 12-16 hours post-fixation at 4°C temperature, the samples were removed from Zamboni's solution and placed into a cryoprotectant solution containing 15% sucrose &

0.1% sodium azide in PBS. Three further rinses were then performed over 36 hours, and the samples were stored at 4°C prior to the preparation of frozen blocks (cf. *2.4.1a*).

2.4 Tissue Sectioning & Staining

2.4.1a Preparation of Frozen Blocks

Small aluminium foil boats were prepared on a Perspex form (10x12mm for DRG's & skin biopsies, 10x27mm for nerve repairs). The base of the boat was filled with OCT™, and the tissue samples were then removed from PBS-Sucrose solution and inserted into the foil boats thus (one sample per block):

a) DRG's: these were placed upon their long axis to allow longitudinal sectioning. The exact orientation along this axis was randomised, in keeping with stereological rules for vertical sectioning.

b) Nerve Repairs: these were trimmed to leave 3mm of both the proximal and the distal nerve stump in continuity with the repair, and were then placed along their longitudinal axis, with a single piece of rat liver placed at the level of the proximal anastomosis, and a double piece at the level of the distal anastomosis (*Figure 2.3a*).

c) Skin Biopsies: these were placed with the epidermal surface flat on the base of the foil boat, and the longitudinal axis of the biopsy randomly oriented relative to the walls.

The tissue samples were then fully covered in OCT™ blocking medium, and immersed into liquid Nitrogen until frozen. Blocks were stored at –40°C prior to sectioning.

2.4.1b Preparation of Blocks for Electron Microscopy

DRG's were post-fixed in 1% osmium tetroxide in 0.1M phosphate buffer at 37°C, dehydrated in acetone and embedded in Vestopal.

2.4.2a Sectioning of Dorsal Root Ganglia for TUNEL & Optical Disection

Each entire DRG was cut into serial 30μm cryosections on a Bright® OTF Cryostat, and every section was collected onto a pair of Vectabond® (Vector, U.K.) coated

Figure 2.3: Tissue Blocking & Sectioning:

A. Blocking Nerve Repairs:

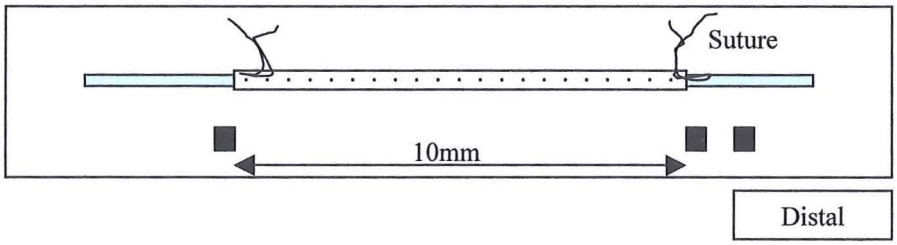

Nerve repairs were blocked into OCT™ with small blocks of liver (■)to indicate the position of the end of the nerve stumps, and to differentiate proximal (single piece of liver) from distal (two pieces of liver).

B. Serial Sectioning of Dorsal Root Ganglia:

#1	2	3	4
5	6	7	8
9	10	11	12
13	14	15	16
17	18	19	19
20	21	22	23
24	25	26	27
Ref:..... Ganglion			A

28	29	30	31
32	33	34	
Ref:..... Ganglion			B

Every serial 30μm cryosection from each dorsal root ganglion was collected in order onto a pair of vectabond® coated glass slides to facilitate subsequent systematic random sampling.

C. Systematic Random Collection of Skin Biopsy Cryosections

# 1	4	7	10	13	16
19	22	25	28	31	34
37	40	43	46	49	52
PGP 9.5	CGRP	VIP	PGP 9.5	CGRP	VIP

After discarding a random number of 15 μm cryosections, every 3rd section was collected onto slides labelled for the primary antiserum to be used. In this way a systematic random sample of vertical sections was collected from each skin biopsy.

glass slides, in rows of 4 sections (*Figure 2.3b*). This facilitated systematic random sampling (for optical disection), counting of the total number of sections from each ganglion (for Cavalieri estimation of ganglion volume), and allowed one to note which sections, if any, detached during subsequent staining.

All sections were air-dried overnight on a warming plate, before being placed into slide racks, sealed in aluminium foil, and stored at –40°C for a maximum of 2 weeks. Sections were thawed at 37°C for 6 hours prior to staining.

2.4.2b Sectioning of Nerve Repairs for Quantitative Immunohistochemistry

The nerve repairs were cut into longitudinal 15μm cryosections. Sections were discarded until the nerve stumps were reached, and seen to be present in the sections, thereafter every second serial section was collected onto 6 Vectabond® coated glass slides. This gave a random sample of sections from the region of the repair containing the majority of regenerating fibres, and ensured that no two sections to be stained with any one antiserum were consecutive.

All sections were air-dried overnight on a warming plate, before being placed into slide racks, sealed in aluminium foil, and stored at –40°C for a maximum of 2 weeks. Sections were thawed at 37°C for 6 hours prior to staining.

2.4.2c Sectioning of Human Skin Biopsies for Quantitative Immunohistochemistry

Human skin biopsies were cut into a systematic random sample of 15μm vertical cryosections. A random number from 1-10 was picked, and this number of sections were discarded before beginning the collection of every third serial section onto a set of 6 Vectabond® coated glass slides (*Figure 2.3c*).

All sections were air-dried overnight on a warming plate, before being placed into slide racks, sealed in aluminium foil, and stored at –40°C for a maximum of 2 weeks. Sections were thawed at 37°C for 6 hours prior to staining.

2.4.3 Triple Staining (DRG's for TUNEL Microscopy & Optical Disection)

Sections were permeabilised by microwave irradiation (478Watts for 1.5 minutes with a 1.5l water load) and rapid cooling in iced PBS. TdT Uptake Nick-End Labelling (TUNEL) (Promega Apoptosis Detection System Fluorescein) was then performed in accordance with the recommended protocol [251], which was adapted ("Triple Staining Protocol", Appendix 5), to allow simultaneous staining with Hoechst 33342 (H33342) and Propidium Iodide (PI). Hoechst 33342 is a non-specific nuclear stain which allows excellent determination of nuclear morphology [137,137,138,138,252]. Although PI exclusion by

an intact plasmalemma is used in vitro to demonstrate cell viability, in permeabilised fixed frozen sections the neuronal cytoplasm is exposed, giving PI at higher concentrations access to demonstrate the cytoplasmic morphology by staining of intracellular organelles. Each stain can be visualised separately using fluorescence microscopy and band specific filters.

The protocol was tested upon cryosections of various tissues that are known to reliably contain apoptotic cells, and in each case TUNEL positive cells were successfully demonstrated (*Figure 2.4*). To ensure that no artefactual errors arose between operated and control sides as a result of possible differences in staining conditions, the DRG's from both the control and axotomised sides of each experimental animal were always sectioned and stained together. A positive biological control (rat testis), and a negative experimental control (normal DRG sections with omission of TdT enzyme during staining) were also included in each staining run.

Slides were mounted with glass coverslips using glycerine in PBS (cf. *Appendix 8.5*). The edges of the coverslips were sealed with DPX, and the slides were stored at 4°C prior to fluorescence microscopic examination for TUNEL within 48 hours.

2.4.4 Immunohistochemistry (Nerve Repairs)

Sections were stained by indirect fluoresence immunohistochemistry according to the protocol given in Appendix 7, using primary antisera against "pan-axonal marker of neurofilaments" (PAMNF, Affiniti U.K.) as a general neuronal marker, and S-100 (DAKO, Denmark) as a Schwann cell marker. Dual staining was performed on all sections.

PAMNF was visualised using a Cy-3 conjugated secondary antibody (Cy-3 horse anti-mouse, Amersham Pharmacia U.K.), whilst S-100 staining was visualised by an FITC-conjugated secondary antibody (FITC goat anti-rabbit, Vector U.K.). Non-specific tissue binding of the secondary antibodies was prevented by pre-incubation of tissue sections with normal goat (Sigma-Aldrich U.K.) or normal horse (Sigma-Aldrich U.K.) sera, and non-specific hydrophobic attachment was reduced by co-incubation with normal rat serum (DAKO, Denmark).

After staining glass coverslips were mounted using glycerine in PBS (cf. *Appendix 8.5*), and stored at 4°C. Sections were then examined within 24 hours of staining (cf. *2.5.4*), and all images for quantification of staining captured (cf. *2.5.5*).

2.4.5 Immunohistochemistry (Skin Biopsies)

Both the pre- and post-treatment biopsies from a patient were processed together in order to eliminate minor variabilities between staining runs. Sections were

Figure 2.4 Verification of TUNEL Protocol in Positive Cells in Positive Biological Control Tissues

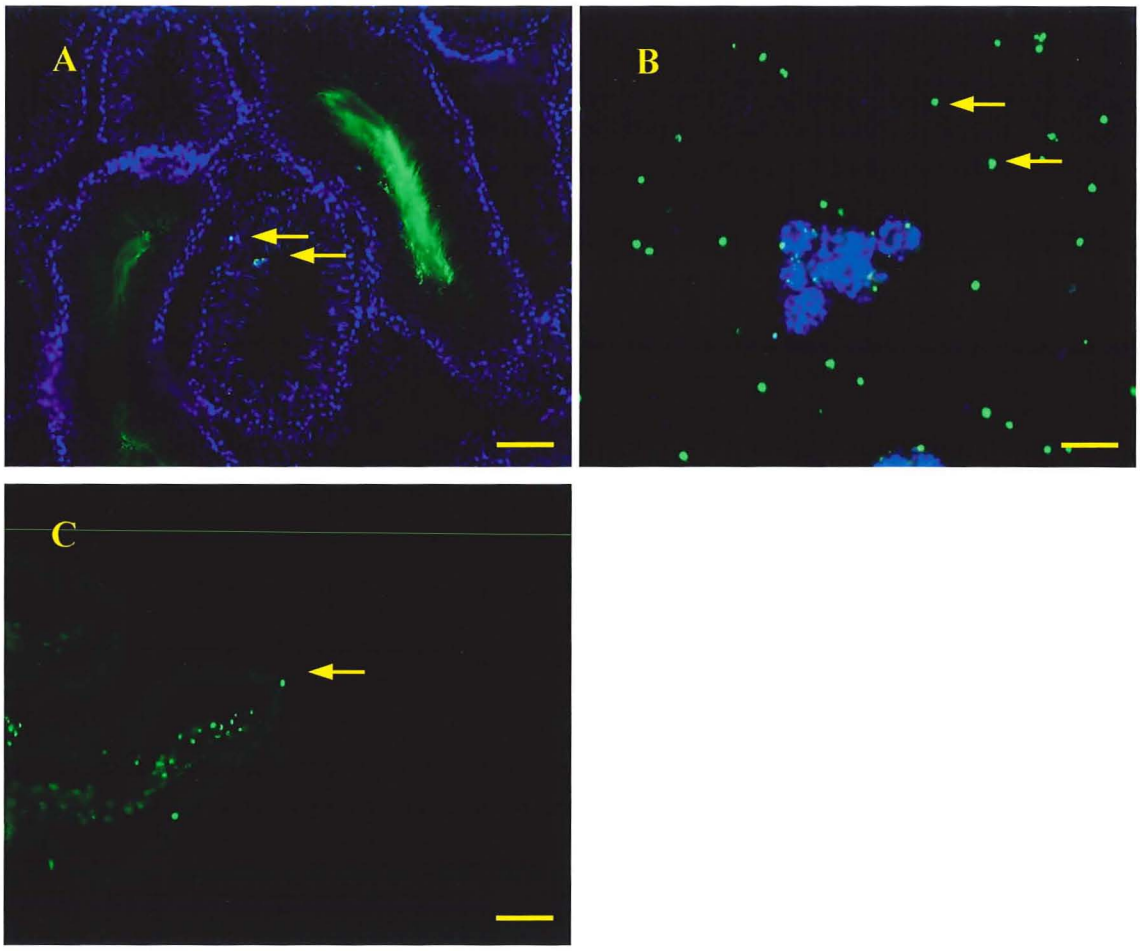

The TUNEL staining protocol was tested in several tissues known to contain apoptotic cells. TUNEL positive cells (arrows) were found in sections of rat testis [A], serum deprived Schwann cells [B], and at the tips of ileal villi [C]. Scale bar equals 40µm.

stained by indirect fluoresence immunohistochemistry according to the protocol given in Appendix 6, using primary antisera against protein gene product 9.5 (polyclonal rabbit antiserum to PGP9.5, Affiniti U.K.), calcitonin gene related peptide (polyclonal rabbit antiserum to CGRP, Affiniti U.K.), and vasoactive intestinal polypeptide (polyclonal rabbit antiserum to VIP, Affiniti U.K.). Antibodies to PGP9.5 bind to all fibre-types, since PGP9.5 is a constitutive cytoplasmic component of all nerve fibres, whereas the peptide neurotransmitter CGRP is specifically found in small, C and Aδ sensory fibres, and the neurotransmitter VIP is present in cholinergic, sympathetic postganglionic efferent fibres. Single antibody staining was used for all sections, and was visualised using a fluorescein conjugated secondary antibody (FITC-conjugated goat anti-rabbit serum, Vector U.K.). Non-specific tissue binding of the secondary antibody was prevented by co-incubation of tissue sections with normal goat serum (NGS, Sigma-Aldrich, U.K.).

After staining, glass coverslips were mounted using glycerine in PBS (cf. *Appendix 8.5*), and stored at 4°C. Sections were then examined within 24 hours of staining, and all images for quantification of staining captured (cf. *2.5.3*).

2.4.6 Staining for Electron Microscopy

Blocks were trimmed on a Pyramitome (LKB, Sweden) and sectioned with a 2128 Ultratome (LKB). Serial 1μm sections were cut from the ganglia and examined by light microscopy. Having identified a representative neuron, ultrathin (60-70nm) sections were collected on formvar-coated one-hole copper grids for electron microscopic examination, and stained with uranyl acetate and lead citrate.

2.5 Analysis & Quantification

In each study all analysis was performed by one individual using coded slides in order to reduce observer error.

2.5.1 TUNEL Staining

Changing between fluorescent filters easily permitted differentiation of neurons from satellite cells on the basis of their size, relative distribution, and their larger, paler nuclei (*Figure 2.5b*). The reliability of these features was previously confirmed in separate experiments where staining with PI and H33342 was combined with immunostaining using antisera to pan-neurofilaments (Affiniti U.K.), and the satellite cell marker S-100 (DAKO, U.K.).

Figure 2.5: Neuron Counting by Optical Disection: The C.A.S.T. Grid System & Morphological Differentiation of Neurons & Satellite Cells

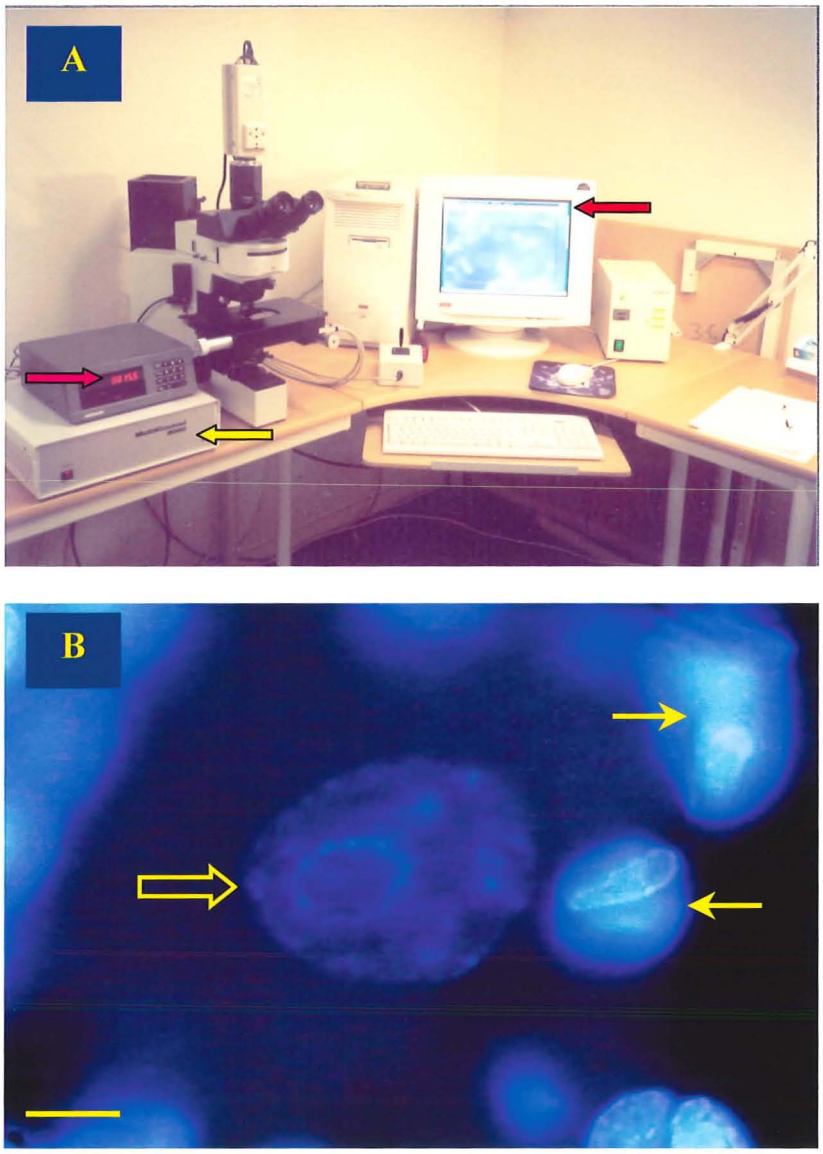

The C.A.S.T. Grid™ stereological system [A] comprised an Olympus BX50 fluorescence microscope, with a continuous interactive video display (red arrow). The stage has a microcator to record manual movement in the Z-axis (pink arrow), and its movement in the X-Y plane is controlled by the C.A.S.T. Grid™ software via a Multicontrol 2000™ unit (yellow arrow) during sampling and optical disection.

Neurons (hollow arrow) were easily differentiated from satellite cells (solid arrows) during optical disection, and TUNEL analysis, on the basis of their larger, nuclei paler which stained less intensely with Hoechst 33342 [B]. Scale bar equals 10μm.

All sections were examined for the presence of TUNEL positive cells using fluorescence microscopy and a 20x objective lens (Olympus BX60 microscope). Cells were confirmed to be neurons, or satellite cells by further examination under a 40x objective, and the morphology of each TUNEL positive neuron was examined by switching filters to visualise the nuclear and cytoplasmic staining. In every case the serial sections immediately before and after the section containing the TUNEL positive neuron were inspected to ensure that each positive neuron was only counted once. Absolute numbers of TUNEL positive neurons were therefore obtained for each ganglion.

At each timepoint the number of TUNEL positive cells was expressed either for individual ganglia (L4 or L5), or as a combined (L4+L5) count. For neurons the total number per experimental group was used, whilst for satellite cells a mean figure per animal (within that experimental group) was calculated.

2.5.2 Stereology

Neuron counts were performed using an Olympus BX50 microscope with parfocalised 60x oil immersion and 4x objectives. Stereology was facilitated by a continuous video output, and a stage which was motorised in the X-Y plane under the control of C.A.S.T. Grid™ software (*Figure 2.5a*). The number of surviving L4 & L5 DRG neurons was estimated by the stereological technique of optical disection [124,135,136], [124,135]using an Olympus WU filter to permit simultaneous visualisation of both PI and H33342 staining. Neurons were easily distinguished from satellite cells on the basis of their size, and their larger, paler staining nuclei (*Figure 2.5b*).

With this technique one initially estimates the ganglion's volume by using the Cavalieri Principle [130], which states that the volume of a structure approximates very closely to its mean cross-sectional surface area multiplied by its height. Mean surface area ($\bar{a}$) is calculated from measurements of the surface area (a) of ten or more serial sections in a systematic random sample from the ganglion. The "height" of the ganglion equals the total number of tissue sections cut from the ganglion (s) multiplied by the mean thickness of those sections ($\bar{t}$). The volume of the ganglion (V_{ref}) is therefore calculated thus:

$$V_{ref} = \bar{a} . \bar{t} . s$$

(V_{ref} = Volume of DRG) ($\bar{a}$ = mean area of section)

($\bar{t}$ = mean section thickness) (s = total number of sections)

In stereology every cell has an equal chance of being counted, obviating any bias due to variations in cell size, or distribution within the ganglion. Central to this tenet are the

counting rules associated with the optical disector bricks, and the process of systematic random sampling at all levels of the process after tissue sectioning. Sampling is achieved by starting from a randomly chosen start point, and then systematically moving through the ganglion, or tissue section, in a series of predetermined steps.

In practise, a systematic random sample of the serial sections from each ganglion was obtained for volume estimation as follows. The start section (1^{st}-3^{rd} of the serial sections) was selected using a random number table, and was examined along with every 3^{rd} subsequent section from the ganglion *(Figure 2.6a)*. Where this randomisation procedure resulted in fewer than the required minimum of ten sections being available, the procedure was altered to select every second section (start section 1^{st} or 2^{nd}).

The neuron containing area (a) of each section was measured using C.A.S.T.-Grid™ (Version 1) software by tracing its margins under a 4x objective *(Figure 2.6b)*. The thickness (t) of every section examined was also directly measured, using a stage-mounted microcator and a 60x oil immersion objective, by focusing down from the surface of the section, to the focal plane at its underside. Results were then used for calculation of mean section thickness ($\bar{t}$), mean surface area ($\bar{a}$), and hence of ganglion volume (V_{ref}).

The density, or "Numerical Volume" (N_v), of neurons within the ganglion was then determined by using a series of optical disector bricks. These are cuboid, computer generated geometrical constructs of a known volume which are placed within the same tissue sections selected for volume estimation (*Figure 2.6d*). Systematic randomisation is performed in the X and Y-axes by movements (X-steps & Y-steps) from a random start point (*Figure 2.6c*). Using an objective lens with a narrow focal plane (<1 μm) the disector bricks are generated by focusing down through a predetermined distance within the thickness (Z-axis) of the tissue section.

In practice, optical disection and systematic random placement of optical bricks within each section was performed by the C.A.S.T.-Grid™ system, which controlled a microscope stage motorised in the X-Y plane *(Figure 2.6c)*. Manual movement in the Z-axis (focusing down through the section) was tracked by the stage-mounted microcator. The disector volume (V_{dis}) was 81702 μm^3, X-steps and Y-steps were 300 μm.

The leading edge of the nucleus was used as the unique point of the neuron for cap counting; standard stereological counting frames [130] and optical disector counting rules were employed [136]. These rules determine that only particles lying entirely within the volume of the bricks, or crossing any of three mutually perpendicular faces are counted. A "cap" is a particle, or neuron in this case, which meets the counting rules employed *(Figure 2.6d)*. Neurons which cross any of the opposite three faces are not counted

Figure 2.6: Estimation of Volume & Neuron Count Within Dorsal Root Ganglia

A

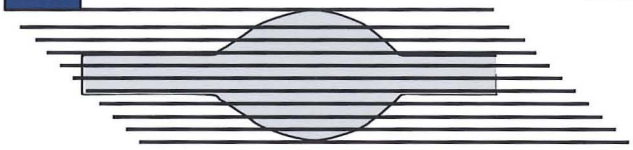

Collect every 30μm serial section (total number of sections = **s**)

Randomly assign start section #1-3

Examine every 3rd section

(total number examined = N_{sect})

B

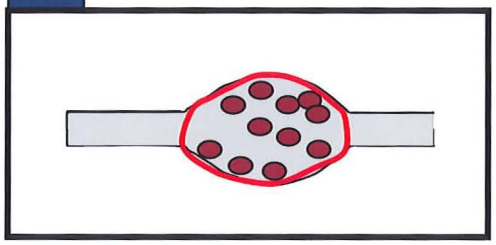

Trace outline of DRG section using 4x objective lens.

Area (**a**) quantified by C.A.S.T. Grid system.

Section thickness (t) measured with microcator.

Calculate mean surface area ($\bar{a}$) & thickness ($\bar{t}$) of DRG sections:

$$\bar{a} = \Sigma\, a / N_{sect} \qquad \bar{t} = \Sigma\, t / N_{sect}$$

Estimate Volume of DRG (V_{ref}) by Cavalieri Principle:

$$V_{ref} = \bar{a} \,.\, \bar{t} \,.\, s$$

C

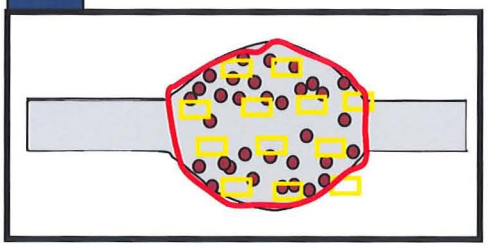

Set x & y steps between disector bricks.

Within each area traced for volume estimation the C.A.S.T. Grid randomly assigns a start point and then systematically moves around the section in predetermined X & Y steps, placing a disector at each point.

D

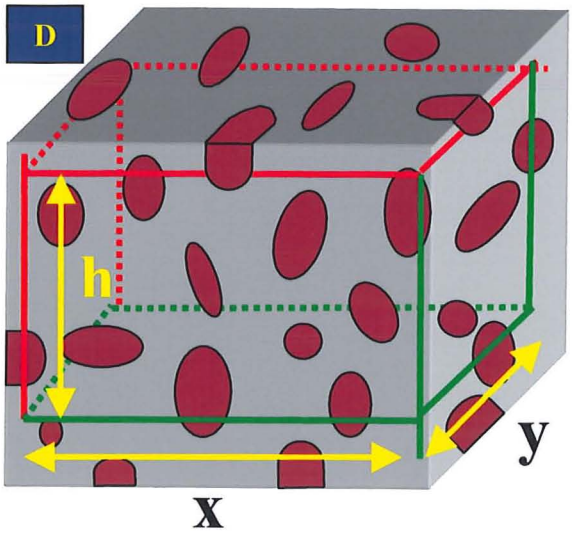

Each optical disector brick is therefore a tissue volume (**x . y . h**) created by focusing down through the tissue section.

There are reference volumes above & below the disector, giving 3 **inclusion** & 3 **exclusion** faces. Neurons crossing an inclusion face ("caps") are included in the count (N_{par}), those crossing an exclusion face are not counted ("profiles").

The density of neurons (N_v) within the total number of disectors used (N_{dis}) is then calculated, and used to estimate the total number of neurons present within the ganglion:

$$V_{dis} = (x \,.\, y \,.\, h) \,.\, N_{dis} \qquad N_v = N_{par} \,/\, V_{dis}$$

$$\textbf{Neuron Count} = N_v \,.\, V_{ref}$$

Due to the systematic random placement (sampling) of the disector bricks, and the equal number of inclusion and exclusion faces, every neuron within a ganglion has an equal chance of being counted, irrespective of its size or relative distribution.

Neuron counts are therefore statistically unbiased.

("profiles"). The mean cap count was 148 (SD27.5) per ganglion, in keeping with the requirement to count between 100 and 200.

The "cap" count thereby obtained is divided by the total volume within which counting was performed (i.e. individual disector brick volume multiplied by the total number employed) to give the density, or "numerical volume" (N_v), of neurons within the ganglion:

$$N_V = \frac{\text{cap count}}{V_{dis} \cdot N_{dis}}$$

(N_V = Numerical volume of neurons) (V_{dis} = Volume of each optical disector brick)
(N_{dis} = Number of optical disector bricks used)

Finally, the numerical volume (N_V) of neurons is multiplied by the volume of the ganglion (V_{ref}) to give the estimated number of neurons within the ganglion:

$$\text{Neuron Count} = N_V \cdot V_{ref}$$

(Neuron Count = estimated number of neurons per ganglion)

The same sampling schedule, stereological counting frame, and optical disector counting rules were used for every count, and the number of neurons was expressed for individual ganglia (L4 or L5) and as a combined (L4 plus L5) count for each side (axotomised, or contralateral control). The combined L4+5 count was used for the studies detailed in *Chapters 3-5*, since this comprises 98.4% of the entire sciatic nerve pool [253], and because individual counts are less sensitive as indicators of the effect of axotomy (cf. *3.4.2*). Neuronal loss was calculated by subtracting the number of neurons in axotomised ganglia from that in their contralateral controls. Loss was then expressed as a percentage of the neuron count in the control ganglia.

2.5.3 Area of Immunostaining (Skin Biopsies)

All quantification was performed upon coded sections by one individual in order to eliminate inter-observer error. After staining, each section was examined by fluorescence microscopy on an Olympus BX60 microscope using a 20x objective lens. For each primary antibody a systematic random sample of 6 visual fields including both epidermis and dermis (PGP9.5 & CGRP), or subcutaneous sweat glands alone (PGP9.5 & VIP) was captured for analysis using a high resolution fluid cooled digital spot camera (Diagnostic

Instruments U.S.A., Model 1.3.0). Similar exposure settings were used for every image captured.

The area of immunostaining in each captured image was subsequently quantified by image analysis using Image-Pro-Plus™ (Version 4.0) software. First the colour immunofluorescent image (*Figure 2.7a*) was converted into greyscale (*Figure 2.7b*), and then the area of interest (epidermis, dermis, or sweat gland) outlined by tracing its margins (*Figure 2.7c*). An intensity threshold was then applied in order to differentiate the bright immunostaining from any low-level background autofluorescence, and the area of staining was calculated by the software package after manually deselecting any residual areas of background staining (*Figure 2.7d*). Similar intensity thresholds were applied to every image quantified.

The area of immunostaining was expressed either as a total area of immunostaining (μm^2) or as a fraction of the total area of interest, whether that was epidermis, dermis, or sweat gland ("fractional area of immunostaining"). The area of immunostaining approximates closely to the actual area of each type of nerve fibre present, and therefore permits quantification of cutaneous innervation by each fibre type.

The innervation present before commencing oral LAC (cf. *8.2*) was compared to that found after 6 months of treatment (i.e. change in fractional area of immunostaining, expressed as a percentage of the pre-treatment value), and both results were compared to the level of innervation found in non-neuropathic HIV negative controls. For Patient 1 the innervation present 6 months after discontinuing LAC treatment was also quantified, and expressed relative to that present before discontinuing treatment.

2.5.4 Regeneration Distance (Late Secondary Nerve Repairs)

Regeneration distance was measured as the distance from the end of the proximal stump, to the tip of the most distal nerve fibre in each nerve graft, or distal stump where fibres had crossed the full 1cm gap (*Figure 2.8a*). After examining all the stained sections from a given repair in order to find the most distal fibres, the regeneration distance was measured under fluorescence microscopy using a graticulated 10X eyepiece, and 10X objective lens, such that each graticule measured a 0.1mm distance. The mean regeneration distance for each type of repair was then calculated, and expressed in millimetres.

2.5.5 Area of Immunostaining (Late Secondary Nerve Repairs)

All the stained sections from a given repair were examined by fluorescence microscopy using a 10X objective lens, in order to identify the two sections exhibiting

Figure 2.7: Quantification of Cutaneous Innervation by Image Analysis and Indirect Immunohistochemistry

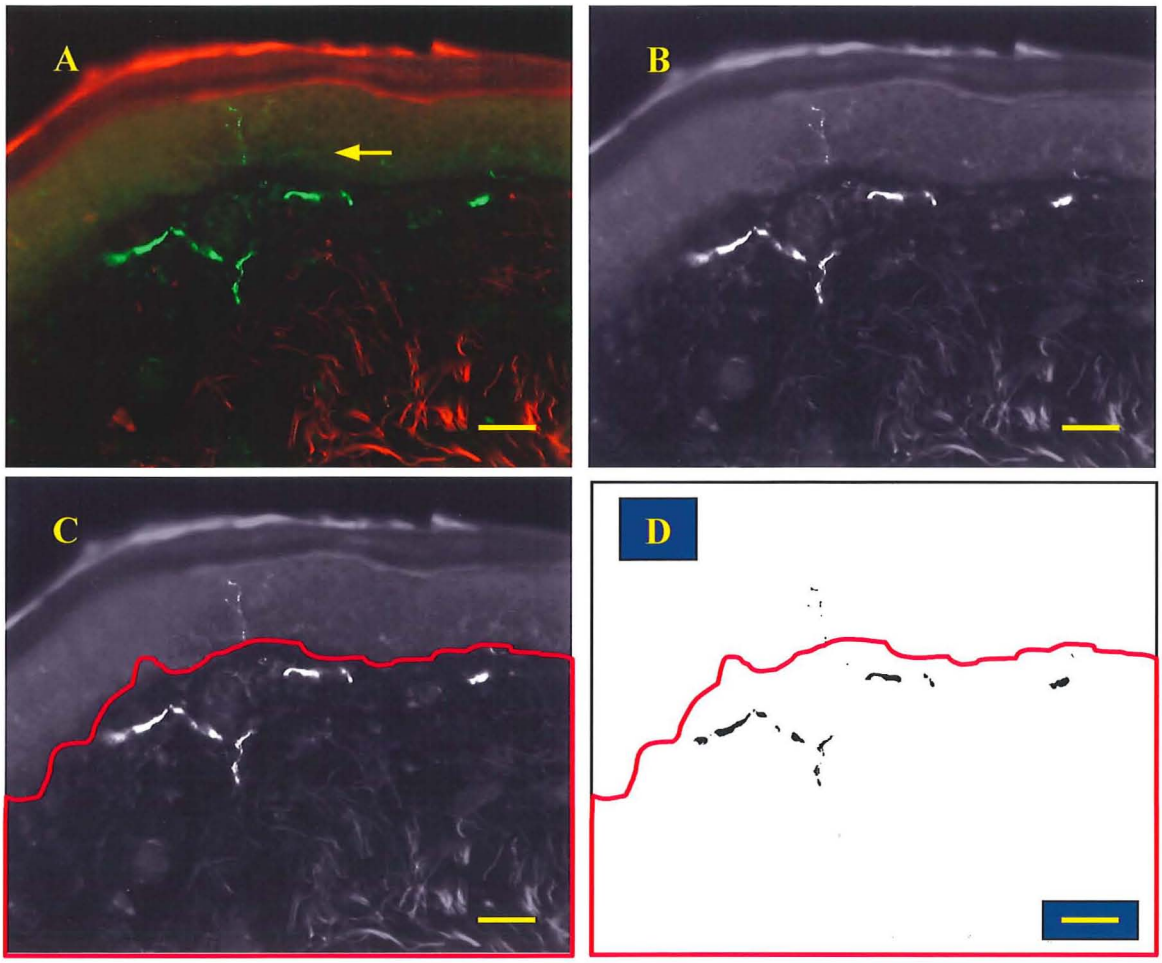

Quantification of cutaneous innervation by image analysis (Image-Pro-Plus®) and indirect immunohistochemistry with a FITC-conjugated secondary antibody. Positive staining shows as green fluorescence against the red background of the non-specific stain Pontamine Sky Blue [A]. First the colour image is converted to a monochrome green image, which in turn is converted to greyscale [B]. The area of interest (epidermis, dermis, or sweat gland) is then outlined manually [C], and an intensity threshold applied to select only the areas of staining, which are brighter than the background [D]. The software then quantifies the selected area, which is expressed either as a total area (μm^2), or as a percentage of the area of interest. Scale bar equals 40μm.

Figure 2.8: Measurement of Regeneration Distance and Area of Immunostaining as Indicators of Nerve Regeneration After Late Secondary Nerve Repair

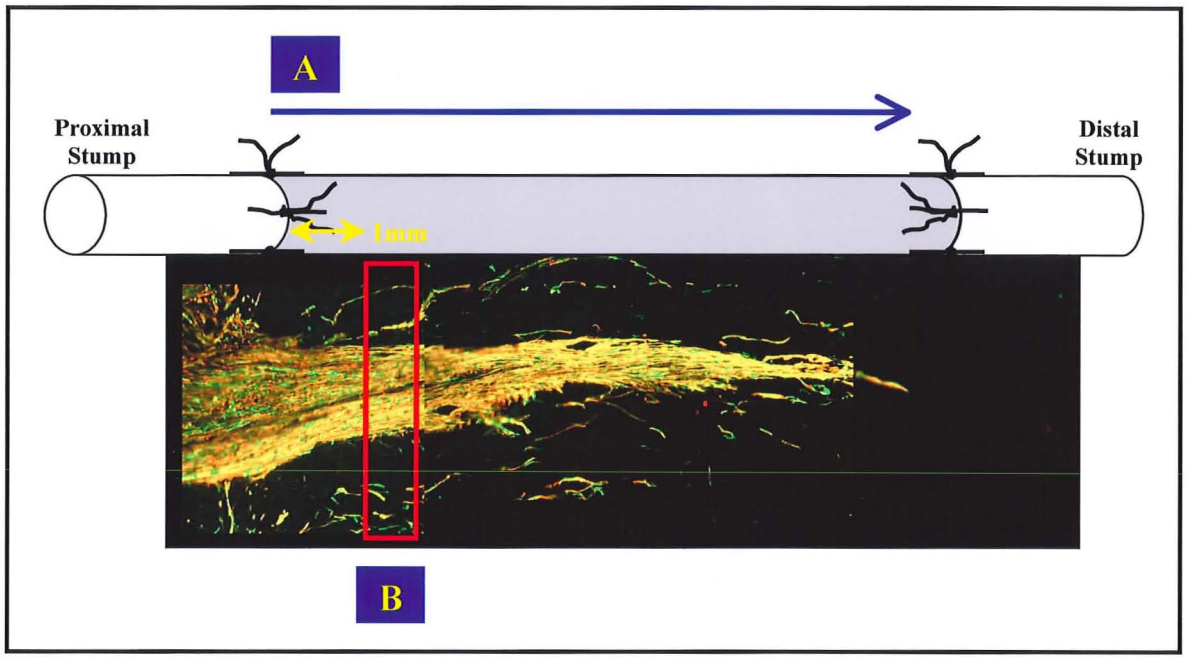

Nerve repairs were cut into 15μm cryosections and stained by indirect immunohistochemistry with antisera against the pan-neuronal marker PAMNF (red fluorescence) and the Schwann-cell marker S-100 (green fluorescence). Where the two stains overlap yellow fluorescence is seen. Regeneration distance [A] was measured from the end of the proximal stump to the tip of the most distal regenerating nerve fibre (blue arrow) using a graticulated eyepiece and a 10x objective lens. Surface area of immunostaining [B] was quantified by image analysis (Image-Pro-Plus™) in a band of images captured at 20x magnification across the full width of the repair, and situated 1mm distal to the end of the proximal nerve stump (red rectangle). Area of immunostaining was expressed either as a total area (μm2), or as a percentage of the whole area of graft within the images captured.

the best nerve regeneration. Due to the pattern in which serial sections were collected onto the slides, the two selected sections were always non-consecutive.

In both the sections selected for measurement, a contiguous band of images lying 1mm distal to the end of the proximal stump was captured across the full width of the graft using a high resolution fluid cooled digital camera (Diagnostic Instruments, U.S.A.), and a 20X objective lens (*Figure 2.8b*). In each band of images the area of immunostaining for either S-100, or PAMNF was then measured using Image-Pro-Plus™ image analysis software.

This process involved converting the monochrome colour image (red for PAMNF, green for S-100) into a greyscale image, and then applying an intensity threshold to select only the bright areas of immunostaining. Occasional areas of bright background staining were then deselected manually, and the total area of staining within that field recorded, along with the total area of the field. This process was repeated for all the images from each section, and the total area of immunostaining summated, along with the total area of the nerve graft present in the fields. The area of immunostaining was also calculated as a percentage of the area of the nerve graft, in order to facilitate comparison between nerve grafts of different diameters.

A total of ten measurements was therefore recorded for each type of repair, and the mean value used for statistical comparison. Total area of immunostaining was expressed in μm^2, and percentage area was quoted directly.

2.5.6 Electron Microscopy Analysis

Ultrathin sections were examined in a JEOL 100CX electron microscope at either 3000X or 5000X magnification, and representative micrographs were taken.

2.5.7 Statistical Analysis

Statistics are like women, mirrors of purest virtue and truth, or like whores, to use as one pleases.
Theodor Billroth

Statistical comparisons were performed using SigmaStat™ (Version 2.0) software. Groupwise comparisons were performed by ANOVA, and pairwise comparisons by Students t-test, or the Mann-Whitney Rank-Sum Test where data distribution was non-parametric, or not normal (assessed by the Kolmogorov-Smirnov Test). Comparison between pre- and post-treatment results within each individual was performed using the Paired t-test, or the Mann-Whitney Rank-Sum Test where data distribution was not normal.

Chapter 3. Timecourse & Morphological Features of Primary Sensory Neuronal Death After Peripheral Axotomy

3.1 Introduction

The extensive primary sensory neuronal death found after experimentally induced peripheral nerve lesions [47,55,97,107,108,111,113,114] (cf. *1.4*) is likely to be a major factor in the poor clinical outcome of peripheral nerve trauma (cf. *1.1*), and although a variety of stimuli may initiate neuronal death, loss of target derived neurotrophic support appears to be the most important determining the magnitude of neuronal death which ensues (cf. *1.5*). The precise timecourse of this neuronal death remains undefined (cf. *1.4*), as does that of satellite cell death within the adult DRG (cf. *1.4*), and yet it should define the most relevant timepoints at which to study the effects of any putative neuroprotective strategies. The timecourse of neuronal death is also of fundamental clinical importance in defining a potential therapeutic window for any future neuroprotective interventions.

The morphological features of post-axotomy primary sensory neuronal death are also of interest since there is debate over the mechanism by which neurons die, and this has clinical implications due to the difference in the therapeutic approaches to apoptosis and necrosis. Neuronal death has classically been deemed to occur by apoptosis [17] in a variety of settings, and there is recent evidence in support of this for axotomised primary sensory neurons [98], however other authors have postulated an active form of cell death that involves mixed morphological features of apoptosis and necrosis [146,254,255].

This study therefore aimed to determine the timecourse of primary sensory neuron, and satellite cell death after a defined peripheral nerve transection. TUNEL was used as a marker of individual cell death in order to identify the onset of neuronal death, and to detect low rates of cell death (cf. *1.4*). The magnitude of neuronal loss was then quantified from neuron counts obtained by the optical disector technique (cf. *1.4*), and the morphological features of neuronal death were established using light and electron microscopy.

3.2 Methods

Under halothane anaesthesia young adult male Sprague-Dawley rats underwent either left or right-sided unilateral sciatic nerve division, and measures were taken to prevent spontaneous regeneration (cf. *2.2.2*). After survival periods of 1, 4 days, 1, 2 weeks, 1, 2, 4 & 6 months (n=6 per timepoint) ipsilateral axotomised, and contralateral

control L4&L5 ganglia were harvested (cf. *2.3.1*) for the preparation of frozen blocks (cf. *2.3.2*). Animals were also harvested (n=3) for electron microscopy of ganglia after a survival period of 2 weeks (cf. *2.3.2*).

For TUNEL and stereological studies, each entire ganglion was cut into serial 30μm cryosections (cf. *2.4.1a & 2.4.2a*), and a microwave permeabilisation technique employed to optimise the sensitivity of a triple staining protocol (cf. *2.4.3*) which incorporated TdT Uptake Nick-End Labelling (TUNEL), nuclear counterstaining with Hoechst 33342 (H33342) and cytoplasmic counterstaining with Propidium Iodide (PI). Each stain was visualised separately using fluorescence microscopy and band specific filters, allowing neurons to be easily distinguished from satellite cells on the basis of their size, relative distribution, and their larger, paler nuclei (*Figure 2.5b*).

All sections were examined for the presence of TUNEL positive cells (cf. *2.5.1*), and absolute numbers of TUNEL positive neurons were obtained for each ganglion. At each timepoint the number of TUNEL positive cells was expressed either for individual ganglia (L4 or L5), or as a combined (L4+L5) count. For neurons the total number per group was used, whilst for satellite cells a mean figure per animal was calculated.

Stereological techniques were employed to obtain statistically unbiased estimates of DRG volume, by the Cavalieri Principle [130], and the number of surviving L4 & L5 DRG neurons by the optical disector technique [124,135,136] (cf. *2.5.2*). During optical disection an Olympus WU filter was used to allow simultaneous visualisation of both PI and H33342 staining. Standard stereological counting frames, and optical disector counting rules were employed, and all stereology was performed using the C.A.S.T. Grid software system.

Neuron counts were expressed both for individual ganglia (L4 or L5) and as a combined (L4 plus L5) count for each side (axotomised, or contralateral control). The number of neurons dying as a result of peripheral axotomy ("neuronal loss") was calculated by subtracting the number of neurons in axotomised ganglia from that in their contralateral controls, and was expressed as a percentage of the neuron count in the control ganglia.

Separate DRG's were prepared for electron microscopy (cf. *2.4.1b*), and representative ultrathin sections cut for the preparation of electron micrographs (cf. *2.4.6*).

Statistical analysis of results was performed using the techniques described previously (cf. *2.5.7*).

3.3 Results

3.3.1a Morphology (Light Microscopy)

TUNEL positive neurons displayed a range of morphologies (*Figure 3.1A-C, E*), although all had abnormal nuclei (H33342 staining) exhibiting pyknosis, chromatin condensation, or even nuclear fragmentation. Whilst many had cytoplasmic features typical of apoptosis (nuclear eccentricity, pyknosis, granulation, vacuolation) (*Figure 3.1A, B*), some exhibited an apparently normal cytoplasmic morphology (*Figure 3.1C*). Satellite cells with abnormal, intensely stained, irregular, condensed or ring-shaped nuclei were frequently seen. Whilst many were TUNEL positive, a substantial minority were negative.

Apart from the classical pattern of chromatolysis and nuclear eccentricity, other morphologically abnormal, but TUNEL negative neurons were seen. "Ghost cells", which are thought to represent the site of fully involuted apoptotic neurons, were occasionally found (*Figure 3.1F*), as were morphologically apoptotic neurons. Grossly dilated and vacuolated cells (*Figure 3.1D*) were found at every timepoint, with a peak incidence 1-2 months after axotomy. These cells were found almost exclusively in axotomised ganglia, and had eccentric, elliptical nuclei, with a degree of chromatin condensation. Two such cells were TUNEL positive (*Figure 3.1E*).

3.3.1b Morphology (Electron Microscopy)

Two weeks after axotomy, many primary sensory neurons showed essentially normal morphology (*Figure 3.2A*). Others exhibited morphological features of axotomy, with nuclear eccentricity and intact, normally distributed intracellular organelles (*Figure 3.2B*). Many neurons in varying degrees of degeneration were also present (*Figure 3.2C-E*), as were apoptotic bodies and occasional dilated, vacuolated cells.

Mitochondrial swelling occurred in the absence of nuclear, or endoplasmic reticular disruption (*Figure 3.2C*), whilst structural disruption of the mitochondrial cristae was accompanied by the prominent nuclear irregularity and a degree of endoplasmic reticular dissolution (*Figure 3.2D*). Complete loss of normal mitochondrial morphology, with the appearance of vacuolation and mitochondrial disruption, occurred in conjunction with nucleolar fragmentation and other morphological features of cell death (*Figure 3.2E*). At higher magnification the extent of the disruption to the normal mitochondrial architecture that precedes nuclear dissolution is apparent, particularly when contrasted to neighbouring cells (*Figure 3.2F*).

Figure 3.1 Light Microscopic Morphological Features of Primary Sensory Neurons After Peripheral Axotomy

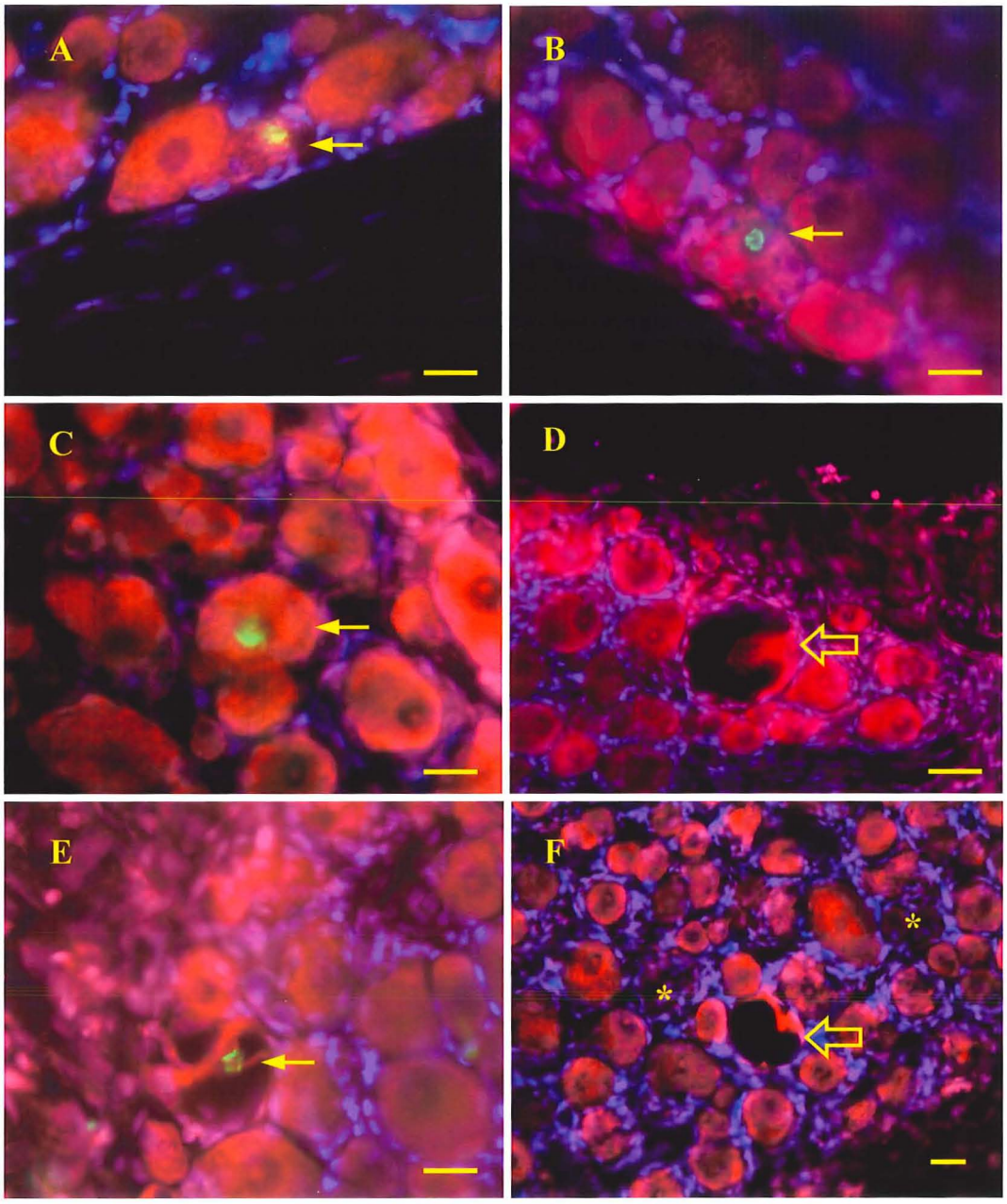

Morphology of primary sensory neurons after peripheral axotomy. Positive TUNEL staining shows as green fluorescence, cytoplasmic staining by Propidium Iodide shows as red, and nuclear staining by Hoechst 33342 shows as blue. TUNEL positive neurons (solid arrows) showed a range of cytoplasmic morphologies (A-C, E). Typical features included pyknosis (A), granulation (A), vacuolation (B), and membrane blebbing (B). However some cells were essentially normal in appearance (C). Numerous enlarged and grossly vacuolated neurons were found at all timepoints studied (D, E, F). Generally such cells were TUNEL negative (outline arrow, D & F), however two TUNEL positive cells were found (E). Ghost cells (asterisks) were found in axotomised ganglia at early timepoints. Scale bar equals 20µm.

Figure 3.2A&B: Electron Microscopy of Primary Sensory Neurons in Axotomised Ganglia

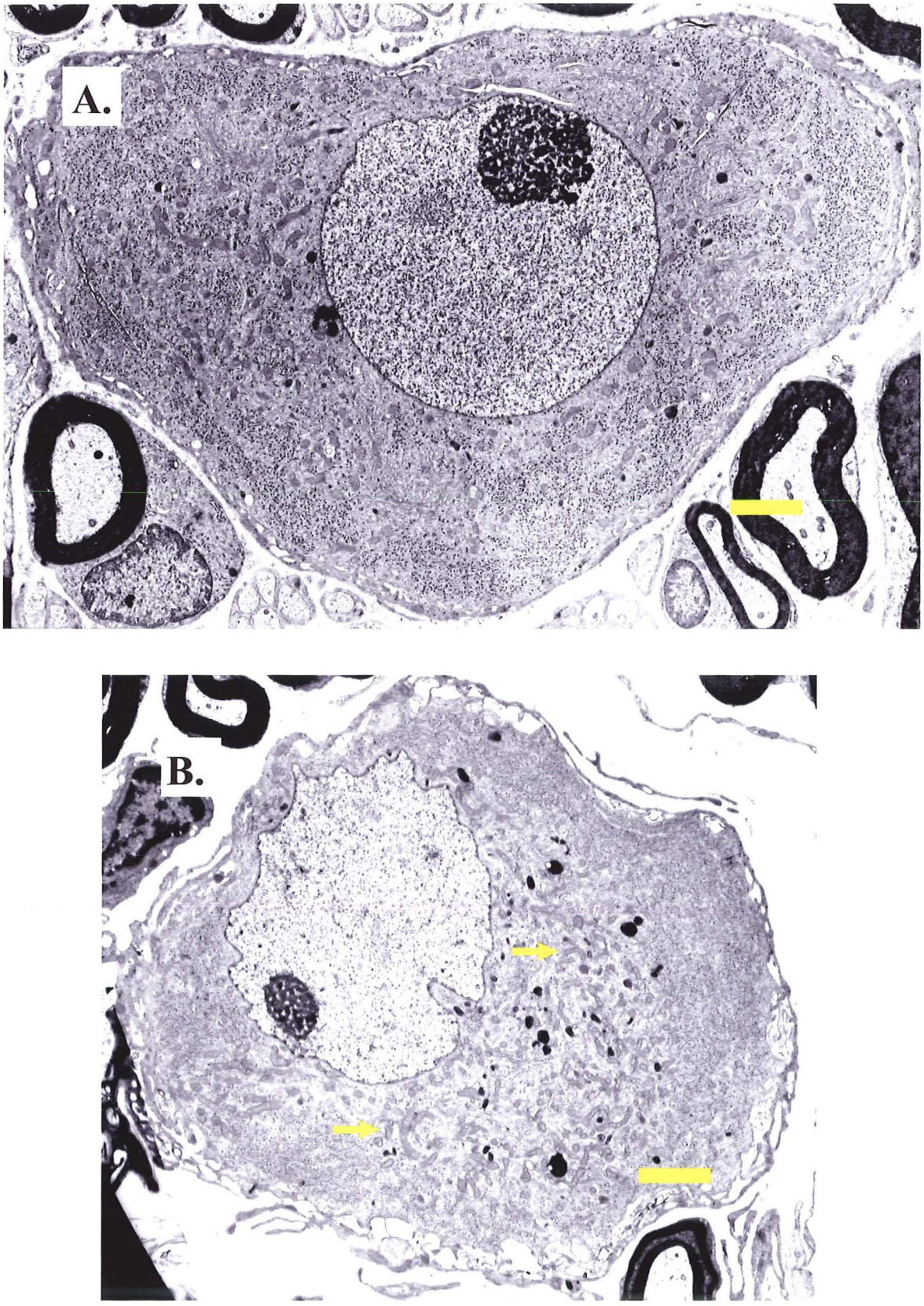

Scanning electron micrographs of primary sensory neurons in axotomised ganglia, progressive deterioration of neuronal morphology can be seen.
A. Cells initially show little morphological abnormality.
B. Chromatin condensation and nuclear irregularity and peripheralisation then occurs, although mitochondria remain generally intact (arrows). Scale bar equals 2μm.

Figure 3.2C&D: Electron Microscopy of Primary Sensory Neurons in Axotomised Ganglia

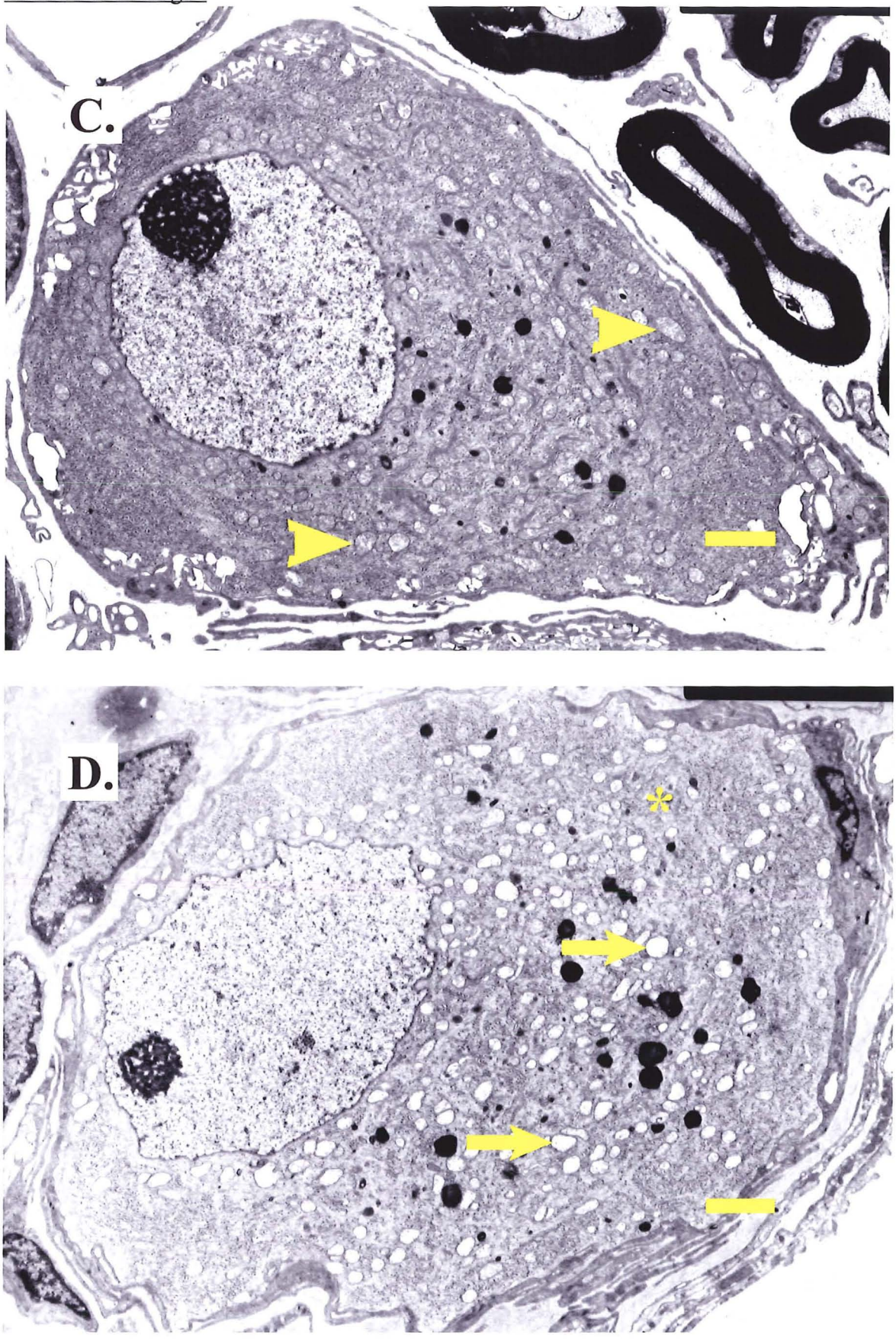

Scanning electron micrographs of primary sensory neurons in axotomised ganglia.
C. Mitochondrial swelling, and disruption of the cristae is evident (arrowheads), although the structure of the endoplasmic reticulum is maintained, and there is little nuclear abnormality.
D. Vacuolation and loss of mitochondrial structure (arrows) is accompanied by nuclear irregularity, and disruption of the endoplasmic reticulum (asterisk). Scale bar equals 2μm.

Figure 3.2E&F: Electron Microscopy of Primary Sensory Neurons in Axotomised Ganglia

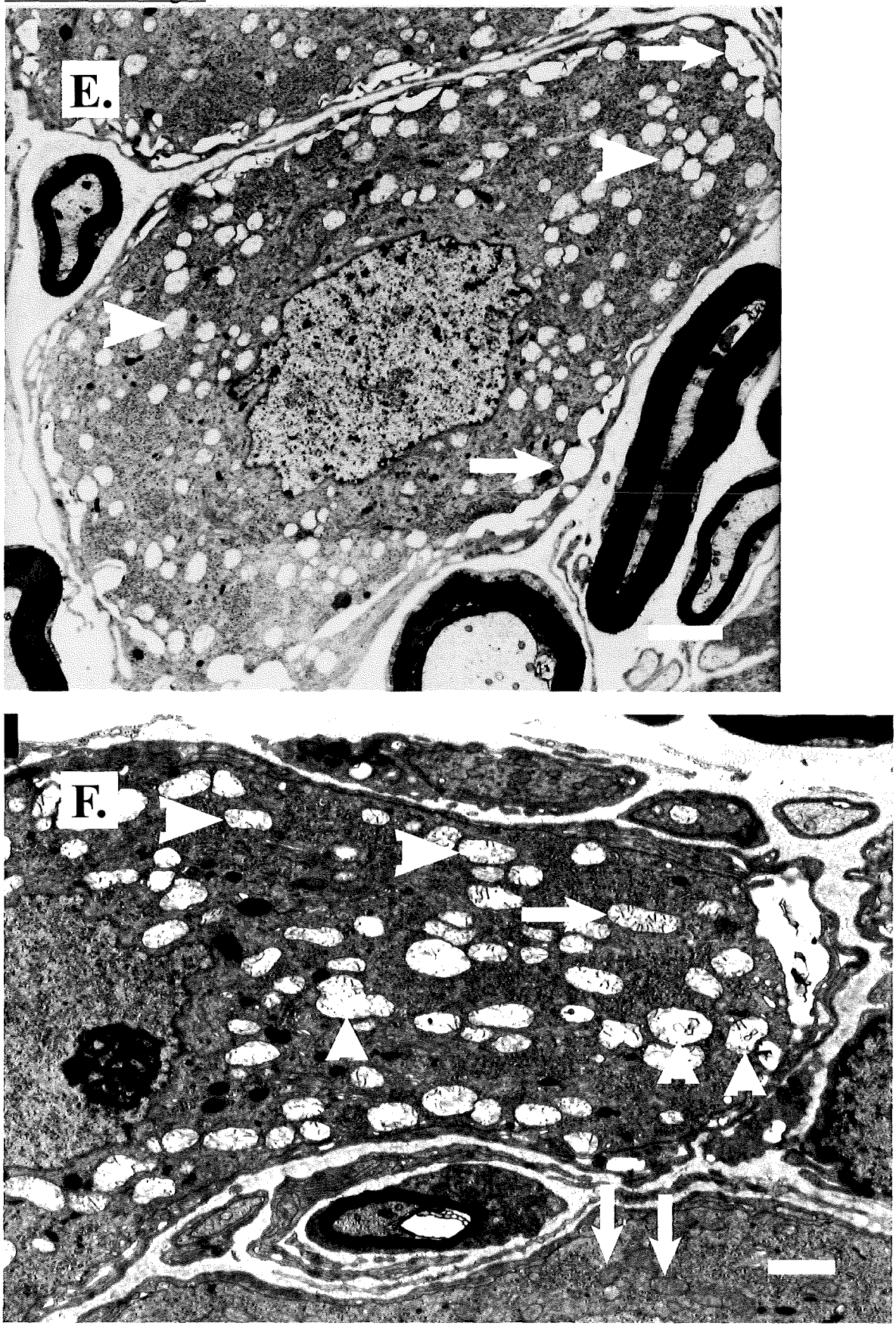

Scanning electron micrographs of primary sensory neurons in axotomised dorsal root ganglia.
E. In a dying neuron prominent nuclear irregularity, and nulcleolar fragmentation occurs in association with mitochondrial disruption, vacuolation (arrowheads), and rupture (arrows). Scale bar equals 2μm.
F. Higher power field illustrating the mitochondrial swelling (arrow), disruption of the cristae (arrowhead), and vacuolation (vertical arrowheads) that accompany nuclear eccentricity and irregularity. Normal mitochondria (inverted arrows) are seen in a neighbouring neuron that did not exhibit the morphological changes of axotomy. Scale bar equals 1μm.

3.3.2 Terminal Deoxyribonucleotidyl Transferase Uptake Nick End Labelling (TUNEL Staining)

TUNEL positive cells were found at all depths within tissue sections. The number found at each timepoint after axotomy is given in Table 3.1.

TUNEL positive neurons were only found in axotomised ganglia, and were present at all timepoints (*Figure 3.3*). The cumulative (L4 plus L5) number of TUNEL positive neurons at 1 day after axotomy was 2 cells/group, and first became significantly different from control ganglia after 1 week (15 cells/group, $p<0.05$). Numbers peaked at 25 cells/group after 2 weeks ($p<0.001$), falling thereafter to 2 cells/group at 6 months. TUNEL positive satellite cells were present at all timepoints, and were more numerous in axotomised ganglia than in control ganglia. Subtracting the mean cumulative (L4+L5) count on the control side from that of the axotomised side gave a reflection of the number of satellite cells which were TUNEL positive due the direct effect of axotomy. This count was 6.8 cells per animal at 4 days, peaked at 20.2 cells at 2 months, and was 10.7 cells at 6 months after axotomy (Table 3.1).

3.3.3 Stereology

The number of neurons surviving after axotomy is given in Table 3.2, along with the calculated percentage neuronal losses. The mean neuron count in control L4 ganglia was 13983 (SD 568) and 16285 (SD 1313) for L5. No statistically significant differences were found between control ganglia at different timepoints (*Figures 3.4-3.6*), or between sides for L4 (right 13648, SD 1633; left 14187,SD 1633) or L5 (right 16574, SD 2853; left 16112, SD 1864) ganglia.

In axotomised ganglia the magnitude of neuronal loss was greater in L5 (peak loss 7878 neurons, 43.6%) than L4 (peak loss 5024 neurons, 34.6%), however the timecourse of neuronal loss was comparable (*Figures 3.4 & 3.5*). No neuronal loss had occurred at 4 days post-axotomy, indeed counts were marginally higher in the axotomised ganglia than in the contralateral controls (hence the calculation of "negative" loss in Table 3.2). Neuronal loss (L4+L5) in axotomised ganglia was first evident at 1 week post-axotomy (14.8% compared to control ganglia, $p=0.045$), reaching 35% at 2 months ($p<0.001$). Despite the fact that loss peaked 4 months after axotomy (39.2%; Table 3.3), the percentage loss found at 4 and 6 months was not statistically different from that found 2 months after axotomy (*Figure 3.6*).

The change in the volume (V_{ref}) of the neuron containing region of ganglia which occurred both as a result of the increasing age of animals over the study period, and due to the effect of peripheral axotomy is shown in Table 3.3. Axotomy caused a significant reduction in V_{ref} (L4 plus L5) at 1 week post-axotomy (87.9% of control, $p=0.04$), which then fell to 80.8% of control by 6 months ($p<0.001$). An age related increase of 68.4% in L4 and 68.3% in L5 occurred in the neuron containing volume of control ganglia, whilst axotomised L4 and L5 ganglia both increased by only 28.0%.

Table 3.1: Timecourse of Positive TUNEL Staining in Neurons & Satellite Cells After Peripheral Axotomy

Timepoint	DRG Neurons (total count per group)				Satellite Cells (mean count per ganglion)						
	Control Ganglia	Axotomised Ganglia			Control Ganglia			Axotomised Ganglia			Axotomised - Control Ganglia
	L4+ L5	L4	L5	L4+ L5	L4	L5	L4+ L5	L4	L5	L4+ L5	L4+L5
1 day	0	1	1	2	5.5	4	10.3	5.5	4.8	10	
4days	0	5	3	8	2.2	4.3	6.5	7	6.3	13	6.8
1week	0	2	13 *	15 *	0.8 *	7.2	8	4.7	12	17 *	8.7
2weeks	0	13 *	12 *	25 **	3.5 *	7.8	11	12	11	22 *	11
1month	0	4	2	6	3	2.7	5.7	4	10	14 *	8.3
2months	0	2	3	5	20	11	31	17	34	51	20
4months	0	1	0	1	7.5	5.2	13	13	9.7	22 *	9.7
6months	0	2	0	2	5	2.3	7.3	8.2	9.8	18	11

Figures are based upon experimental groups of 6 animals at each timepoint.

* P Value <0.05 ** P Value <0.001 (compared to contralateral control ganglia).

Figure 3.3: TUNEL Positive Primary Sensory Neurons After Peripheral Axotomy

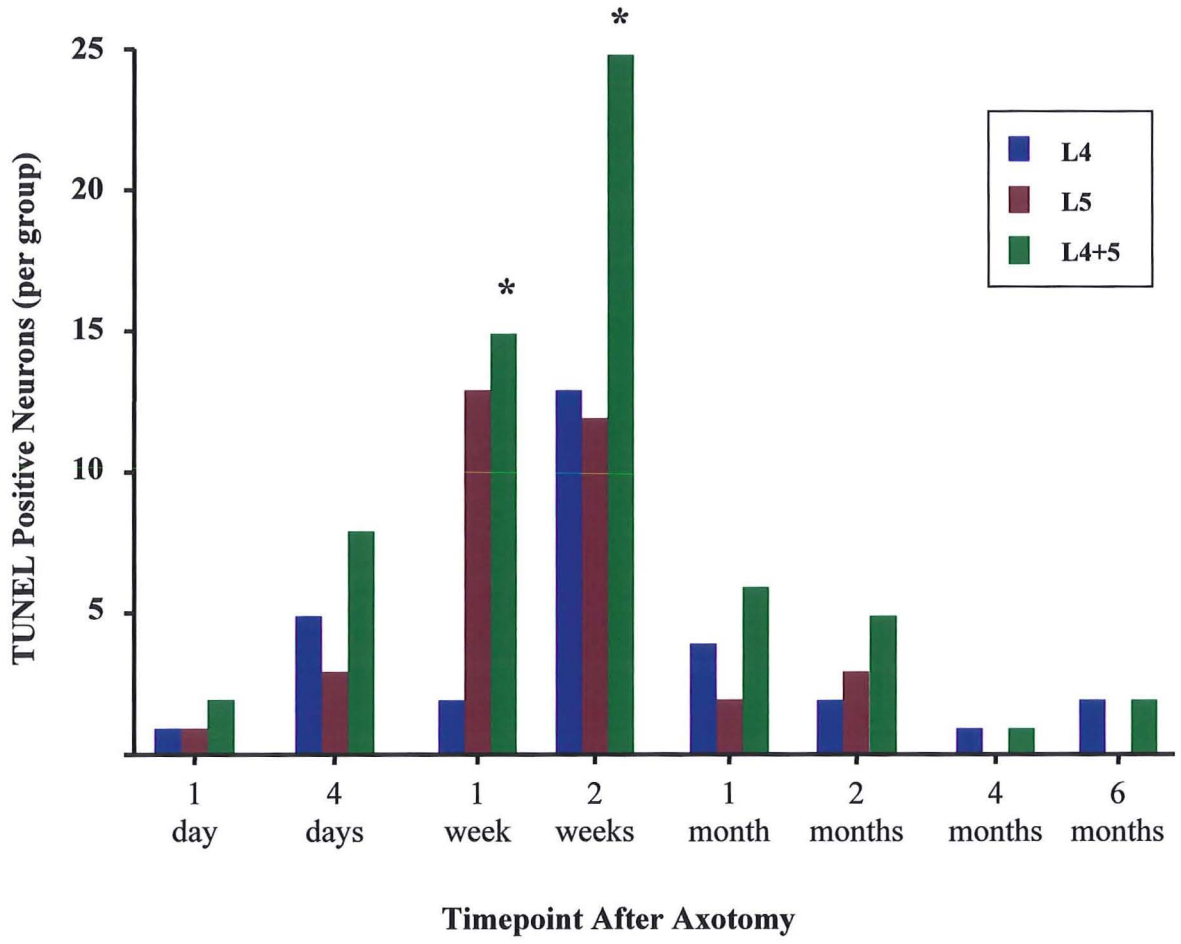

Total number of TUNEL positive neurons per group of 6 animals at each timepoint from 1 day up to 6 months after sciatic nerve transection. Counts from L4 ganglia are in blue, from L5 in brown, and the combined L4+5 count is in green. TUNEL positive neurons are present 24 hours after axotomy, numbers peak 2 weeks after axotomy, and positive neurons are still present 6 months later

(* $p<0.05$ compared to control).

Table 3.2: Change in Primary Sensory Neuron Counts After Peripheral Axotomy

Timepoint	Control Ganglia Mean (SD)			Axotomised Ganglia Mean (SD)			Percentage Neuronal Loss		
	L4	L5	L4+L5	L4	L5	L4+L5	L4	L5	L4+L5
4days	14233 (2810)	15972 (669)	30205 (1122)	15138 (4829)	16413 (1377)	31551 (3322)	-6.0%	-3.0%	-4.5%
1week	13517 (2064)	14966 (2193)	28483 (1447)	11005 (452)	13256 (939)	24261 (2352)	18.6% *	14.3%	14.8% *
2weeks	13949 (1193)	15692 (2198)	29641 (926)	11239 (1305)	12077 (1500)	23317 (876)	19.0% *	23.0% *	21.3% **
1month	14658 (1953)	14647 (948)	29305 (474)	11349 (2497)	11520 (1727)	22869 (1295)	22.6% **	25.6% **	22.0% **
2months	13948 (1007)	17597 (2524)	31545 (999)	9751 (1230)	10709 (1082)	20460 (873)	30.1% **	39.1% **	35.1% **
4months	14536 (801)	18055 (2279)	32591 (791)	9511 (655)	10315 (621)	19826 (237)	34.6% **	43.6% **	39.2% **
6months	13039 (1392)	17066 (2289)	30105 (843)	9370 (519)	10341 (1601)	19711 (711)	28.1% **	39.4% **	34.5% **

Figures are based upon experimental groups of 6 animals at each timepoint.

*P Value <0.05 **P Value <0.001 (neuron count in axotomised ganglia compared to contralateral control).

Figure 3.4 Effect of Peripheral Axotomy Upon L4 DRG Neuron Counts

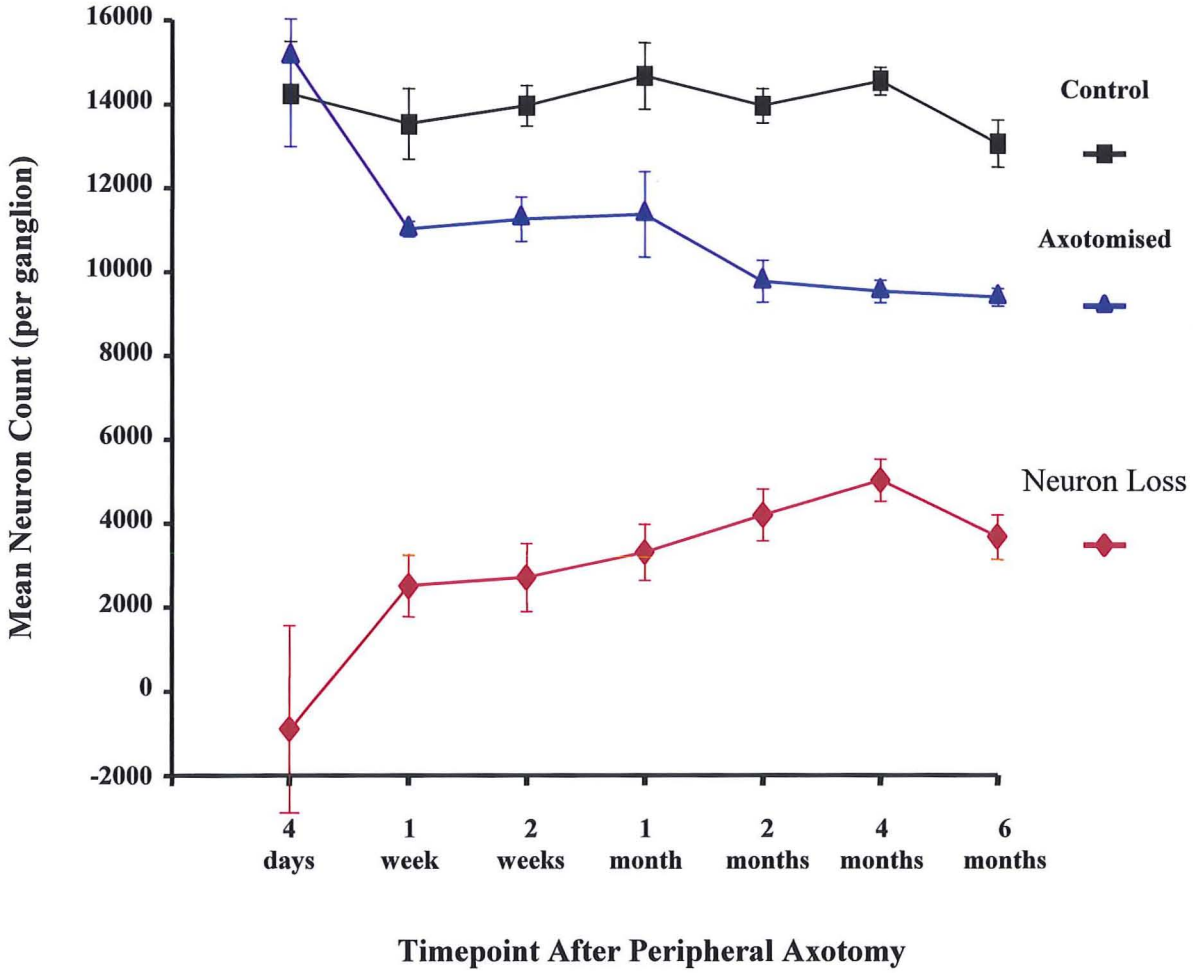

The timecourse of neuronal loss within the L4 dorsal root ganglia is shown. No loss had occurred 4 days after peripheral axotomy, however by 1 week an 18.6% loss had occurred ($p<0.05$). Loss then continued to increase until reaching 35% at 4 months after injury ($p<0.001$). The neuron loss found at 6 months was not significantly lower ($p>0.05$) than at 4 months.

Figure 3.5 Effect of Peripheral Axotomy Upon L5 DRG Neuron Counts

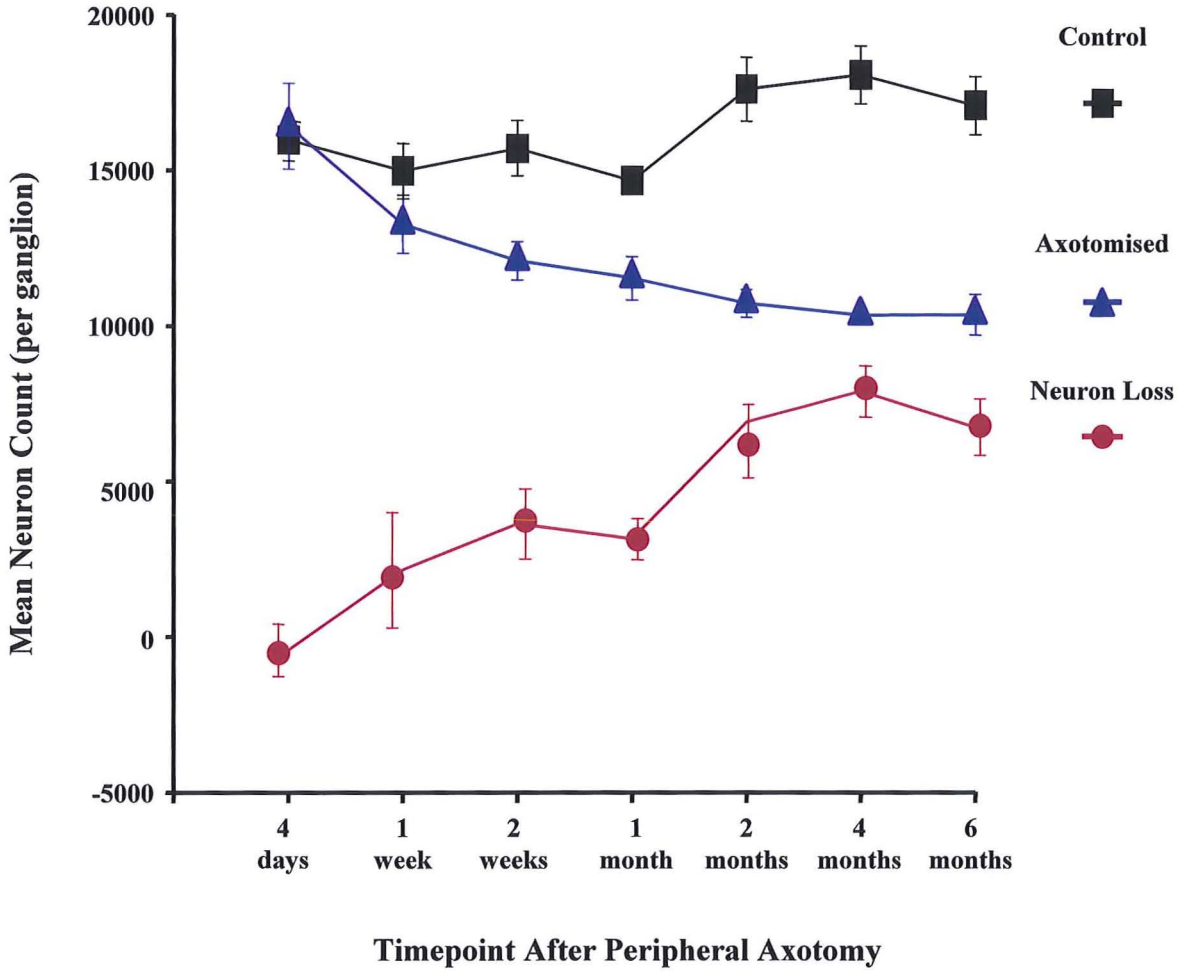

The timecourse of neuronal loss within the L5 dorsal root ganglia is shown. No loss had occurred 4 days after peripheral axotomy, however by 1 week a 14.3% loss had occurred ($p>0.05$). Loss then continued to increase until reaching 23% ($p<0.05$) at 2 weeks, and 39.1% at 2 months after injury ($p<0.001$). The neuron loss at 4, and 6 months was not significantly greater ($p>0.05$) than at 2 months.

Figure 3.6 Effect of Peripheral Axotomy Upon Cumulattive L4 + L5 DRG Neuron Counts

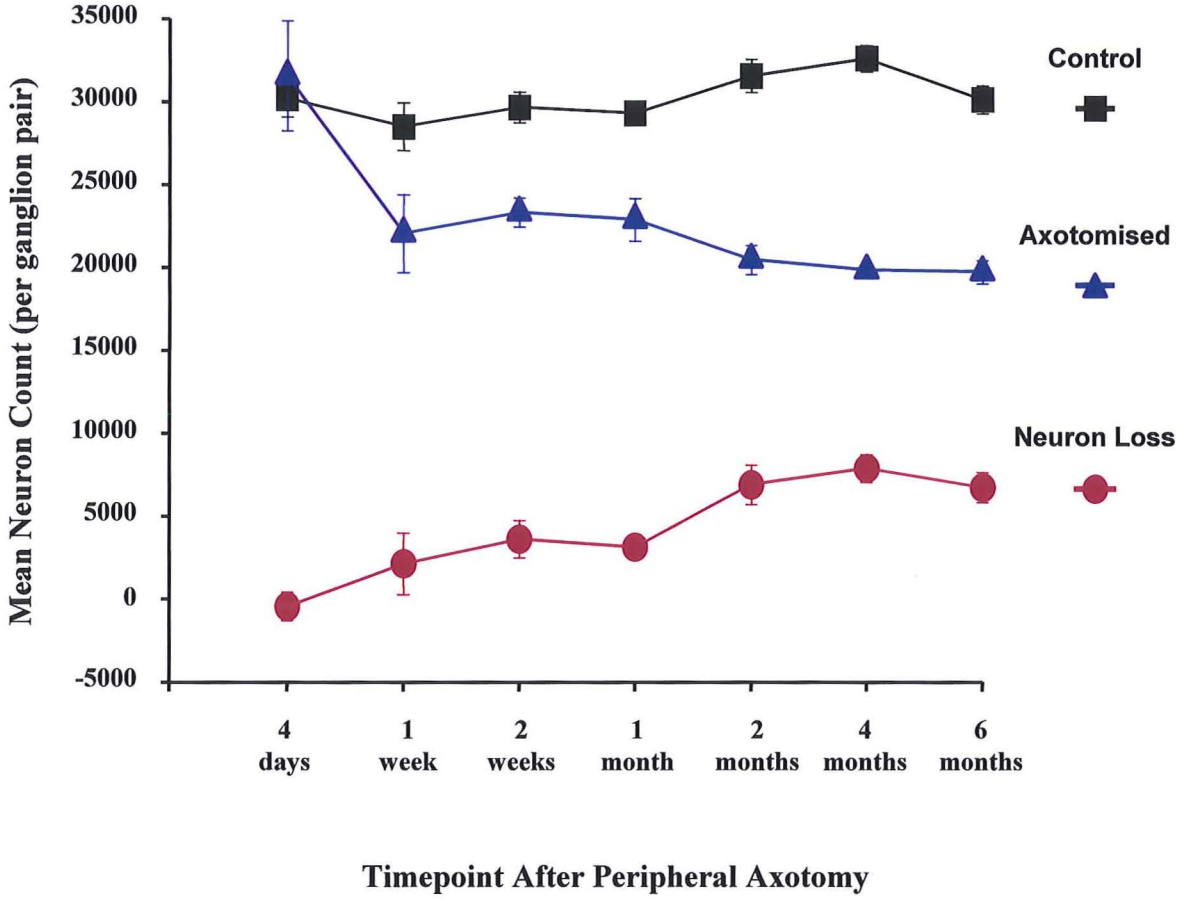

The timecourse of sensory neuronal loss after peripheral nerve injury is shown. The number of neurons present in control ganglia (black) remained constant throughout the study period at ~30,000 neurons per ganglion pair. The number of neurons in axotomised ganglia is shown in blue, and the calculated neuron loss (control – axotomised counts) is shown in brown. Four days after axotomy no neuron loss had occurred, however by 1 week after injury a 14.8% loss had occurred ($p<0.05$ compared to control). Loss then gradually increased, reaching a plateau by 2 months after injury (35% loss, $p<0.001$), and the neuron loss found at 4 & 6 months (39.2% & 34.5% respectively) was not significantly greater ($p>0.05$) than that found at 2 months.

Table 3.3: Effect of Age & Peripheral Axotomy Upon Neuron Containing Volume of Dorsal Root Ganglia

Timepoint	Age Related Increase (from 4 days post-axotomy) In Neuron Containing Volume of Ganglia				Neuron Containing Volume of Axotomised Ganglia (% of Control)		
	Control L4	Axotomised L4	Control L5	Axotomised L5	L4	L5	L4+L5
4 days					111%	105%	108%
1week	19.3% *	3.0%	35.9% *	3.7%	95%	80% *	87. 9% *
2weeks	30.1% *	-3.2%	22.7%	-2.7%	82% *	82% *	82.6% *
1month	15.0%	-11.2%	-2.3%	-26.7% *	85% *	79% *	82.2% *
2months	32.2% *	-4.6%	0.0%	-3.1% *	80% *	69% *	73.4% **
4months	63.4% **	17.3%	69.3% **	16.4% *	80% *	72% *	75.5% **
6months	68.4% *	28.0% *	68.3% **	28.0% *	82% *	80% *	80.8% **

Figures are based upon experimental groups of 6 animals at each timepoint.

*P Value <0.05, **P Value <0.001 (left hand columns compared to to volume at 4 days post-axotomy, right-hand columns compared to contralateral control).

3.4 Discussion

3.4.1 Methodology

The experimental model was standardised as far as possible, since factors such as age and the proximity of the nerve transection to the ganglia affect the DRG neuronal response to injury [256,257], and the magnitude of DRG neuronal loss [118]. All animals therefore underwent sciatic nerve division at the same age, and the level of transection was standardised against an anatomical landmark in the mid-thigh. Spontaneous regeneration of the transected sciatic nerves (which would restore distal trophic support) was prevented by ligating and capping both nerve stumps, and burying the proximal stump in an intermuscular pocket. This procedure also created significant physical barriers to the uptake by the proximal stump of distal stump derived neurotrophic factors, thereby clarifying the role of withdrawal of target organ and distal stump derived neurotrophins in determining the magnitude of neuronal death in vivo.

TUNEL was initially proposed as a specific marker for apoptosis [140], however positive staining has subsequently been found in necrosis [141,142], and in the S-Phase of mitosis [143]. Despite this, TUNEL remains a valid technique for detecting DNA fragmentation, which is the earliest irrefutable point of neuronal death. The results presented herein should therefore be interpreted as referring simply to cell death, and not specifically to apoptosis.

Methodological concerns have previously been expressed over the sensitivity of TUNEL and ISEL staining due to inadequate tissue permeabilisation by traditional enzymatic methods, such as digestion with Proteinase-K [98,139]. Microwave irradiation of tissue sections increases the efficacy of permeabilisation sufficiently to give a sensitivity of >90% with no reduction in specificity [139], and we therefore optimised a microwave permeabilisation protocol to maximise the sensitivity of TUNEL staining. Despite using thick (30μm) tissue sections, penetration of the TUNEL reagents was not impaired, since TUNEL positive cells were found at all depths within tissue sections and not just in the surface layer. The specificity of TUNEL staining was confirmed by the fact that all TUNEL positive cells exhibited abnormal nuclear morphology.

Since optical disection avoids both the statistical bias of assumption based techniques [258] and the potential underestimates inherent to the physical disector technique, due to lost caps [124,131,259], it has been proposed as the ideal technique for estimation of neuron numbers. Although the technique has been validated both theoretically, and

empirically against serial reconstruction counts of DRG neurons [125,134], accuracy is dependent upon adherence to certain rules [129]. Volume estimation by the Cavalieri Principle [130] requires the use of at least ten sections, whose thickness must be known accurately. Accordingly, section thickness was measured directly from the sections after staining, rather than assumed to be equal to that at which the sections were cut (tissue shrinkage during staining may invalidate such an assumption [135]. Adequate numbers of caps were counted (cf. *2.5.2*) to meet the requirement of 100-200 per ganglion [129], and at 28% and 19% respectively the X & Y dimensions of the disector frame employed were >4% of the X & Y step distances [135].

3.4.2 Neuron Counts

The mean neuron counts in control ganglia (L4 13983, SD 568; L5 16285, SD 1313; L4+L5 30268, SD 2548) were in agreement with other results in the literature obtained by optical [132,260,261] and physical [98] disector methods. There was no difference between the counts obtained from the left or right sides, negating concerns over other experimental models involving lesions on one side only [98].

Combined L4+5 counts have been calculated since this comprises 98.4% of the entire sciatic nerve pool [253]. Furthermore, the variance in counts from individual control ganglia is greater than that found for combined counts (coefficient of variation L4 12%, L5 14%, L4+5 8%). This suggests that biological constancy is maintained in the total number of neurons in the sciatic nerve root pool, rather than in the number of neurons present in any one ganglion. As indicators of the effect of axotomy, changes in the combined counts are therefore more sensitive than changes in counts from individual ganglia.

3.4.3 Neuronal Loss

At 39.2%, the peak neuronal loss was broadly in keeping with results in the literature [55,113,114], although smaller losses have been reported [98,107,108]. Variations may be due to different animal models, counting techniques, or levels of axotomy. Also, the procedure used to prevent spontaneous regeneration in this study may have excluded trophic support from the distal stump more completely than in other studies, resulting in greater neuronal death. One may estimate that 56-75% of the neurons that were actually axotomised died, since only 54-70% of neurons in L4 & L5 DRG's contribute axons to the sciatic nerve at the mid-thigh [108,253,262]. That neuronal loss was greater in L5 than L4 ganglia reflects the greater contribution of L5 neurons to the sciatic nerve at the mid-thigh [262].

3.4.4 Timecourse of Neuronal Death

Primary sensory neuronal death was found to commence within 24 hours of sciatic nerve transection, as shown by the presence of TUNEL positive neurons at 1 day post-axotomy. Whilst previous studies have given the exact onset of neuronal loss as being at 4 [55] to 10 [108] days, we demonstrate that statistically significant neuronal loss in fact begins at 7 days after sciatic nerve transection in the mid-thigh. The delay between the start of neuronal death, and that of neuronal loss reflects both the time taken for individual neurons to progress from DNA fragmentation to complete involution, and for the rate of death to increase sufficiently to overcome the masking effect of the normal biological variation in neuron numbers.

Neurons take a few hours to progress from DNA fragmentation, and therefore positive TUNEL staining, to eventual involution in vitro [239,263] whilst a delay of days was found to be the case in axotomised neonatal facial motoneurones in vivo [123]. In this study, at most 6 days passed between positive TUNEL staining and the occurrence of significant neuronal loss. Although cell death in the first few days may have occurred at too slow a rate to translate into significant neuronal loss, the full course of sensory neuronal death in vivo, from beginning (DNA fragmentation) to end (neuronal loss), appears to last some days.

TUNEL staining also exhibits an earlier peak (at 2 weeks post-axotomy) than neuronal loss (at 4 months post-axotomy). ISEL staining (a marker specific for single, rather than double-strand DNA breaks) was similarly found to peak at 3 weeks post-axotomy [98], although the count was only a single neuron less at 2 weeks. The peak incidence of DNA fragmentation, and so of neuronal death, therefore occurs some 2-3 weeks after peripheral nerve transection.

Neuronal loss was found to occur predominantly during the first 2 months after injury, since the losses found at 4 and 6 months were not significantly different to that found 2 months after axotomy. This is broadly in keeping with the literature although no previous study has involved sufficiently long survival times [55], and been as detailed [55,98,108].

The discrepancy between the timecourse of TUNEL staining, and that of neuronal loss reflects a difference in what each technique detects. As a marker of DNA fragmentation TUNEL staining detects the beginning of a cell's death, rather than the subsequent elimination reflected by neuronal loss. TUNEL positivity therefore precedes loss, with the number of positive neurons at any timepoint reflecting the rate of cell death, whilst neuronal loss quantifies the total number of cells which have died up until then.

It was unclear for exactly how long neuronal death continues after a peripheral nerve injury. As discussed previously, neuronal loss is a relatively crude measure of this, and various studies have not found any statistically significant increase in neuronal loss beyond 1-2 months after axotomy [55,98,108]; current results). Indeed there is a trend (not statistically significant) for neuronal loss to be less at 6 months post-axotomy than at 2 months (Groves et al., 1997 [98]; current study). However it is clear from the presence of morphologically apoptotic [98], and TUNEL positive neurons, that neuronal death does continue for at least 6 months after axotomy. Death is likely to be due to axotomy rather than old age, since control ganglia showed no evidence of neuronal death, and since L4 neuron counts at 3 months and 3 years of age in male Sprague-Dawley rats are not statistically different [260]. In the cat however, neuronal loss may continue up to 18 months post-axotomy [264], although this result was obtained using assumption-based counting techniques and may not be entirely accurate as a result.

It is the large discrepancy between the number of TUNEL positive neurons found, and the magnitude of neuronal loss that remains to be adequately explained. The number of TUNEL positive neurons found in this study was low (although greater than in other studies), yet this was unlikely to be due to inadequate permeabilisation since microwave irradiation was used, as discussed previously. It is not clear from the literature for how long a dying cell will stain positively with TUNEL in vivo, although estimates range from as little as 2-5 minutes [139]. In Gavrieli's original description cells are described as being TUNEL positive before they are morphologically apoptotic [139], and it is likely that cells are potentially TUNEL positive for only a few hours before condensation into nucleosomes masks the DNA fragments [122]. This condensation precedes the more advanced morphological features of apoptosis, and indeed whilst positive ISEL staining of neurons peaks at 3 weeks post-axotomy, numbers of morphologically apoptotic neurons are still increasing at 4 weeks [98]. This brief time window for staining is therefore the most likely explanation for the discrepancy between the small number of TUNEL positive neurons, and the large number lost. Additionally, some neuronal death may occur without any potentially stainable DNA strand breakage, as has been demonstrated in other cell types [146].

3.4.5 Mechanism of Neuronal Death

Electron microscopy (EM) revealed a similar pattern of morphological findings to those previously described for axotomised or dying neurons [56,98,146,265], with a mixture of apoptotic and other features (cf. *3.3.1b*). Although a more extensive study would be

required in order to attempt an accurate morphological consideration of the mode of death [265], the relationship between neuronal death and mitochondrial accumulation, swelling and disruption was highlighted. This has previously been shown in retrogradely degenerating neurons of the dorsal lateral geniculate nucleus [53], but has not been specifically demonstrated in axotomised primary sensory neurons.

TUNEL positive neurons exhibiting no abnormalities of cytoplasmic morphology were found at the light microscopic level, and may represent apoptotic cells caught just prior to the development of visible morphological features [143,155]. Many neurons did display cytoplasmic granulation, vacuolation, pyknosis and membrane irregularities in keeping with apoptosis, however the morphological findings were not all classically apoptotic, and these limited findings may therefore add to the current debate over the precise morphological pattern of neuronal death.

The grossly dilated and vacuolated cells which were predominantly found in axotomised ganglia have been previously described [57], and demonstrated to be large, GAP-43 positive, myelinated neurons containing proteinaceous material [56]. Since none of the neurons were ISEL positive [56] the features were ascribed to regeneration rather than cell death. However our finding of two TUNEL positive neurons may mean that such dilation is in fact a morphological feature of post-axotomy adult primary sensory neuronal death. The previous failure to demonstrate DNA fragmentation could merely be a result of the small number of such neurons, and the small percentage of dying neurons detected by DNA fragment labelling. Furthermore, the number of such cells present closely matches the timecourse of neuronal loss, and is reduced by NT3 administration [56], which might be expected to increase regeneration [47]. Recent electron microscopical studies reviewed by Clarke [146] have cast doubt upon the classical apoptotic description of adult neuronal death, and his Type 3B ("cytoplasmic") cell death has morphological features similar to those found here. Apoptosis has been discounted as the mechanism in other forms of adult neuronal death [266], and it may be the case therefore that the dilated vacuolated morphology is another pattern of death in myelinated primary sensory neurons.

3.4.6 Effect of Axotomy Upon Ganglion Volume

The 27% rise in control L4 dorsal root ganglion volume between 2 and 6 months of age matches the previously described 28% increase in volume from 3 to 30 months of age [260], since ganglion volume reached its maximum by 4 months of age in this study (Table 3.3). A 68% increase in volume was found in both L4 and L5 control ganglia over the first 6 months of life, however in axotomised ganglia volume increased by only half as much

(28%), presumably reflecting their reduced cellularity. Axotomy caused a volume reduction in both L4 and L5 ganglia when compared to controls that commenced 1 week after axotomy and plateaued after 2 months. Axotomised ganglia were not only smaller than controls, they also shrank from their baseline volume (before neuronal loss commenced 4 days after axotomy), and did not begin to exhibit the normal age related increase in ganglion volume until after the main period of neuronal death had finished (i.e. after 2 months post-axotomy). Loss of volume may therefore reflect the actual loss of cells, but since it was of a lesser magnitude than neuronal loss it must also reflect the reduction in volume of surviving neurons [55]. This implies that as neurons die the spatial relationship of surviving cells is altered, which may have implications for local neuron-glia interactions, and for local concentrations of trophic factors.

3.4.7 Axotomy Induced Satellite Cell Death

ISEL positive satellite cells have previously been noted [98] in control and axotomised ganglia, however the timecourse of cell death was not reported. TUNEL positive satellite cells were consistently found within axotomised ganglia, and showed a definite temporal relationship to sciatic nerve division with a peak 2 months after axotomy. In this adult study the TUNEL positive neuronal peak preceded the satellite cell peak by 6 weeks, as opposed to 3 days in neonates [100], implying a difference in the precise relationship. Delayed oligodendrocyte death after optic nerve [121], and spinal cord injury [138] has been noted in adults, where it was thought to be due to axonal degeneration, and was implicated in demyelination of surviving axons, and expansion of the cord lesion. The presence of TUNEL positive satellite cells in control ganglia may represent constant physiological turnover in this potentially labile cell population, although the marked increase in the number of positive cells 2 months after axotomy suggests a direct effect of contralateral axotomy, perhaps mediated by degeneration of neurites in crossed tracts. These facts imply that adult primary sensory neuronal death induces delayed secondary death of satellite cells, perhaps mediated by trophic interdependence mechanisms or neurotoxic cytokines. The significance of satellite cell death is unclear, however it merits further investigation given the key role which satellite cells play in maintaining the neuronal capacity to resist oxidative stress and cell death.

3.4.8 Conclusions

These results therefore offer a logical time-structure for in vivo experiments on primary sensory neuronal death, and for testing any potential therapies to prevent neuronal death. The secondary satellite cell death described remains to be fully characterised, as do

the precise mechanisms of neuronal death, and the features that differentiate the neurons which survive from those that die.

Chapter 4. The Effect of Peripheral Nerve Repair Upon Axotomy Induced Sensory Neuronal Death

4.1 Introduction

As previously discussed (cf. *Chapter 2*), it is likely that the single most important determinant of the poor sensory outcome after peripheral nerve injury is the death of a substantial proportion of the primary sensory neurons in the injured nerve's sensory neuronal pool (cf. *3.4.3*). Reducing this neuronal death ought therefore to improve outcome. Surgical repair is the standard treatment for peripheral nerve injuries, yet despite the known protective effects of exogenous neurotrophic factors [47,105,109,217], the effect of nerve repair (which restores trophic support from the distal stump [17]) upon sensory neuronal death is not clear. Nor is it known whether the timing of the nerve repair after injury affects the extent of neuronal death.

Sensory neuronal death after crush injuries (axonometsis) is markedly less than that found after nerve transections (neurometsis) [107,116], yet in both cases neurons are peripherally axotomised. The principal difference is that with a crush injury the connective tissue structure of the nerve remains intact, and so the axon stumps therefore remain in contact with the distal segment of the nerve which produces the neurotrophic factors that are so essential for neuronal survival [17]. By reapproximating the proximal and distal nerve stumps, surgical repair of a transected nerve may result in a situation more akin to a crush injury and so have a protective effect against sensory neuronal death [116,117]. If this were the case, then one would expect that the earlier the nerve is repaired the greater the protective benefit would be.

The importance of the timing of peripheral nerve repair upon neuronal death is also of great clinical importance, since it would affect not only the planning of elective nerve repairs (as in brachial plexus injuries), but potentially influence the way in which trauma surgery services are structured. Currently, peripheral nerve repairs are not generally considered to require immediate repair, and cases are frequently postponed for some days due to lack of theatre availability. If the timing of nerve repair were to determine the magnitude of sensory neuronal death, and so the potential for the return of normal sensation, then the current situation would be unacceptable and a restructuring to allow patients more rapid access to surgical nerve repair would become necessary.

This study therefore aimed to establish, in principle, whether or not the timing of nerve repair does affect the magnitude of sensory neuronal death occurring after a peripheral nerve transection, as determined by TUNEL, and stereological neuron counts.

4.2 Methods

In two groups of young adult male Sprague-Dawley rats (n=6 per group) a unilateral sciatic nerve transection was performed, and the nerve was then repaired by epineurial suture coaptation either immediately (cf. *2.2.5*), or following a 1 week delay (cf. *2.2.6*). The animals were terminated (cf. *2.3.1*) and the L4 & 5 dorsal root ganglia (DRG) harvested (cf. *2.3.2*), 2 weeks after the initial nerve transection. The ganglia were processed (cf. *2.4.1a, 2.4.2a & 2.4.3*) for quantification of neuronal death by TUNEL (cf. *2.5.1*), and by stereological determination of the number of sensory neurons using the optical disector technique (cf. *2.5.2*).

A control group, whose nerves were not repaired, was provided by a group of animals whose ganglia were harvested 2 weeks after sciatic nerve transection, as described in the previous chapter (cf. *Chapter 3*).

4.3 Results

The timing of peripheral nerve repair affected the number of TUNEL positive neurons present in axotomised DRG's, as is displayed in Table 4.1, and *Figure 4.1*. Contralateral control ganglia did not contain any TUNEL positive neurons, and the number present in axotomised L4+5 ganglia 2 weeks after axotomy was 25cells/group ($p<0.001$ compared to contralateral control ganglia) when the sciatic nerve was not repaired. This count was almost halved when the nerve was repaired after a 1 week delay (14cells/group, $p=0.016$ vs. contralateral control ganglia), and immediate nerve repair resulted in an even greater reduction in the number of TUNEL positive neurons, to 11 cells/group ($p=0.002$ vs. control ganglia), which reached statistical significance ($p<0.05$ vs. no repair). The difference between the counts obtained after immediate and delayed repair was not statistically significant however.

A similar pattern was found when the number of dying neurons (neuronal loss) was quantified. In the group whose sciatic nerves were not repaired 21.3% of all L4+5 DRG neurons had died (6324 neurons, $p<0.001$ compared to contralateral control ganglia) within 2 weeks of nerve transection (Table 4.1, *Figure 4.1*). Neuronal loss was reduced after nerve repair, being 12.4% (2450 neurons, $p>0.05$ vs. control ganglia) in the group whose nerves were repaired after a 1 week delay, and 4.80% (1236 neurons, $p>0.05$ vs. control

Table 4.1: Effect of the Timing of Nerve Repair Upon Sensory Neuronal Death

	No Nerve Repair	Delayed Nerve Repair	Immediate Nerve Repair
Mean Neuronal Loss L4+L5Combined	6324 **	2450	1236
TUNEL Positive Neuron Count (per Group) L4+5 Combined	25 **	14 *	11 *

Figures are based upon experimental groups of 6 animals at each timepoint.

*P Value <0.05, **P Value <0.001 (compared to contralateral control).

Figure 4.1: Effect of the Timing of Nerve Repair Upon Sensory Neuronal Death

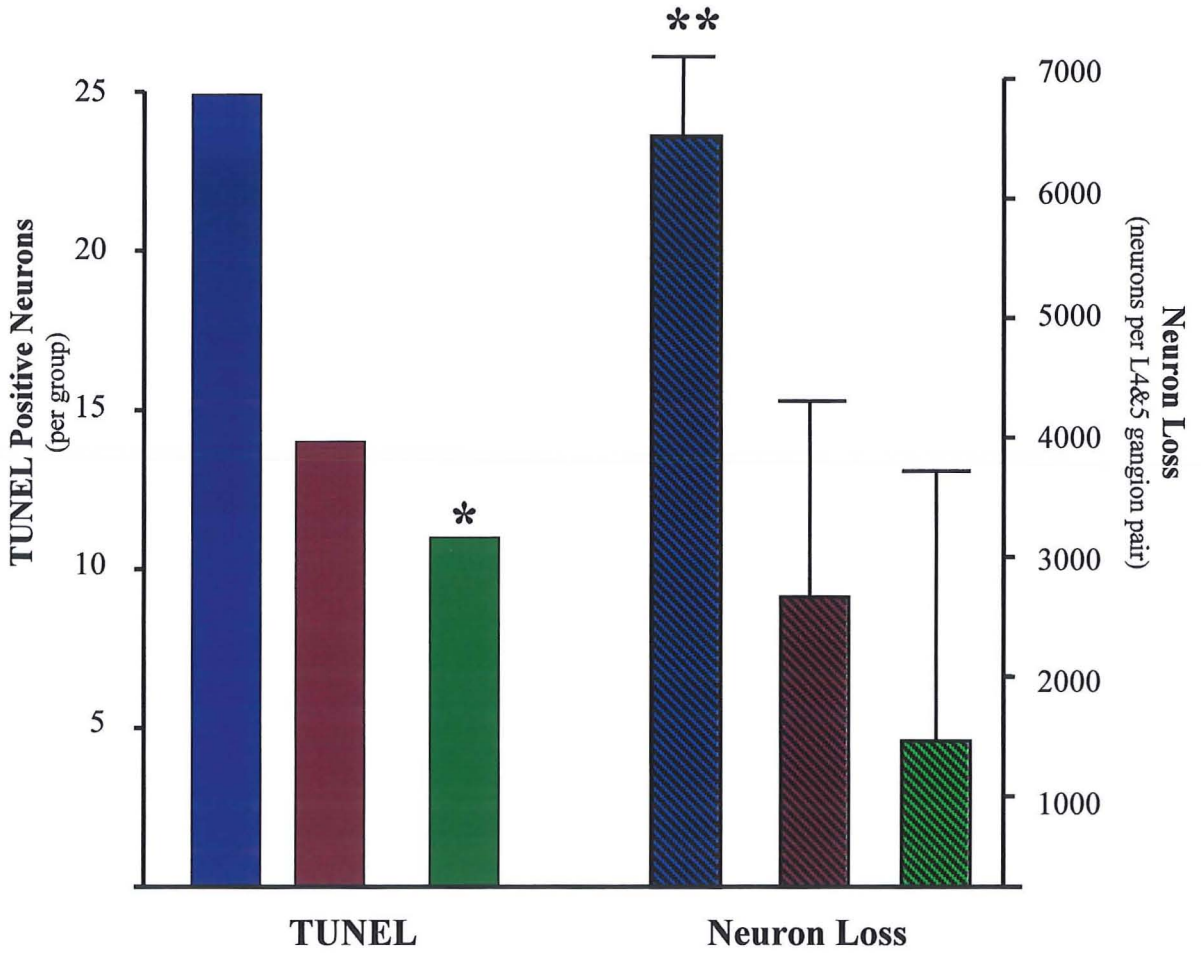

Both the number of TUNEL positive neurons (plain bars), and the neuron loss (hatched bars) found 2 weeks after sciatic nerve transection are reduced by peripheral nerve repair. Immediate repair (green) is more protective than repair after a 1 week delay (pink), when to compared to nerves which were not repaired (blue).

(* p<0.05 compared to no nerve repair; ** p<0.001 compared to contralateral control ganglia).

ganglia) after immediate nerve repair. However the effect upon neuronal loss was not statistically significant.

4.4 Discussion

4.4.1 Methodology

In order to limit confounding factors such as the proximity of the nerve transection to the ganglia, the experimental model was standardised as far as possible (cf. *3.4.1*), and the nerve repairs were performed using standard clinical techniques in order to maximise the clinical applicability of the results. The merits of TUNEL as a marker of neuronal death, particularly when combined with microwave tissue permeabilisation have been discussed previously, as have the benefits of optical disection in producing statistically unbiased neuron counts for the calculation of neuronal loss (cf. *3.4.1*).

DRG's were harvested 2 weeks after transection of the sciatic nerve, since this was when neuronal death peaked in animals whose nerves were not repaired (cf. *3.4.4*), and was the earliest timepoint at which neuronal loss was highly statistically significant ($p<0.001$). Cumulative results for L4 & L5 ganglia were also used to maximise the sensitivity of the experiment in detecting any effect upon the death of sensory neurons in the sciatic nerve pool (cf. *3.4.1*). This is also the reason that a mid-thigh lesion was employed, rather than a more distal lesion comparable to the more common clinical injuries to the median or ulnar nerves at the wrist, or to digital nerve injuries. By using a lesion that induces a greater magnitude of neuronal death [17], the chance of detecting a protective effect against neuronal loss is enhanced. Results still ought to be directly applicable to distal nerve injuries, since the lesser magnitude of neuronal loss found with these injuries [118] probably reflects the smaller number of neurons which are actually axotomised, and the response of neurons which are actually injured may remain constant [267] (cf. *1.4*).

4.4.2 Nerve Repair Reduces Primary Sensory Neuronal Death

Nerve repair, and its timing, was found to reduce sensory neuronal death. The number of TUNEL positive neurons present 2 weeks after axotomy was almost halved by repair after a one week delay, and was further reduced after immediate nerve repair, an effect which reached statistical significance ($p<0.05$). The same pattern was found for neuronal loss; 21.3% of all L4 & L5 DRG neurons had died two weeks after transection of the sciatic nerve, yet when the nerve was repaired after a one week delay this loss was halved, to 12.4%. Neuronal loss was further halved after immediate repair, to 4.8%,

thereby demonstrating the protective effect of early nerve repair. During the first week after sciatic nerve transection 14.8% of neurons die (Table 3.2), so the fact that the loss found in the delayed repair group one week later (2 weeks after nerve injury) was no greater would further suggest that surgical nerve repair is indeed highly neuroprotective.

The fact that the differences in neuronal loss between groups with or without nerve repair were not statistically different is most probably due to the fact that 2 weeks is not long enough to develop a difference of the magnitude required for statistical differentiation. Additionally, the fact that the difference between the neuron counts obtained from axotomised, and control ganglia was highly statistically significant ($p<0.001$) when the sciatic nerve was not repaired, but did not reach statistical significance in either of the nerve repair groups suggests that the effect of nerve repair upon neuronal loss was real.

Peripheral crush injuries do not involve physical disruption of the nerve trunk and cause less neuronal death than transections [107,116], whilst immediate nerve repair reduces sensory neuronal death to the same level as that found after a crush injury at the same site [107]. It would therefore seem likely that although the mechanism by which nerve repair reduced neuronal death remains to be clarified, restoration of physical continuity between the proximal and distal nerve stumps is likely to be involved.

The reduction in neuronal death is unlikely to be due to a reduction in the local production of neurotoxic inflammatory cytokines or antidromic electrical activity by the distal stump, since delayed repair was protective despite potentially involving additional trauma to the nerve during the second procedure. The most likely explanation for the reduction in sensory neuronal death is therefore that by repairing the nerve the axons in the proximal stump are brought into close proximity with the distal stump, whose Schwann cells are the principal source of neurotrophic factors after nerve injury [17,90]. Further confirmation of this has come from subsequent experiments in our laboratory in which a primary 1cm gap repair was performed using either an acellular bioresorbable conduit, or one containing cultured autologous Schwann cells. Whilst sensory neuronal death was not affected by repair with an acellular conduit, a substantial reduction in neuronal death occurred after repair with a conduit containing Schwann cells.

4.4.3 Conclusions

These results therefore give further support to the hypothesis that loss of distal stump neurotrophic support is the major factor determining the magnitude of neuronal death after peripheral axotomy, however the clinical implications of this study are more

profound. It would appear that surgical nerve repair does reduce sensory neuronal death after peripheral nerve injury, and that the earlier the repair is performed, the greater the protective effect. This has obvious clinical importance for both elective and emergency nerve surgery, since it would seem that sensory outcome might be improved by repairing the nerve as soon after injury as is clinically feasible.

Further work is required to establish whether nerve repair is equally protective in more distal nerve injuries, and to define the maximum acceptable delay between injury and performing nerve repair. However from the results of the timecourse study (cf. *Chapter 3*) it is clear that neurons begin to die within 1 day of peripheral nerve injury, so that it would seem inadvisable to delay repair even by 24 hours where there is no contraindication to primary repair. Equally it would seem advisable to perform early secondary nerve repairs within two weeks of injury, as that is when neuronal death reaches a peak, and to perform late secondary nerve repairs within two months of injury since neuronal loss is virtually complete by this timepoint (cf. *3.4.4*).

Chapter 5. Therapeutic Potential of N-acetyl-cysteine in Peripheral Nerve Trauma

5.1 Introduction

Sensory neuronal death is probably the single most important factor determining the poor sensory outcome of peripheral nerve injuries (cf. *1.1*), and yet no therapies are currently clinically available that reduce it. Despite the reduction in neuronal death achieved by immediate nerve repair (cf. *4.4.2*) there is still a need for an adjuvant therapy, since immediate nerve repair did not eliminate neuronal death, nor is it likely to be clinically feasible for the majority of patients (cf. *1.6*). Although the administration of exogenous neurotrophic factors (NTF's) is neuroprotective after experimental peripheral and central nervous system lesions [17,105,106,214,215], their immediate clinical applicability remains doubtful (cf. *1.6*).

In contrast to the specificity of neurotrophic factors [47], there appears to be relative homogeneity in the way that the initiation of neuronal death is signalled and then effected in different subpopulations [103,166] (cf. *1.5*). A therapeutic agent acting at this level of the cell death process therefore ought to be protective for a wide range of neuron subtypes against a wide range of stimuli. As described previously (cf. *1.6*), the apparent role of reactive oxygen species generation in neuronal death (cf. *1.5*) makes N-acetyl-cysteine, and other antioxidants potentially attractive as clinically applicable neuroprotective agents [268] after ischaemia reperfusion or trauma [269]. The additional roles of abortive entry into the cell cycle, and glutathione dependent nitric oxide mediated mitochondrial bioenergetic dysfunction (cf. *1.5*) makes N-acetyl-cysteine particularly attractive (cf. *1.6*) since it not only has direct antioxidant properties, but may also affect regulation of the cell cycle, and is a glutathione substrate.

NAC is currently in clinical use as a mucolytic agent in respiratory disease and as a treatment for paracetamol (acetominophen) poisoning [241], where it acts to maintain glutathione levels in hepatocytes. Glutathione acts a free radical scavenger in neurons [270], it helps maintain mitochondrial oxidative metabolism by protecting the cytochrome oxidase complex I from NO mediated damage [199], and improves neuronal survival in response to a range of insults in vitro [197,242,243]. By acting as a cysteine donor NAC maintains intracellular glutathione levels [191], and is neuroprotective for a range of neuronal cell types against a variety of stimuli in vitro [160,206,271-273]. NAC may therefore reduce neuronal death

by blocking attempted entry into the cell cycle, and by improving the capacity to maintain redox balance, and normal mitochondrial function.

Similarities exist between the mechanisms underlying post-axotomy neuronal death throughout the entire nervous system, both peripheral and central [166], and as a result, any intervention that reduces primary sensory neuronal death may also have therapeutic implications for the management of brain, and spinal cord trauma. This study therefore investigated the effect of systemic NAC treatment upon primary sensory neuronal death after peripheral nerve injury with the aim of determining its potential for therapeutic use in clinical practice. A combination of TUNEL staining, and neuron counting by the optical disector technique was used to assess the effect of treatment upon neuronal survival (cf. *1.4*).

5.2 Methods

Groups of young adult male Sprague-Dawley rats (n=6) underwent unilateral sciatic nerve division (cf. *2.2.2*), and immediately after nerve transection parenteral treatment with N-acetyl-cysteine (NAC) was commenced at either 150mg/kg/day ("high-dose"), or 30mg/kg/day ("low-dose") as detailed in section *2.2.4*. Another experimental group ("sham treatment") received an identical volume of 5% dextrose solution (cf. *2.2.4*), and all animals were dosed until termination (cf. *1.2.1b*). Two further control groups were provided by the animals whose DRG's were harvested 2 and 4 months after sciatic nerve transection in the timecourse study (cf. *Chapter 4*).

The L4 & L5 DRG's were harvested from both the axotomised, and contralateral control sides (cf. *2.3.2*) at either 2 weeks (all treatment groups), or 2 months (one "high-dose treatment", and one "no treatment" group) after sciatic nerve transection (cf. *2.2.4*). The ganglia were then processed (cf. *2.4.1a, 2.4.2a & 2.4.3*) for quantification of neuronal death by TUNEL (cf. *2.5.1*), and by stereological determination of the number of surviving neurons using the optical disector technique (cf. *2.5.2*). The mean cap count was 152 (SD25.6) per ganglion, in keeping with the requirement to count between 100 and 200, and all sampling other parameters were the same as discussed previously (cf. *3.2, 2.5.1. & 2.5.2*).

5.3 Results

No adverse effects upon animal behaviour were found, and weight gain during the study period was not significantly affected at either 2 weeks (p=0.87) or 2 months (p=0.30) by NAC treatment.

5.3.1 Morphology

When compared to normal ganglia (*Figure 5.1A*), prominent morphological changes were present in the axotomised ganglia of untreated animals, with the majority of neurons exhibiting nuclear eccentricity, and chromatolysis (*Figure 5.1B*). Neurons displaying features of apoptosis (cytoplasmic granulation, vacuolation, membrane irregularities) were seen, as were numerous enlarged, and grossly vacuolated neurons. Although the morphological findings were unchanged by sham treatment with 5% dextrose solution (*Figure 5.1C*), NAC caused a qualitative improvement in neuronal morphology, which was more pronounced after high-dose NAC treatment (*Figure 5.1E*) than after low-dose treatment (*Figure 5.1D*).

5.3.2 TUNEL Staining

The effect of NAC treatment upon the number of TUNEL positive neurons, and the neuronal loss found 2 weeks after axotomy is summarised in Table 5.1, whilst Table 5.2 gives the equivalent findings 2 months after axotomy.

TUNEL positive neurons were only found in axotomised ganglia, and all exhibited nuclear morphological features of cell death (chromatin condensation, and nuclear irregularity, or fragmentation). These neurons displayed a similar range of cytoplasmic morphologies to those described in chapter *3.3.1a* (*Figure 3.1*). Two weeks after sciatic nerve transection the total number of TUNEL positive neurons present in the axotomised L4&5 ganglia of untreated animals was 25 neurons per group of 6 animals, and sham treatment had no significant effect (19 neurons/group, p=0.405). Treatment with NAC at both the low (7 neurons/group), and high (2 neurons/group) doses used did however cause a reduction in the number of TUNEL positive neurons, when compared to either sham treatment (low-dose p=0.065; high-dose p=0.003), or no treatment (low-dose p=0.015; high-dose p=0.002). The number of TUNEL positive neurons found in axotomised ganglia 2 months after axotomy was also reduced by high-dose NAC treatment (Table 5.2).

Figure 5.1: Effect of N-acetyl-cysteine (NAC) Treatment Upon Primary Sensory Neuronal Morphology After Sciatic Nerve Transection

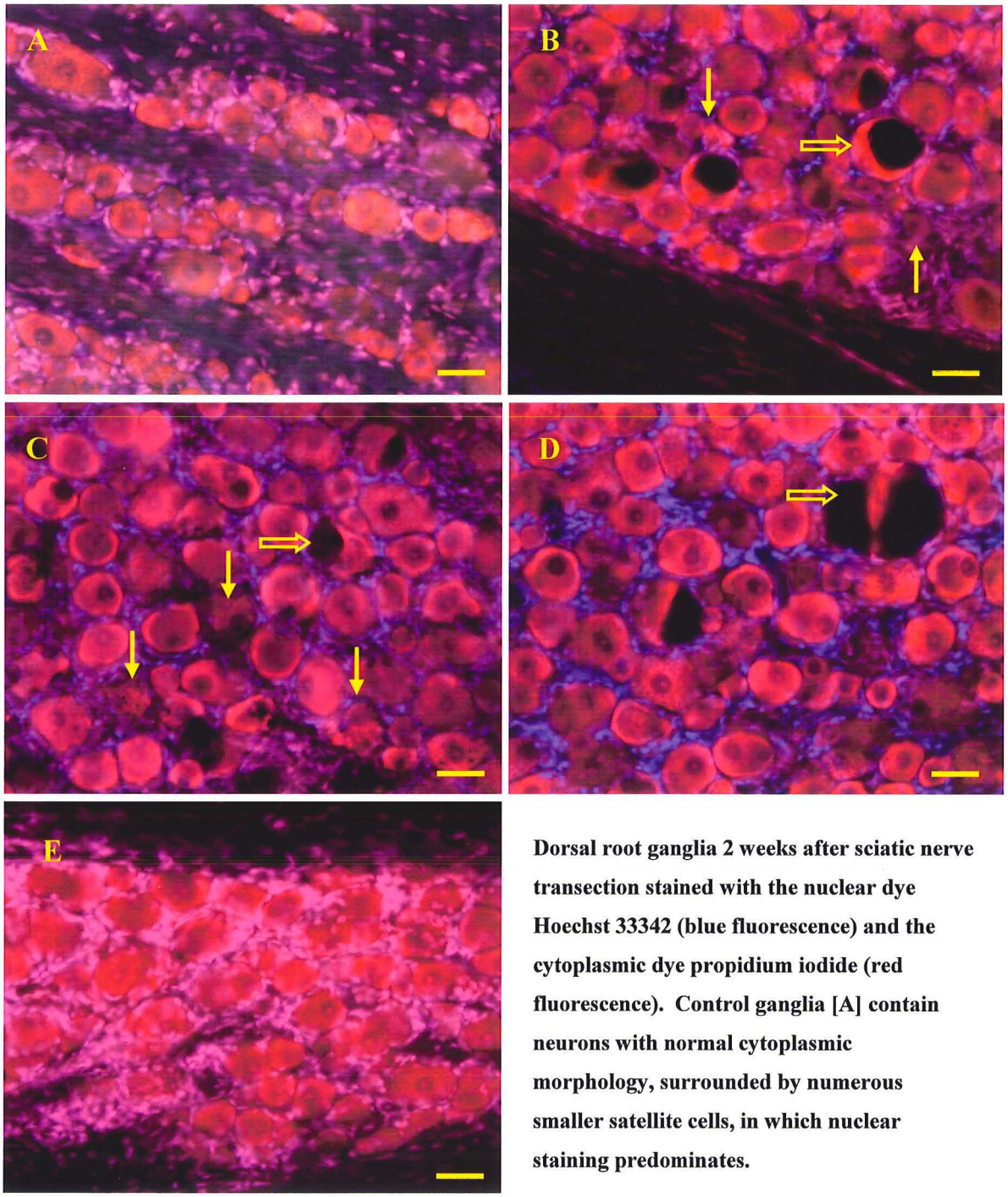

Dorsal root ganglia 2 weeks after sciatic nerve transection stained with the nuclear dye Hoechst 33342 (blue fluorescence) and the cytoplasmic dye propidium iodide (red fluorescence). Control ganglia [A] contain neurons with normal cytoplasmic morphology, surrounded by numerous smaller satellite cells, in which nuclear staining predominates.

Two weeks after sciatic nerve transection [B] gross morphological changes are evident, with most neurons displaying nuclear eccentricity, membrane irregularities, and cytoplasmic granulation or vacuolation (hollow arrow). Apoptotic neurons are also evident (solid arrow). Morphology was not affected by injections of sterile 5% glucose (sham treatment) [C], and was only slightly improved after low-dose NAC treatment [D]. After high-dose NAC treatment neuronal morphology is significantly more normal [E]. Scale bar equals 40µm.

Table 5.1: Effect of N-acetyl-cysteine (NAC) Treatment Upon Sensory Neuronal Death 2 Weeks After Axotomy

Treatment Group	Control Ganglia (L4+5) Mean (SD)		Axotomised Ganglia (L4+5) Mean (SD)		Percentage Neuronal Loss (L4+5)
	TUNEL Count	Neuron Count	TUNEL Count	Neuron Count	
No Treatment	0	29641 (2268)	25	23317 (2146)	21%
Sham Treatment	0	29845 (1553)	19	23625 (1899)	21%
Low Dose NAC (30mg/kg/day)	0	30844 (1567)	7	30441* (2321)	1%*
High Dose NAC (150mg/kg/day)	0	31761 (2804)	2*	30699* (4942)	3%*

The total number of positive neurons present in the axotomised, or contralateral control ganglia of each experimental group (n=6) is shown. Neuron counts are the mean (standard deviation) number of neurons present in either the axotomised, or contralateral control L4 & L5 dorsal root ganglia of each experimental group. Neuronal loss was calculated by subtracting the mean neuron count in the axotomised ganglia from that in the contralateral control ganglia, and is expressed as a percentage of the control value. * P value <0.05 compared to sham treatment.

Table 5.2: Effect of N-acteyl-cysteine (NAC) Treatment Upon Sensory Neuronal Death 2 Months After Axotomy

Treatment Group	Control Ganglia (L4+5) Mean (SD)		Axotomised Ganglia (L4+5) Mean (SD)		Percentage Neuronal Loss (L4+5)
	TUNEL Count	Neuron Count	TUNEL Count	Neuron Count	
No Treatment	0	31545 (2446)	5	20460 (2138)	35%
High Dose NAC (150mg/kg/day)	0	30034 (4539)	3	29243* (4100)	3%**

The total number of positive neurons present in the axotomised, or contralateral control ganglia of each experimental group (n=6) is shown. Neuron counts are the mean (standard deviation) number of neurons present in either the axotomised, or contralateral control L4 & L5 dorsal root ganglia of each experimental group. Neuronal loss was calculated by subtracting the mean neuron count in the axotomised ganglia from that in the contralateral control ganglia, and is expressed as a percentage of the control value. * P value <0.05, ** P Value <0.005 compared to no treatment.

5.3.3 Neuronal Loss

The effect of NAC treatment upon the number of neurons present in both axotomised, and contralateral control DRG's 2 weeks after nerve injury is shown in Table 5.1, and 2 months after injury in Table 5.2. Two weeks after axotomy the mean number of neurons present in the non-axotomised, contralateral control ganglia (L4+5) of untreated animals was 29641 (SD2268), and this was not significantly affected by sham treatment with 5% dextrose solution (29845 neurons, SD1553; p=0.86), or by treatment with NAC (low-dose 30844 neurons, SD3839, p=0.58; high dose 31761 neurons, SD2804, p=0.18). Two months after axotomy there was still no difference between the counts obtained from untreated animals (31545 neurons, SD2446), and those from animals which received high dose NAC treatment (30034 neurons, SD4539; p=0.52).

Two weeks after axotomy 21% (p=0.002 vs. control ganglia) of all neurons in the axotomised L4&5 ganglia had died in the groups receiving sham treatment (Table 5.1), and this was the same as occurred in animals which received no treatment (21% loss, p=0.96). This loss of neurons was almost completely eliminated by treatment with NAC (low-dose NAC 1% loss, p=0.019; high-dose NAC 3% loss, p=0.031) (*Figure 5.2*), and the same protective effect was still present 2 months after axotomy (no treatment 35% loss; high-dose NAC 3% loss, p=0.002) (Table 5.2). Although the number of neurons in axotomised L4 & L5 DRG's was significantly less than in the contralateral control ganglia of the "sham treatment" (p=0.002), and "no treatment" groups (p=0.002 at 2 weeks post-axotomy, p<0.001 at 2 months), there was no significant difference in the groups receiving NAC treatment at either 2 weeks (low-dose p=0.83; high-dose p=0.64) or 2 months (high-dose p=0.41) after axotomy.

Statistical analysis of results was performed using the techniques described previously (cf. *2.5.7*).

Figure 5.2 Effect of N-acetyl-cysteine (NAC) Treatment Upon Primary Sensory Neuronal Death After Peripheral Nerve Injury

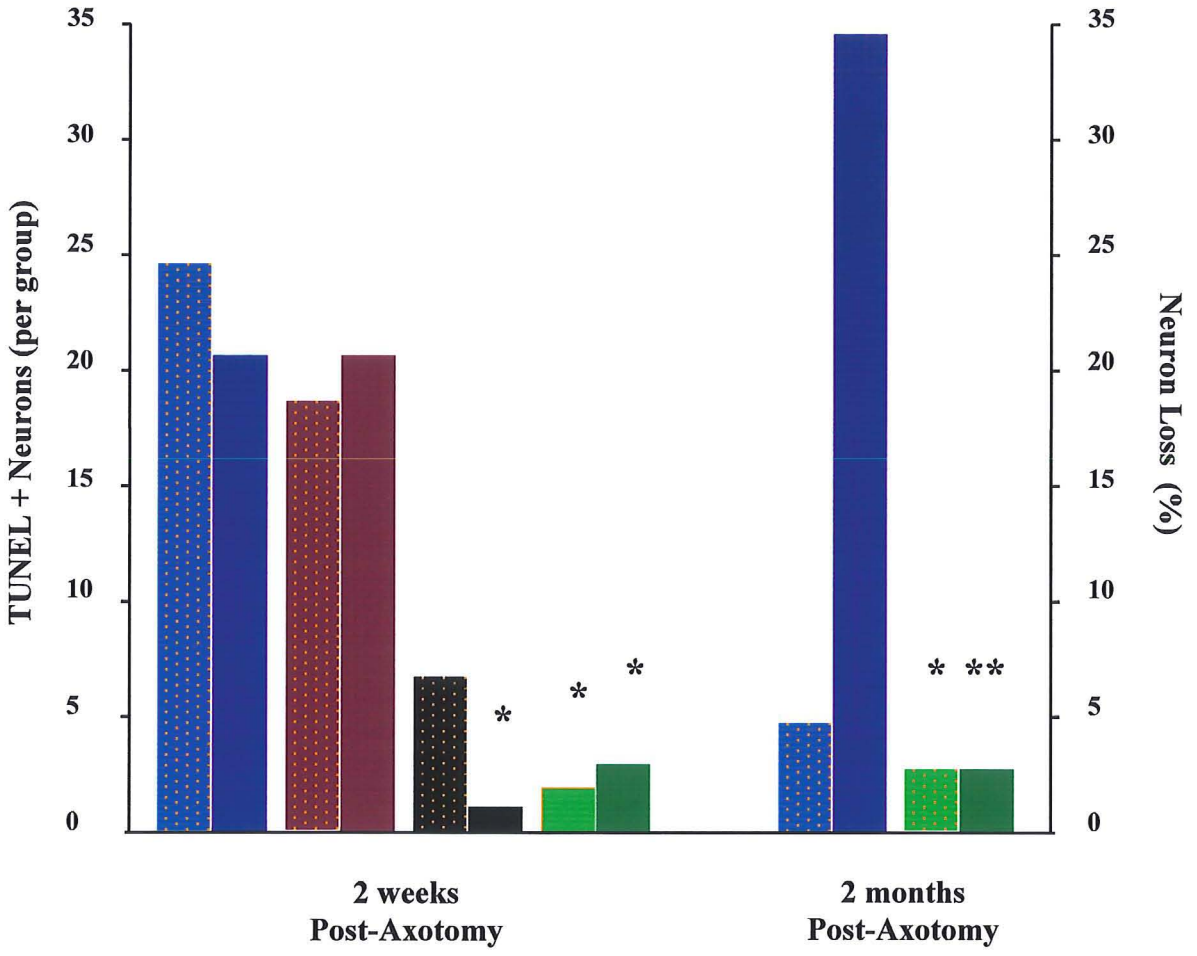

The total number of TUNEL positive neurons per experimental group of 6 animals (stippled bars), and the percentage neuron loss (plain bars) at both 2 weeks, and 2 months after sciatic nerve transection is shown. There was no significant difference between groups receiving sham treatment (5% glucose injections; maroon bars) and no treatment (blue bars). Both low-dose (30mg/kg/day; black bars) and high-dose (150mg/kg/day; green bars) NAC treatment was associated with a reduction in both the number of TUNEL positive neurons, and in the percentage neuron loss (* $p<0.05$ compared to sham treatment, ** $p<0.005$ compared to no treatment).

5.4 Discussion

5.4.1 Methodology

After sciatic nerve transection, numbers of TUNEL positive neurons reach a peak 2 weeks after peripheral axotomy, in contrast neuronal loss begins one week after axotomy and is virtually complete 2 months later (cf. *3.4.4*). A 2 week timepoint was therefore initially used in this study to reveal the effect of NAC treatment at a time when neuronal death, as demonstrated by TUNEL staining, reaches a peak in the absence of any intervention. Having demonstrated an overall protective effect 2 weeks after axotomy, the experiment was repeated with a 2 month timepoint in order to determine whether the neuroprotective effect was lasting, and to establish its magnitude, since by 2 months after injury neuronal loss is essentially complete.

The mean neuron counts obtained from control ganglia (30618, SD 2969) were in agreement with other results in the literature obtained by stereological methods [98,102,132,260,261], verifying the accuracy of the counting technique used and the neuronal losses that were calculated.

NAC treatment was given parenterally in order to bypass variabilities in gastrointestinal absorption, and the considerable effects of first pass metabolism [241]. Treatment was initially given intravenously in order to achieve peak tissue levels as quickly as possible after peripheral nerve injury, and animals were not pre-treated since this would not be clinically possible in the majority of nerve injuries. Maintenance treatment was then administered intraperitoneally, since this route is associated with a more sustained increase in serum levels, and has considerable animal welfare benefits compared to intramuscular injection. After an initial 2 weeks of twice daily dosing, the same total dose of NAC was administered once daily for welfare reasons, and because the principal period of neuronal death then been passed (cf. *3.4.4*).

5.4.2 NAC Treatment Reduces Neuronal Loss and DNA Fragmentation After Peripheral Nerve Transection

Systemic treatment with NAC (150mg/kg/day) brought about a significant reduction in both the number of TUNEL positive neurons and the neuron loss found 2 weeks after peripheral axotomy. Neuronal death was prevented, rather than just delayed, since this protective effect was found to be preserved 2 months after axotomy, by which time neuronal loss has effectively finished in the absence of treatment. Even at a reduced dose, NAC (10mg/kg/day) was still significantly effective in preventing neuronal death,

and evidence of a dose response was apparent in the increased number of TUNEL positive neurons, and in the worsened morphological findings. The neuronal loss at 2 weeks was slightly higher in the high-dose group than in the low-dose group, but the difference lies comfortably within the variability of the counting technique, and probably does not reflect a less protective effect since the TUNEL count was lower than with low-dose NAC. As previously discussed, TUNEL is a more sensitive marker of cell death at 2 weeks post-axotomy than neuronal loss and it is likely that if both treatment doses were given for 2 months, then the neuronal loss would be less in the high-dose group.

Neuronal death cannot have been completely eliminated, since TUNEL positive neurons were present in NAC treated ganglia, however it was reduced to the extent that the overall neuronal loss in both treatment groups was only 2% at 2 weeks after axotomy (control count 31323, SD 3238; operated count 30581; SD 3793). The neuroprotective effect was still present 2 months after axotomy, when loss was only 3%. This represents the salvage of around 5,500 neurons per animal at 2 weeks, and of more than 10,000 neurons, at 2 months after axotomy, amounting to over a third of the total sensory neuronal pool. The massive reduction in neuronal loss was not merely an artefact of the way in which it is calculated, since NAC treatment did not affect upon the number of neurons in control ganglia. Equally it is evident that neuroprotective effect is due to NAC, and not merely to the act of intraperitoneal injection, since treatment with the vehicle solution (sterile 5% dextrose) had no effect upon either the number of TUNEL positive neurons, or upon neuronal loss.

5.4.3 Mechanism of Action

There are a variety of mechanisms by which N-Acetylcysteine (NAC) may potentially exert its neuroprotective effect, however since studies using primary sensory neurons are scarce, it is necessary to draw upon other experimental models of neuronal death.

Axotomy causes a loss of distal neurotrophic support, which initiates neuronal death possibly via an effect upon cellular redox balance, and oxidative stress. NGF, the prototypic neurotrophin, stimulates L-cysteine uptake for glutathione synthesis [274-276], and BDNF & bFGF also induce glutathione peroxidase activity within neurons [277]. BDNF deprivation induces nitric oxide synthase (NOS) activity in cultured motorneurons (MN), which precedes the onset of cell death, and is prevented by antioxidants [278]. The antioxidant effect of NAC may therefore mimic some of the effects of neurotrophic support, and NAC also has complex effects upon neurotrophic factor signalling pathways

within neurons, for example by uncoupling NGF activation of mitogen activated protein kinases (MAPK's) from that of Ras [279]. NAC also blocks the activation of c-Jun Kinase (JNK), and so prevents apoptosis in trophic factor deprived PC12 cells [175].

Axotomy induced retrograde degeneration occurs in association with perikaryal accumulation of mitochondria, and oxidative stress that may be worsened by mitochondrial dysruption [53] (cf. *3.4.5*). Root avulsion induces 30% MN death, and involves oxidative stress [193], and NOS activity [194,195]. Nerve injury therefore increases mitochondrial nitric oxide (NO) production, due to an increase in the activity of both inducible nitric oxide synthase (iNOS) in neuroglia, and constitutive NOS (nNOS) within neurons. This is one of the mechanisms by which the mitochondrial electron transport chain may be disrupted, since transient increases in NO cause reversible inhibition of complex IV, and sustained increases may cause permanent inhibition of cytochrome C (complex I) [197]. This effect is enhanced by mitochondrial glutathione depletion [197], and blocked by augmenting glutathione levels in vitro [280]. Disruption of the electron transport chain disturbs the cell's redox balance, and favours the generation of reactive oxygen species (ROS) which can disturb mitochondrial membrane potential (MMP) [200], disrupt calcium homeostasis, and lead to cell death [197,201]. NAC protects mtDNA from damage due to increased NO, or oxidative stress, similarly to the anti-apoptotic Bcl-2 [281], which also has antioxidant, mitochondrial protective effects [282].

Glutathione depletion, particularly depletion of mitochondrial glutathione [270,283], increases the susceptibility of neurons to a variety of toxic stimuli, such as glutamate toxicity, ischaemia reperfusion, oxidative stress [197,242,284], and serum or trophic factor withdrawal [175]. Neurons have a less resistance to oxidative stress than astroglia [240,285,286], due to limited capacity for glutathione synthesis, and increasing glutathione levels may therefore be protective [197,242,270], since glutathione is one of the principal defenses against ROS and oxidative stress within neurons [197]. However glutathione does not cross the blood-brain barrier, and neurons cannot synthesise thiols, being dependent upon astrocytes for the supply of precursor peptides in order to maintain glutathione levels in response to oxidative stresses [287,288]. Cysteine is the rate limiting precursor in glutathione synthesis [287], and can be readily taken up as NAC [240]. In vitro NAC causes an increase in neuronal glutathione levels [240,272,279,289,290], an effect enhanced by co-culture with astroglia [291], and NAC protects glia in culture [286], working synergistically with CNTF to protect oligodendrocytes [206]. Given the key role that glia play in neuronal glutathione synthesis, and survival, this protective effect may be of importance in vivo, and NAC, which crosses the blood-brain barrier, does reduces retinal ganglion cell death after axotomy in vivo [292].

At high doses NAC has direct reductant [272,279] and antioxidant effects, and can block lipid peroxidation by peroxyntitrate (ONOO-) [290]. However the antioxidant role of NAC, and of the glutathione which it produces, is not sufficient to fully explain its neuroprotective effect, since the D-stereoisomer (D-NAC) is also protective for PC12 neuronal cells after trophin withdrawal, unlike other antioxidants studied, but cannot be used for glutathione synthesis [160]. Mice deficient in NT-3 (a neurotrophic factor) exhibit primary sensory neuronal death due to disco-ordinated cell cycling [207], and this may explain the protective action of L- and D-NAC, since both regulate cell cycling, and DNA synthesis [160]. This effect requires protein synthesis, gene transcription, and activation of the Ras-extracellular signal-related kinase pathway (ERK), but is independent of the PI3 kinase pathway, unlike the protective effect of NGF [293]. However, since NAC blocks DNA synthesis, but not cell death, independently of ERK activation, cell cycle control is not the sole mechanism [293].

The neuroprotective effect of NAC may therefore be due to a combination of its antioxidant, and reductant properties, the promotion of glutathione synthesis, and to preventing abortive entry into the cell cycle by injured neurons.

5.4.4 Conclusions & Clinical Relevance

This study has demonstrated that NAC, which may also have analgesic properties [289], is highly neuroprotective in an in vivo model of peripheral nerve injury. This further confirms the postulated roles of NO induced mitochondrial dysfunction, reactive oxygen species, glutathione depletion, and abortive cell cycling in the death of adult primary sensory neurons. Further research is required to define the precise mechanism of action, and so to increase the understanding of the events culminating in neuronal death. NAC is currently under investigation in a model of brachial plexus injury, and research is required to establish whether NAC and similar compounds may have therapeutic roles in other forms of trauma to the nervous system, such as brain and spinal cord injury. A further question is whether or not NAC will improve peripheral nerve regeneration, as well as neuronal survival.

A pressing clinical need exists for a treatment that reduces sensory neuronal death after peripheral nerve trauma, and the results of this study strongly suggest that NAC may be a suitable agent. Unlike other antioxidant agents under investigation for their neuroprotective effects, such as BN80933[269], NAC already has a proven safety profile in the clinical environment, and clinical trials in peripheral nerve trauma could therefore

begin in the near future, once the effect of NAC upon peripheral nerve regeneration has been determined.

Chapter 6. Clinical Potential of L-acetyl-carnitine in the Treatment of Peripheral Nerve Injuries

6.1 Introduction

The neuroprotective potential of NAC was described in the previous chapter, where it was argued that NAC's principal mechanism of action was likely to be via maintaining neuronal glutathione levels and so countering the effects of reactive oxygen species, or possibly by inhibiting NO mediated mitochondrial bioenergetic dysfunction and abortive cell-cycling. It would be theoretically preferable to intervene earlier in the cascade of events, although not sufficiently far upstream that the protective effect would cease to be applicable in a range of neuronal subpopulations against a variety of insults would be lost. The apparent ubiquity of mitochondrial bioenergetic dysfunction as a prelude to the generation of reactive oxygen species and neuronal death [53,185,191,192] makes it an intriguing target for therapeutic intervention, and one agent which may act at this level is L-acetyl-carnitine (LAC).

LAC is the acetyl ester of L-carnitine, and is the predominant acylcarnitine in human tissues. Both peptides have a physiological role in the transport of long-chain free fatty acids (FFA) across mitochondrial membranes [247,294], although there are differences in their other actions. LAC is also an acetyl-group donor in oxidative metabolism [246,247], has antioxidant activity [295,296], and increases the expression and affinity of neurotrophin receptors for nerve growth factor (NGF) [244,245,297]. In-vitro LAC is neuroprotective [244,245,248] and prevents mitochondrial uncoupling [248], whilst in-vivo it increases peripheral nerve regeneration after peripheral nerve lesions [298,299]. LAC is currently showing promising results in clinical trials for diabetic neuropathy [249,300] and HIV-associated peripheral neuropathy [301], where regeneration of neurites into target tissues has been demonstrated (cf. *8.4*).

This study therefore investigated the effect of systemic LAC treatment upon primary sensory neuronal death after peripheral nerve injury, using TUNEL to identify individual dying neurons, and neuron counting by the optical disector technique to quantify the overall neuronal loss which occurred (cf. *1.4*).

6.2 Methods

Groups of young adult male Sprague-Dawley rats (n=6) underwent unilateral sciatic nerve division (cf. *2.2.2*), and immediately after nerve transection parenteral treatment with L-acetyl-carnitine (LAC) was commenced at either 50mg/kg/day ("high-

dose"), or 10mg/kg/day ("low-dose") as detailed in section *2.2.3*. Another experimental group ("sham treatment") received injections of an identical volume of sterile saline (cf. *2.2.3*), and all animals were treated until termination (cf. *2.2.1b*). Two further control groups were provided by the animals whose DRG's were harvested 2 and 4 months after sciatic nerve transection in the timecourse study (cf. *Chapter 4*).

The L4 & L5 DRG's were harvested from both the axotomised, and contralateral control sides (cf. *2.3.2*) at either 2 weeks (all treatment groups), or 2 months (one "high-dose treatment", and one "no treatment" group) after sciatic nerve transection (cf. *2.3.2*). The ganglia were then processed (cf. *2.4.1a, 2.4.2a & 2.4.3*) for quantification of neuronal death by TUNEL (cf. *2.5.1*), and by stereological determination of the number of surviving neurons using the optical disector technique (cf. *2.5.2*). The mean cap count was 158 (SD25.8) per ganglion, in keeping with the requirement to count between 100 and 200, and all other sampling parameters were the same as discussed previously (cf. *3.2, 2.5.1. & 2.5.2*).

TUNEL counts were expressed as the total number of positive neurons in the L4 and L5 DRG's of each experimental group of 6 animals, and neuron counts were expressed as a mean combined (L4 plus L5) count for each side (axotomised, or contralateral control). Neuronal loss was then calculated by subtracting the neuron count in a pair of axotomised ganglia from that of their contralateral controls, and the mean loss was then expressed as a percentage of the mean neuron count in the control ganglia.

Statistical analysis of results was performed using the techniques described previously (cf. *2.5.7*).

6.3 Results

No adverse effects upon animal behaviour were found, and weight gain during the study period was similar in all groups at both 2 weeks ($p=0.198$) and 2 months ($p=0.343$).

6.3.1 Morphology

Prominent morphological changes were evident in the axotomised ganglia of untreated animals (*Figure 6.1B*), with the majority of neurons exhibiting nuclear eccentricity, and chromatolysis. Neurons displaying features of apoptosis (cytoplasmic granulation, vacuolation, membrane irregularities) were seen, as were numerous enlarged, and grossly vacuolated neurons. Morphological findings were unchanged by sham treatment with normal saline, however low-dose LAC caused a qualitative improvement in

Figure 6.1: Effect of L-acetyl-carnitine (LAC) Treatment Upon Primary Sensory Neuronal Morphology After Sciatic Nerve Transection

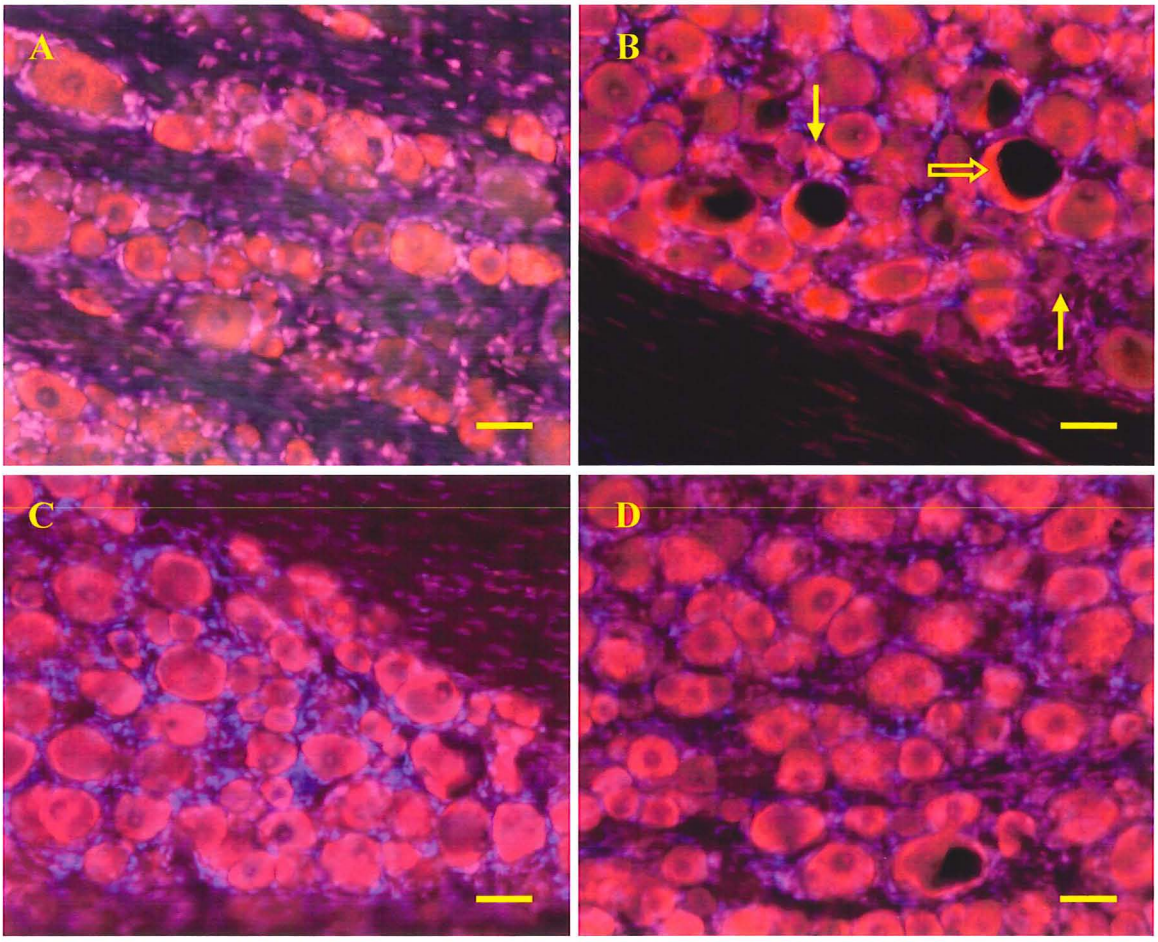

Dorsal root ganglia 2 weeks after sciatic nerve transection stained with the nuclear dye Hoechst 33342 (blue fluorescence) and the cytoplasmic dye propidium iodide (red fluorescence). Control ganglia [A] contain neurons with normal cytoplasmic morphology, surrounded by numerous smaller satellite cells, in which nuclear staining predominates. Two weeks after sciatic nerve transection [B] gross morphological changes are evident, with most neurons displaying nuclear eccentricity, membrane irregularities, and cytoplasmic granulation or vacuolation (hollow arrow). Apoptotic neurons are also evident (solid arrow). Morphology is somewhat improved after low-dose LAC treatment, although nuclear eccentricity and membrane irregularity remains frequent [C]. After high-dose LAC treatment neuronal morphology is significantly more normal [D]. Scale bar equals 40µm.

neuronal morphology (*Figure 6.1C*), which was even more pronounced after high-dose LAC treatment (*Figure 6.1D*).

6.3.2 TUNEL Staining

The effect of LAC treatment upon the number of TUNEL positive neurons, and upon the neuronal loss found 2 weeks after axotomy is summarised in Table 6.1, while Table 6.2 gives the equivalent findings 2 months after axotomy.

TUNEL positive neurons were only found in axotomised ganglia. There was no difference between the treatment groups in the morphology of the TUNEL positive neurons, which exhibited a range of cytoplasmic morphologies identical to those described previously (cf. *3.3.1a & 5.3.1*). Two weeks after sciatic nerve transection the total number of TUNEL positive neurons present in the axotomised L4&5 ganglia of untreated animals was 25 neurons per group of 6 animals. Whilst sham treatment had no significant effect upon the number of TUNEL positive neurons (33 neurons/group, $p=0.937$), a significant reduction in the number of TUNEL positive neurons did occur with LAC treatment at both the low (6 neurons/group, $p=0.009$), and high (3 neurons/group, $p=0.004$) doses used (*Figure 6.2*). A reduction in TUNEL positive neurons was also found with high-dose LAC 2 months after axotomy (Table 6.2, *Figure 6.2*).

6.3.3 Neuronal Loss

Two weeks after axotomy the mean number of neurons present in the unoperated contralateral control ganglia (L4+5) of untreated animals was 29641 (SD 2268). This was similar to the equivalent count in sham treated (30257, SD 3261; $p=0.61$), or low-dose LAC treated (30167, SD 1877; $p=0.67$) animals, but lower than that in the high-dose LAC treated group (33646, SD 875; $p<0.05$). However, by 2 months after axotomy the contralateral control ganglia of untreated animals (31545, SD 2446) once again contained a similar number of neurons to those in the high-dose LAC treated group (30560, SD 4294; $p=0.36$).

In the animals receiving no treatment a loss of 21% of all L4&5 neurons (axotomised mean 23317, SD 2146; unoperated control mean 29641, SD 2267) occurred during the first two weeks after axotomy, and this rose to 35% after 2 months (axotomised mean 20460, SD 2138; control mean 31545, SD 2446) (*Figure 6.2*). Two weeks after axotomy neuronal loss was not affected by sham treatment (21% loss, $p=0.99$), but was almost completely eliminated by LAC treatment (low-dose LAC 0% loss, $p=0.001$; high-dose LAC 2% loss, $p=0.006$), and this protective effect was preserved 2 months after axotomy (high-dose LAC -4% loss, $p<0.001$) (*Figure 6.2*).

Table 6.1: Effect of L-acetyl-carnitine (LAC) Treatment Upon Neuronal Death 2 Weeks After Axotomy

Treatment Group	Control Ganglia (L4+5) Mean (SD)		Axotomised Ganglia (L4+5) Mean (SD)		Percentage Neuronal Loss (L4+5)
	TUNEL Count	Neuron Count	TUNEL Count	Neuron Count	
No Treatment	0	29641 (2268)	25	23317 (2146)	21%
Sham Treatment	0	30257 (3261)	33	23958 (2510)	21%
Low Dose LAC (10mg/kg/day)	0	30167 (1877)	6*	30270** (2100)	0%**
High Dose LAC (50mg/kg/day)	0	33646* (875)	3*	33077** (2410)	2%*

TUNEL positive neuron counts are expressed as the total number of positive neurons present in the axotomised, or contralateral control ganglia of each experimental group. Axotomised, and contralateral control ganglia neuron counts are stated as the mean (standard deviation) count per experimental group. Neuronal loss is calculated as the mean neuron count in the axotomised ganglia subtracted from that in the control ganglia, expressed as a percentage of the control value.
* P value <0.05, ** P value <0.001 compared to no treatment.

Table 6.2: Effect of L-acetyl-carnitine (LAC) Treatment Upon Neuronal Death 2 Months After Axotomy

Treatment Group	Control Ganglia (L4+5) Mean (SD)		Axotomised Ganglia (L4+5) Mean (SD)		Percentage Neuronal Loss (L4+5)
	TUNEL Count	Neuron Count	TUNEL Count	Neuron Count	
No Treatment	0	31545 (2446)	5	20460 (2138)	35%
High Dose LAC (50mg/kg/day)	0	30560 (4294)	1	31642* (3775)	-4%**

TUNEL positive neuron counts are expressed as the total number of positive neurons present in the axotomised, or contralateral control ganglia of each experimental group. Axotomised, and contralateral control ganglia neuron counts are stated as the mean (standard deviation) count per experimental group. Neuronal loss is calculated as the mean neuron count in the axotomised ganglia subtracted from that in the control ganglia, expressed as a percentage of the control value.
* P value <0.05, ** P value <0.001 compared to no treatment.

Figure 6.2 Effect of L-acetyl-carnitine (LAC) Treatment Upon Primary Sensory Neuronal Death After Peripheral Nerve Injury

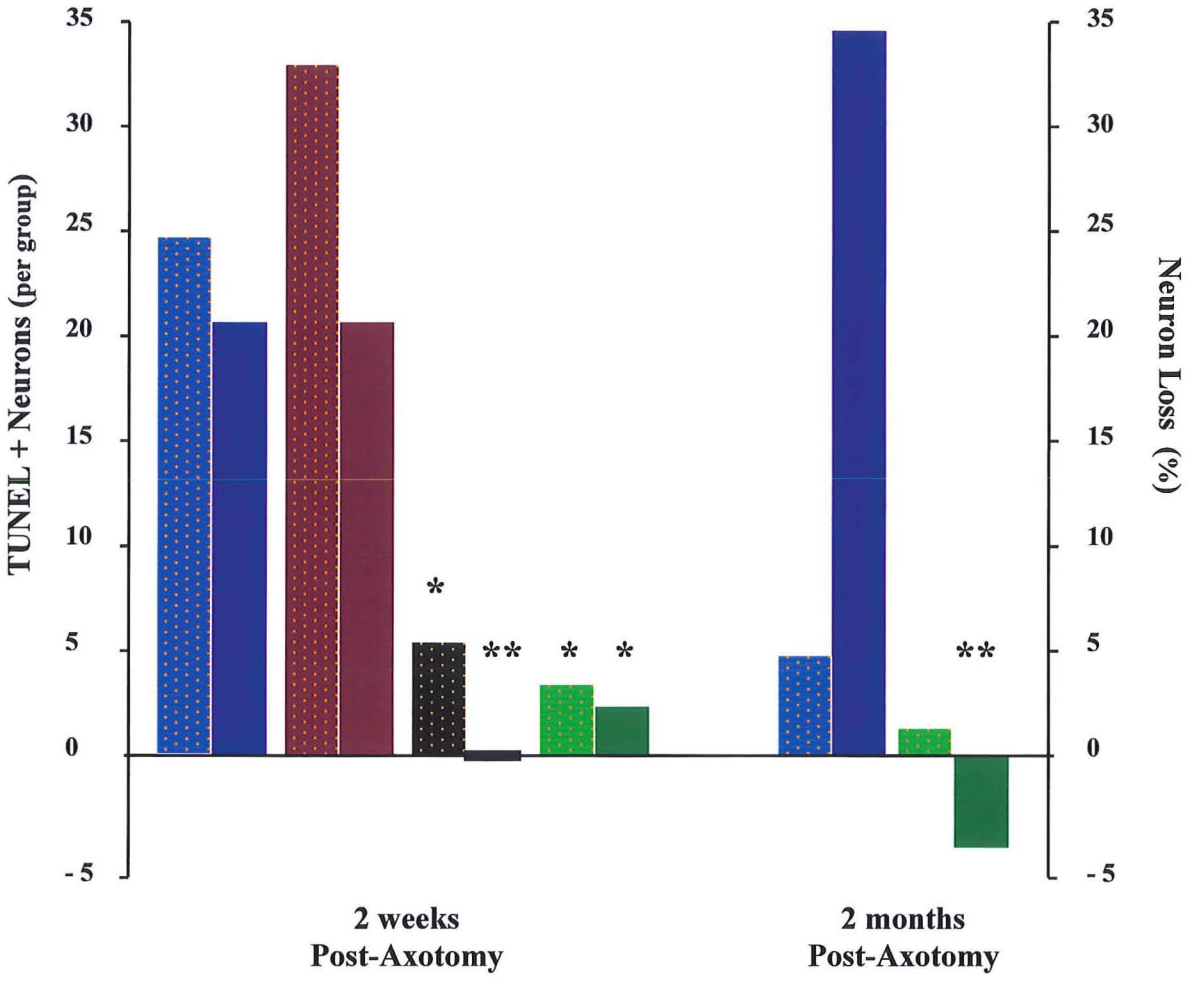

The total number of TUNEL positive neurons per experimental group of 6 animals (stippled bars), and the percentage neuron loss (plain bars) at both 2 weeks, and 2 months after sciatic nerve transection is shown. There was no significant difference between groups receiving sham treatment (sterile normal saline; maroon bars) and no treatment (blue bars). Both low-dose (5mg/kg/day; black bars) and high-dose (50mg/kg/day; green bars) L-acetyl-carnitine (LAC) treatment was associated with a reduction in the number of TUNEL positive neurons, and a reduction in percentage neuron loss to zero in some groups

(* $p<0.05$ compared to sham treatment, ** $p<0.001$ compared to no treatment).

6.4 Discussion

6.4.1 Methodology

As a marker of DNA fragmentation TUNEL staining detects the beginning of an individual neuron's death and therefore precedes the cell's subsequent elimination, which will be reflected by neuronal loss (cf. *1.4, Figure 1.1*). TUNEL staining is therefore a more sensitive marker of cell death, as very small neuronal losses may be entirely masked by the normal biological variability in neuron numbers (cf. *3.4.4*).

The timepoints of 2 weeks, and 2 months after sciatic nerve transection were used as they reflect both the peak of neuronal death, and of neuronal loss, as has been discussed previously (cf. *3.4.4*), along with the use of combined L4 & L5 counts (cf. *3.4.2*). Adequate numbers of caps (158, SD 25.8) were counted to meet the requirement of 100-200 per ganglion [129], and the mean neuron count obtained from control ganglia was 30969 (SD 2858) per ganglion pair. This is in agreement with other results in the literature [98,102,132,260,261], and with the results obtained in the previous two studies (cf. *3.4.2 & 5.4.1*), verifying the accuracy of the counting in this study.

LAC levels were not measured in this study since both parenteral and enteral administration of LAC have previously been demonstrated to increase plasma and CNS levels [302,303]. The dose of 50mg/kg/day is comparable to the dose of LAC used clinically for the treatment of peripheral neuropathies (cf. *8.2*), and in diabetic rats was sufficient to normalise sciatic nerve LAC content [304], when given by intraperitoneal injection. Parenteral administration was used in order to eliminate variability due to gastrointestinal absorption, and treatment was initially given 12 hourly in order to maintain peak serum levels of LAC. Once the principal period of neuronal death was over at 2 weeks after injury, the same total daily dose was administered once daily for reasons of animal welfare.

6.4.2 LAC Treatment Reduces Neuronal Death and Eliminates Neuronal Loss After Peripheral Nerve Transection

At both timepoints studied, systemic treatment with LAC (50mg/kg/day) led to a significant reduction in all the markers of neuronal death. The reduction in the number of TUNEL positive neurons found 2 weeks after peripheral axotomy was matched by an even greater reduction in neuronal loss, and neuronal death was prevented, rather than just delayed, since this protective effect was found to be preserved 2 months after axotomy. Even at the reduced dose of 10mg/kg/day LAC therapy was still significantly effective in preventing neuronal death, with a dose response effect being evident in the worsened

morphological changes and in the number of TUNEL positive neurons, when compared to high-dose LAC treatment. Hence the low-dose regime was not used in the 2 month groups. The lack of any apparent dose response in neuronal loss after 2 weeks of LAC treatment most likely reflects both the small difference in the number of dying neurons (TUNEL results) between dose levels, and the fact that 2 weeks is a relatively early timepoint for minor differences in rates of neuronal death to translate into differences in neuronal loss.

When all three treatment groups are considered together, LAC treatment was found to have completely eliminated the neuronal loss normally found after sciatic nerve transection (control ganglia count 31457, SD 3041; operated ganglia count 31663; SD 2931). Since occasional TUNEL positive neurons were present in LAC treated ganglia neuronal death cannot have been completely eliminated, but the protective effect was dramatic nonetheless. Around 6,000 neurons per animal at 2 weeks, and over 10,000 neurons at 2 months after axotomy, were salvaged by LAC treatment, and this amounts to protection of almost the entire sensory neuronal pool.

The reduction in calculated neuronal loss was not merely an artefact of changes in the number of neurons in control ganglia, since LAC treatment did not appear to have any effect upon the number of neurons in the control ganglia. A minor, but statistically significant increase was found 2 weeks after axotomy in the group treated with high-dose LAC (33646, SD 875), but this was likely to be an artefact of the unusually low standard deviation in this group, rather than a real effect of treatment, since the mean count lay well within the normal distribution of counts for untreated and sham treated animals (mean 29949, SD 2697). Two months after axotomy there was no difference between the untreated, and high-dose LAC groups.

Finally, it is evident that the reduction in neuronal death was due to LAC rather than the act of drug administration, since 2 weeks after axotomy sham injections of sterile normal saline had had no effect upon either neuronal loss, or upon the number of TUNEL positive neurons.

6.4.3 Mechanism of Action

The precise mechanism by which LAC prevents primary sensory neuronal death after peripheral axotomy remains to be determined, although it is likely that its activity is due to attenuation of both the initiator, and effector mechanisms of cell death.
Firstly, LAC may attenuate the loss of distal neurotrophic support by enhancing neurotrophin responsiveness, since it is known to increase NGF binding capacity [297], and to potentiate the effects of NGF [244,245]. Secondly, LAC facilitates the transport of cytosolic

long-chain free fatty acids across mitochondrial membranes and provides acetyl groups for maintenance of aerobic glycolytic pathways [246,247], in preference to the normal shift into the less efficient pentose phosphate shunt [305,306]. LAC may therefore prevent failure of mitochondrial oxidative metabolism, which is integral to the cell death pathway [185,191], at a time when energy requirements are increased in support of the regenerating neurites [305], and this effect has been demonstrated in-vitro [248]. Finally, the antioxidant role of LAC [295] may be of benefit in preventing cell damage by the free oxygen species [296] whose generation is thought to be of major importance in the effector mechanism of cell death [197,198].

6.4.4 Conclusions & Clinical Relevence

Experimentally, LAC enhances sensory neuronal survival in vitro [244,245] and has been demonstrated to increase motor nerve regeneration after peripheral axotomy [298], which in neonates may be due to recruitment of ectopic motorneurones, or to increased motorneuronal survival [307]. Clinically, LAC has an excellent safety profile, and is under investigation as a treatment for diabetic neuropathy, and HIV-associated peripheral neuropathy where it is known to reduce analgesic requirements [301,308], and to cause cutaneous nerve fibres to regenerate to normal control levels in the dermis and sweat glands [308].

Further work needs to be undertaken to clarify the required duration of treatment with LAC, its precise mechanism of action, and studies are now underway to determine its effects in other models of trauma to the nervous system. However the evidence would suggest that LAC is a clinically safe drug when administered either orally or parenterally, and that it promotes sensory neuronal survival after peripheral nerve trauma, as well as enhancing the capacity for peripheral nerve regeneration. The results presented herein therefore suggest that LAC may indeed be the first effective, clinically applicable agent for adjuvant pharmacotherapy in the management of major peripheral nerve trauma such as brachial plexus injuries, and clinical trials are now being scheduled.

Chapter 7. L-acetyl-carnitine Improves Nerve Regeneration Indepently of Neuronal Survival

7.1 Introduction

L-acetyl-carnitine (LAC) is known to improve nerve regeneration after acute nerve injuries [298], and this has been ascribed to improvements in neuronal metabolic capacity, and nerve growth factor (NGF) responsiveness [244,245,297]. However in light of the demonstration that LAC virtually abolishes sensory neuronal death after sciatic nerve transection (cf. *Chapter 6*), it is now unclear whether the reported improvement in regeneration is due to an increase in the regenerative potential of individual neurons, or to an increase in the number of regenerating neurons, secondary to a reduction in cell death.

This question is of clinical importance in two scenarios; firstly in the setting of peripheral nerve surgery, and secondly in the setting of chronic neuropathy. If LAC proves to be clinically effective in reducing sensory neuronal death after peripheral nerve injury it will then become important to determine the appropriate duration of treatment after nerve repair. If LAC improves regeneration only via its neuroprotective role, then treatment need only be given for the first 2 months, until the period of sensory neuronal death is over (cf. *3.4.4*). However if LAC also improves the regenerative potential of individual neurons then treatment should be continued until target reinnervation is completed, which may take many months in the case of proximal injuries [5,11].

Secondly, in the case of the chronic neuropathies that occur in conditions such as diabetes [309] and HIV disease [26,204], the problem is not merely sensory neuronal death [310,311], but also the inability of neurons to maintain long peripheral axons and to regenerate into the target tissues as a result of chronic metabolic insufficiency [26]. If LAC can be demonstrated to improve nerve regeneration after injury independently of its effect upon neuronal death, then it may have greater therapeutic potential in these chronic disease states.

The effect of LAC treatment upon nerve regeneration following late secondary sciatic nerve repair 2 months after nerve transection was therefore determined by quantitative immunohistochemistry. The sensory neuronal death induced by nerve transection will have been virtually complete by this time after injury, and any effect upon nerve regeneration ought therefore to primarily reflect an improvement in the regenerative capacity of individual neurons.

7.2 Methods

Two groups of young adult male Sprague Dawley rats (n=5) underwent an initial unilateral sciatic nerve division, followed by repair with a 1cm reversed sciatic nerve graft two months later (cf. *2.2.7*). In one group the animals were treated with L-acetyl-carnitine (50mg/kg/day) by intraperitoneal injection, as detailed in section *2.2.7*, from the time of nerve repair until termination (cf. *2.2.1b*) six weeks after repair. The sciatic nerves were harvested (cf. *2.3.3*), and processed for (cf. *2.4.1a, 2.4.2b & 2.4.4*) for immunohistochemical quantification of regeneration distance (cf. *2.5.4, Figure 2.8*), and percentage area of immunostaining against S-100 as a Schwann cell marker, and PAMNF as a pan-neuronal marker (cf. *2.5.5*). Area of immunostaining was measured in a band of images captured with a 20X objective lens, and situated 1mm distal to the end of the proximal nerve stump (cf. *2.5.5, Figure 2.8*).

All quantification was performed by the same observer, and care was taken to ensure that similar settings were employed for both experimental groups during the image capturing and thresholding process. Statistical analysis of results was performed using the techniques described previously (cf. *2.5.7*).

7.3 Results

7.3.1 Regeneration Distance

In both experimental groups axons had crossed the full width of the repair, and reached the cut end of the distal nerve stump in all cases, and as a result no effect of LAC treatment upon mean regeneration distance could be demonstrated (LAC treatment 12.9mm, SD 0.90; control 13.3mm, SD 1.53). There was no visible gastrocnemius contraction in response to pinching the nerve proximal to the repair in any animal.

7.3.2 Area of Immunostaining

The effect of LAC treatment upon the area of immunostaining is summarised in Table 7.1 and Figure 7.1. The total area of immunostaining in LAC treated nerve repairs was significantly greater than control both for PAMNF (LAC 212245μm^2, SD 41861; control 58259 μm^2, SD 25405; $p<0.001$), and for S-100 (LAC 236641μm^2, SD 41841; control 112295 μm^2, SD 29902; $p<0.001$).

The mean percentage area of immunostaining was also significantly greater in the LAC treated group than control, both for PAMNF (LAC 24%, SD 9.5; control 7.3%, SD 2.3; $p=0.008$), and S-100 (LAC 26%, SD 10; control 14%, SD 2.1; $p=0.012$). The total area

Table 7.1: Effect of L-acetyl-carnitine (LAC) Treatment Upon Nerve Regeneration

Treatment Group	**Total Area of Immunostaining (μm^2)** Mean (SD)		**Percentage Area of Immunostaining** Mean (SD)	
	PAMNF	S100	PAMNF	S100
No Treatment	58259 (25405)	112295 (29902)	7.3% (2.3)	14% (2.1)
High Dose LAC (50mg/kg/day)	212245** (41861)	236641** (41841)	24%* (9.5)	26%* (10)

The mean area of immunostaining for nerve fibres (PAMNF), or Schwann cells (S-100) within reversed sciatic nerve grafts harvested 6 weeks after a late secondary repair of a 1 cm gap in the rat sciatic nerve (2 month interval between transection & repair). Percentage area of immunostaining equals the total area expressed as percentage of the total area of graft within which staining was measured. * P value <0.05, ** P value <0.001 compared to no treatment.

Figure 7.1 Effect of L-acetyl-carnitine (LAC) Upon Nerve regeneration After Late Secondary Repair

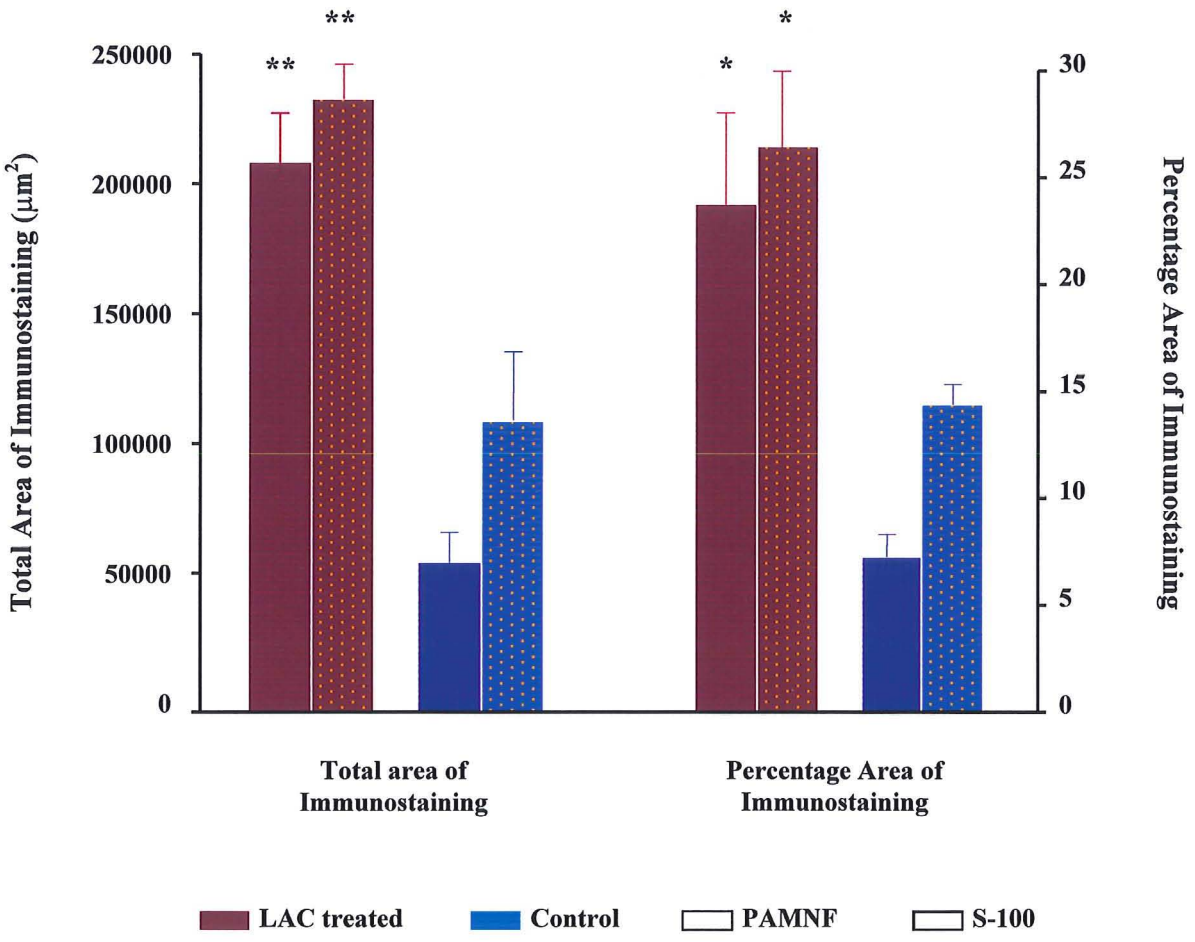

The effect of LAC treatment (50mg/kg/day; maroon bars) upon the total, and percentage areas of immunostaining for PAMNF (plain bars) and S-100 (stippled bars) 6 weeks after late secondary nerve repair is shown compared to untreated controls (blue bars). LAC treatment resulted in significant increases in both total, and percentage areas of immunostaining for nerve fibres (PAMNF) and Schwann cells (S-100). (* $p<0.05$, * $p<0.001$ compared to untreated control).

of nerve graft present in the quantified sections was slightly higher in the LAC treated group (967046 μm^2, SD 279641) than in the controls (774571 μm^2, SD 146813), but the difference was not statistically significant (p=0.21).

7.4 Discussion

7.4.1 Methodology

Repairs were performed 2 months after nerve transection as sensory neuronal loss has reached a plateau value by this timepoint (cf. *3.4.4*). This delay made end-to-end epineurial repair unfeasable due to retraction of the nerve stumps, and nerve grafts were therefore used to bridge the resulting gap since this is the standard clinical technique.

PAMNF is a constitutive component of all mammalian nerve fibres, and so the area of immunostaining with antisera against it gives a reliable determination of the area of nerve fibres present in a tissue section. Similarly S-100 is a marker of all Schwann cells, and so it provides a means to quantify the Schwann cell response to regenerating neurites. Grafts were harvested 6 weeks after nerve repair, and the area of immunostaining was measured 1mm distal to the end of the proximal nerve stump, as this site had proved the most informative in previous unpublished research into nerve regeneration through bioartificial nerve conduits.

Artefactual variations in the total area of immunostaining may arise if there are differences in the area of nerve graft in which staining is measured. Such differences may arise either because of actual differences in the diameters of the nerve grafts used, or because of variability in the exact position within the graft at which the section was cut. Since the nerve is cylindrical, longitudinal sections cut at slightly different positions in the graft will inevitably have different diameters. Hence the area of immunostaining was also expressed as a percentage of the area of the graft to compensate for this effect.

The dose of LAC, dosage schedule, and route of administration was chosen for the reasons explained in the previous chapter (cf. *6.4.1*), and no sham injection group was included since there was no effect found in the previous study (cf. *6.3.2 & 6.3.3*).

7.4.2 L-acetyl-carnitine (LAC) Improves Nerve Regeneration Independently of Neuronal Survival

Two months after sciatic nerve transection sensory neuronal loss within the L4 & L5 DRG's has reached a peak plateau value (cf. *3.4.4*), and so nerve repair at this timepoint relies upon a relatively stable pool of surviving neurons. Any effect of LAC treatment

upon nerve regeneration therefore ought to be primarily the result of an effect upon the regenerative capacity of individual neurons, rather than upon neuronal survival. Although the nerve repair involves limited trimming of the proximal nerve stump, this is unlikely to cause such substantial neuronal death as the original transection, since the neurons which were most susceptible to axotomy induced death will have died already. Furthermore the nerve is then immediately repaired, and this will limit any death that might have occurred otherwise (cf. *4.4.2*).

Although there was no demonstrable difference in regeneration distance as a result of LAC treatment, this may simply be due to the manner in which regeneration distance was calculated. The distal nerve stumps were trimmed ~3mm distal to the nerve repair, and so any difference in the distance which fibres travelled beyond that point would not be detected. Such a difference could be detected by studies using earlier timepoints, or by seeking evidence of target organ reinnervation at later timepoints.

The total area of immunostaining with antisera against PAMNF, hence the total area of regenerating nerve fibres, was significantly greater in the LAC treated group than in the untreated controls (Figure 7.1), and this was matched by a comparable increase in the total area of immunostaining for Schwann cells (S-100). The increase was not an artefact of the slightly greater area of nerve graft present in the LAC treated tissue sections, since the percentage area of immunostaining for both nerve fibres (227% increase), and Schwann cells (87% increase) was also significantly greater in the LAC treated group. Neurite ingrowth causes Schwann cell proliferation [47,90], and this may explain why LAC treatment also caused an increase in the percentage area of immunostaining for Schwann cells.

7.4.3 Mechanism of Action

The precise mechanism by which LAC improved nerve regeneration after late secondary repair is not yet certain. Neuronal energy requirements are increased during regeneration [305], and it is postulated that by improving free fatty acid transport into mitochondria, and supporting aerobic glycolysis [246-248], in preference to the less efficient pentose-phosphate pathway [305,306], then regeneration will be facilitated. The effect of LAC treatment to increase neuronal NGF binding capacity [297], and responsiveness [244,245] may also be significant, since exogenous NGF is known to improve peripheral nerve regeneration [47,216].

7.4.4 Implications

L-acetyl-carnitine may therefore improve peripheral nerve regeneration independently of its effect upon the number of surviving neurons, although further electrophysiological studies and the demonstration of target organ reinnervation would be required to conclude that the increased regeneration is of functional benefit. The regenerative capacity of individual neurons may be enhanced either by a direct effect to support axonal growth, or by a more facilitative effect whereby LAC treatment enhances the regenerative response to physiological neurotropic cues.

This might suggest that LAC treatment should be continued until target organ reinnervation has occurred after peripheral nerve repair, and that it may also be of benefit even after nerve repairs which have been delayed for several months. Furthermore, LAC is likely to be of benefit in causing peripheral nerve regeneration in chronic neuropathic conditions where impaired regenerative capacity, rather than sensory neuronal death, is the principal pathogenetic mechanism.

Chapter 8. L-acetyl-carnitine: a Pathogenesis Based Treatment for HIV-Associated Distal Symmetrical Polyneuropathy

8.1 Introduction

In the previous two chapters it has been proposed that L-acetyl-carnitine (LAC) treatment may be neuroprotective, possibly acting via the promotion of mitochondrial bioenergetic function, or its NGF agonist activity. Results also suggested that LAC may be of benefit in promoting nerve regeneration in chronic conditions where there is a continuing metabolic insult to the neurons, for example in diabetic neuropathy. However the pathogenesis of diabetic neuropathy is complicated by microvascular changes, and so a neuropathy whose pathogenesis is more identifiably due to impaired mitochondrial function, and loss of target derived NGF [229] was chosen for testing the clinical efficacy of LAC.

HIV-associated peripheral neuropathies (PN) [204] are a cause of significant morbidity in 10-35% of HIV positive patients [26,312,313], and distal symmetrical polyneuropathy (DSP) is the commonest form. It is a chronic condition that affects 11-66% of patients on nucleoside analogue reverse transcriptase inhibitor (NRTI) drug therapy [204,314], and the dideoxynucleotide analogue agents stavudine (D4T), zalcitabine (ddC), and didanosine (ddI) are particularly implicated in its pathogenesis [26,204,315]. A striking feature of HIV-associated DSP is the development of severe dysaesthetic pain [26] which may be unresponsive to analgesia, even in combination with anticonvulsants [204], tricyclic antidepressants [316], mexiletine [316], or Peptide T [317]. Accordingly, withdrawal of certain NRTI's often becomes necessary [26,204] since no effective therapies for DSP are currently available, despite the recent promise shown by recombinant nerve growth factor (rhNGF) [229], and changes in the prescribing pattern of these drugs have led to a reduction in the incidence of PN [26]. As a result there is a need for a pathogenesis-based treatment for DSP which would allow patients to remain upon NRTI therapy, which remains the keystone of current highly active antiretroviral therapy (HAART) regimes [318].

DSP is currently thought to be a result of disrupted mitochondrial oxidative metabolism [203,315] secondary to a reduction in neuronal mitochondrial DNA content [202,315,319], which makes the neurons unable to maintain long peripheral axons, resulting in the glove and stocking distribution of DSP [204] (cf. *1.4*). In keeping with this die-back hypothesis, epidermal innervation is known to be reduced in DSP [320], although the

innervation of the dermis and sweat glands remains to be formally quantified. The development of an abnormal sweating pattern in DSP suggests that an autonomic neuropathy also develops, and this may also be a factor in the nocturnal sweating common in HIV disease [321].

Since DSP is a chronic condition that involves axonal die-back, there are considerable similarities with the situation found after chronic peripheral nerve transection as a result of trauma. In both conditions the target organs and distal segments of peripheral nerve are chronically denervated, and axonal regeneration is the key to restoring normal sensory function and target derived neurotrophic support. Although there is a persistent insult to the neurons in DSP, unlike chronic nerve transection, both conditions are likely to involve disruption of mitochondrial energy metabolism. In nerve transection this leads to significant sensory neuronal death, whereas in DSP the effect is more subtle, making neurons unable to sustain long peripheral axons. A therapy that could induce peripheral nerve regeneration in DSP may therefore be of benefit in the setting of peripheral nerve trauma, and regeneration after repair.

L-Acetyl-Carnitine (LAC) has been proposed as a therapeutic agent for DSP. The acetyl ester of L-carnitine, LAC is vital for normal mitochondrial function, being a physiological transport molecule for free fatty acids, and an important acetyl-group donor in high energy metabolism and β-oxidation of free fatty acids [246,247]. In addition, LAC potentiates the actions of NGF [244,245,297], promotes peripheral nerve regeneration [298], and has been shown to be neuroprotective both in vitro [244,248] and in animal models of diabetic neuropathy [322]. LAC has analgesic properties, possibly mediated by increasing ACTH and β-endorphin levels [323], whilst its non-acetylated form, L-carnitine, also has favourable immunological benefits [324] in HIV infection. Furthermore, short term LAC treatment [301] has shown symptomatic benefits in DSP, although it is not known if this effect is long-lasting, or whether it is due to neuronal regeneration, or merely to an analgesic effect.

This study was therefore designed to determine the effect of long term LAC therapy upon symptoms and cutaneous innervation in patients with DSP, by using quantitative immunohistochemistry with fibre-type specific antisera, a technique that has previously been found to be more sensitive than clinical assessment of diabetic neuropathy [25].

8.2 Methods

This study was performed in agreement with the terms of the Helsinki Declaration, after appropriate review by the local research ethics committee. Five asymptomatic HIV negative controls, and an open observational cohort of 5 patients with established NRTI therapy related DSP (Grade 2-4/4 by analgesic requirement) were recruited. Selection criteria included anyone aged 20-50 years, of either sex, with a documented positive licensed HIV-antibody ELISA test [Roche v1.5, or Cobas v1.5], and a diagnosis of stable DSP (onset within 6-12 months of commencing NRTI therapy, symptoms stable for >3 months, and no other neuropathic aetiological factors or therapies associated with DSP). The median age of the neuropathic patients at recruitment was 34 years (range 30-44), and was 32 years (range 29-53) for controls. The controls had tested negative for HIV antibodies within the previous 3-12 months, had no neuropathic symptoms or signs, and had no history of diabetes, metabolic disorders, alcohol abuse, or treatment with potentially neurotoxic agents.

Patients received six months of treatment with oral LAC capsules [Sigma-Tau, Italia] at a dose of 1500mg b.d., and all other medications were managed on a clinical basis.

As an outpatient procedure under local anaesthesia 1cm x 0.5cm skin biopsies were excised from an anatomically standardised point in the lower third of whichever leg was felt to be more symptomatic by the patient (cf. *2.3.4*). Biopsies were taken prior to commencing LAC therapy ("pre-treatment"), and again from a neighbouring site in the same leg after 6 months of treatment ("post-treatment"). A single biopsy was taken from an equivalent site in each control.

All staining and quantification (cf. *2.4.5, 2.5.3*) was performed by one masked individual to eliminate inter-observer error, and both pre- and post-treatment biopsies were processed together in order to eliminate minor variabilities between staining runs. A systematic random sample of 15μm vertical cryosections [325] from each biopsy was collected (cf. *2.4.1a & 2.4.2c*), and stained (cf. *2.4.5*) by indirect immunohistochemistry using primary antisera against protein gene product 9.5 (PGP9.5.), calcitonin gene related peptide (CGRP), and vasoactive intestinal polypeptide (VIP). Antisera against PGP9.5 bind to all fibre-types, since PGP9.5 is a constitutive component of all nerve fibres, whereas antisera against the peptide neurotransmitter CGRP are specific for the C, Aδ fibres of small sensory neurons, and antisera against VIP are specific for cholinergic,

sympathetic postganglionic efferent fibres. Staining was visualised using a fluorescein conjugated secondary antibody (FITC-conjugated goat anti-rabbit serum,).

The area of immunostaining with each antibody, approximates closely to the actual area of each type of nerve fibre present, was then quantified (cf. *2.5.3*) in a systematic random sample of 6 visual fields including both epidermis and dermis (PGP9.5 & CGRP), or subcutaneous sweat glands alone (PGP9.5 & VIP). Innervation was then expressed either as a total area (μm^2), or as a fraction of the total area of interest, whether that was epidermis, dermis, or sweat gland ("fractional area of immunostaining"). The pre-treatment level of innervation could then be compared to that found after treatment with LAC (i.e. change in fractional area of immunostaining, expressed as a percentage of the pre-treatment value), and both results compared to the level of innervation found in non-neuropathic HIV negative controls. Statistical comparison was performed using the techniques described previously (cf. *2.5.7*).

8.3 Results

8.3.1 Clinical and Immunological Parameters

In the patients with established DSP the mean duration of neuropathy prior to recruitment was 34 (standard deviation 42) months, and none had a history of diabetes, or metabolic disorders. Patient 1 had persistent NRTI induced DSP, which had remained constant despite withdrawal of ddI therapy 8 years prior to recruitment, whilst the other 4 patients remained on NRTI therapy during the full course of the study (patient 2, lamivudine (3TC); patient 3, 3TC & D4T; patients 4 & 5, D4T & ddI). Only patient 5 had a previous history of alcohol excess, but had no alcohol related illness and had stopped drinking three years before recruitment (18 months prior to onset of neuropathy). Similarly, only patient 3 had received treatment with another potentially neurotoxic agent, having taken a course of dapsone 100mg/day several years prior to the onset of his neuropathy.

Clinical grade of neuropathic pain fell significantly from a median of 3 (range 2-4) at recruitment, to 2 (range 1-2) after six months of LAC treatment ($p=0.016$), and patients also described an improvement in general well-being and quality of life, although this was not formally assessed. Viral load (pre-treatment 204650 copies/ml (cpm), SD 311517; post-treatment 192550cpm, SD 284473; $p=0.923$), CD4 positive T-cell count (pre-treatment 232/μl, SD 127; post-treatment 264/μl, SD 244; $p=1.00$), and CD4 count as percentage of total T-cell count (pre-treatment 13.0%, SD 4.90; post-treatment 17.4%, SD 11.6; $p=0.457$) did not alter significantly over the study period, however the CD4/CD8

ratio did increase (pre-treatment 0.20, SD 0.094; post-treatment 0.43, SD 0.68; p=0.008). LAC treatment was well tolerated; no side effects were described, and no adverse events, or wound complications at biopsy sites occurred.

8.3.2 Immunohistochemistry – Morphology of Cutaneous Innervation

Representative photomicrographs are shown in Figures 8.1-8.4.

A normal pattern of cutaneous innervation was present in the control biopsies. The cutaneous innervation derived from a plexus of fibres in the reticular dermis which fed either into plexi enveloping individual sweat glands, or into the plexus of finer sub-epidermal fibres which ran parallel to the surface of the skin within the papillary dermis (*Figures 8.1C, 8.2C*). These fibres either terminated in sensory organs lying in the region of the dermo-epidermal junction, or sent branches up the dermal papillae to enter the epidermis as free-end terminals. Within the epidermis fibres either ran perpendicular to the surface of the skin, or ended in fine branches lying parallel to the base of the stratum corneum. PGP9.5 immunoreactive fibres predominated in all regions of the skin, whilst CGRP positive fibres lay principally in the sub-epidermal plexus (*Figure 8.3C*), and deeper layers of the epidermis, and VIP positive fibres enveloped the sweat glands (*Figure 8.4C*).

In the skin of patients with established DSP there was an almost complete absence of fibres within the epidermis, and both the sub-epidermal plexus, and the plexi surrounding individual sweat glands were atrophied (*Figures 8.1A & 8.2A*), as were the sweat glands themselves. LAC treatment was associated with a general normalisation of morphology, although epidermal fibres remained less evident than in the skin of controls (*Figures 8.1B, 8.2B*).

8.3.3 Immunohistochemical Quantification - All Fibre Types (PGP9.5)

The effect of LAC treatment upon cutaneous innervation in each of the patients with established DSP, as determined by quantitative immunohistochemistry is given in Table 8.1, where positive values reflect an increase in innervation after treatment and negative values reflect a decrease. Table 8.2 shows the cutaneous innervation of the DSP cohort as a whole, compared to that of the asymptomatic controls.

In summary, the data presented in these tables show that when compared to controls, patients with established DSP exhibited reduced innervation of the epidermis (51% of control), dermis (49%) and, most markedly, of the sweat glands (25%) (Table 8.2). LAC treatment subsequently caused a significant ($p<0.05$) overall increase in innervation within the epidermis and dermis, and a highly significant ($p<0.001$) increase within the sweat glands (Table 8.1), although Patient 4 exhibited insignificant reductions in

Figure 8.1: Effect of LAC Treatment Upon Cutaneous Innervation by All Fibre Types

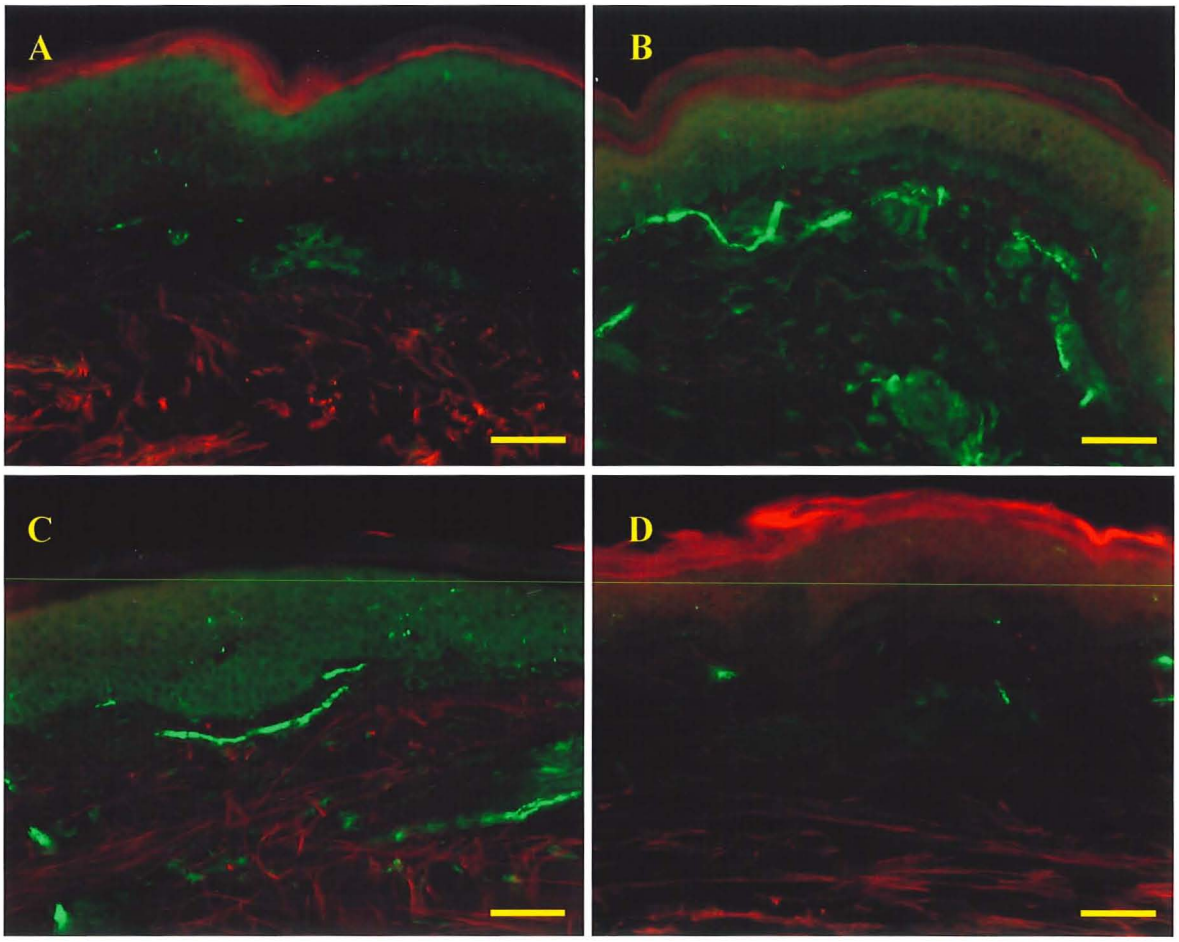

Photomicrographs of vertical sections through skin biopsies stained by indirect immunofluorescence using a primary antiserum to PGP 9.5. Nerve fibres show as green fluorescence, against the red of the non-specific stain Pontamine Sky Blue. Cutaneous nerve fibres are scarce, and atrophic in established DSP [A], but after 6 months of LAC treatment (1500mg b.d.) [B] innervation increases to normal levels in the dermis, although epidermal innervation remains less than that found in normal controls [C]. Six months after stopping LAC treatment innervation is reduced [D]. Scale bar equals 40µm.

Figure 8.2: Effect of LAC Treatment Upon Sweat Gland Innervation by All Fibre Types

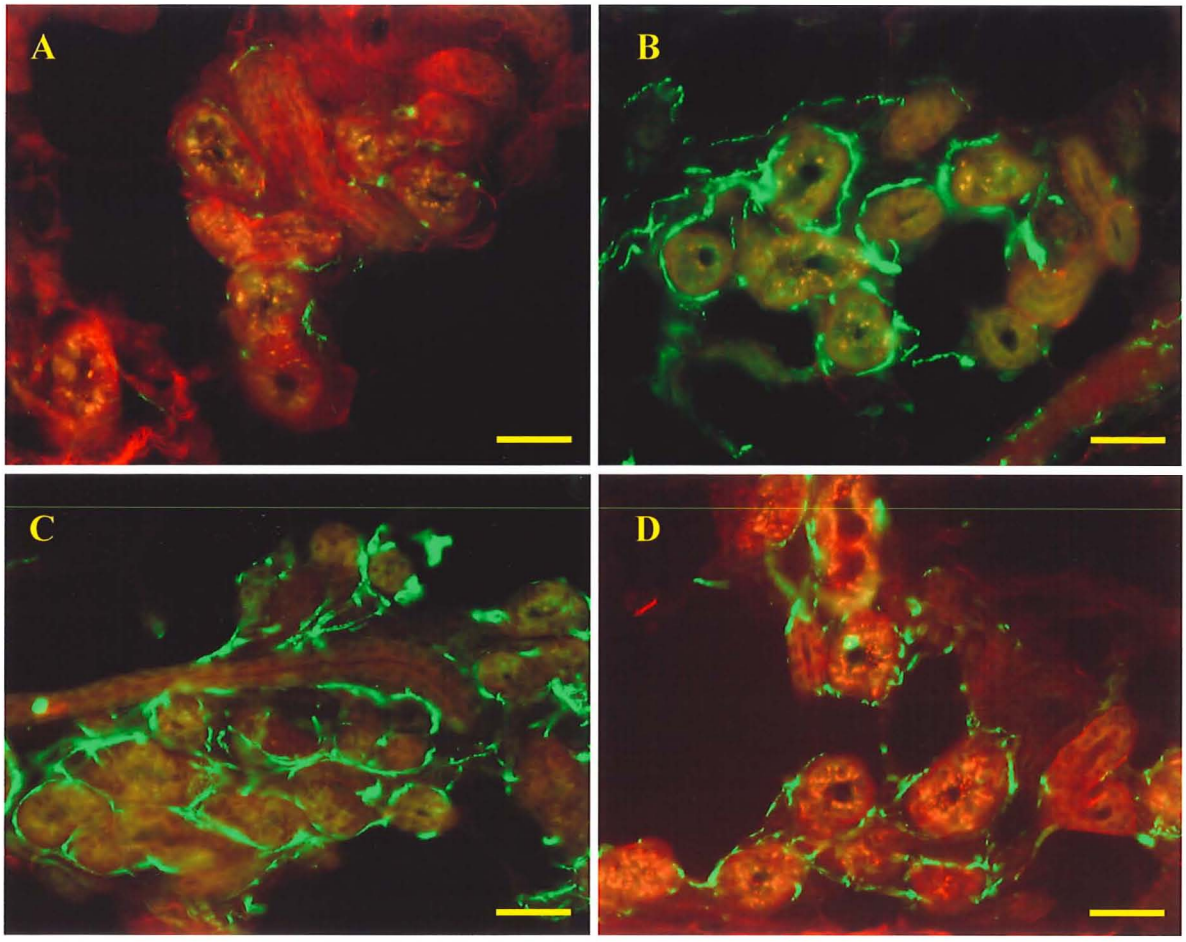

Photomicrographs of sections through skin biopsies stained by indirect immunofluorescence using a primary antiserum to PGP 9.5, and showing the innervation of the dermal sweat glands. Nerve fibres show as green fluorescence, against the red of the non-specific stain Pontamine Sky Blue. Nerve fibres are scarce, and atrophic in established DSP [A], but after 6 months of LAC treatment (1500mg b.d.) [B] innervation by all fibre types increases to normal levels [C]. Six months after stopping LAC treatment innervation is reduced [D]. Scale bar equals 40μm.

Figure 8.3: Effect of LAC Treatment Upon Cutaneous Innervation by Small Sensory Fibres

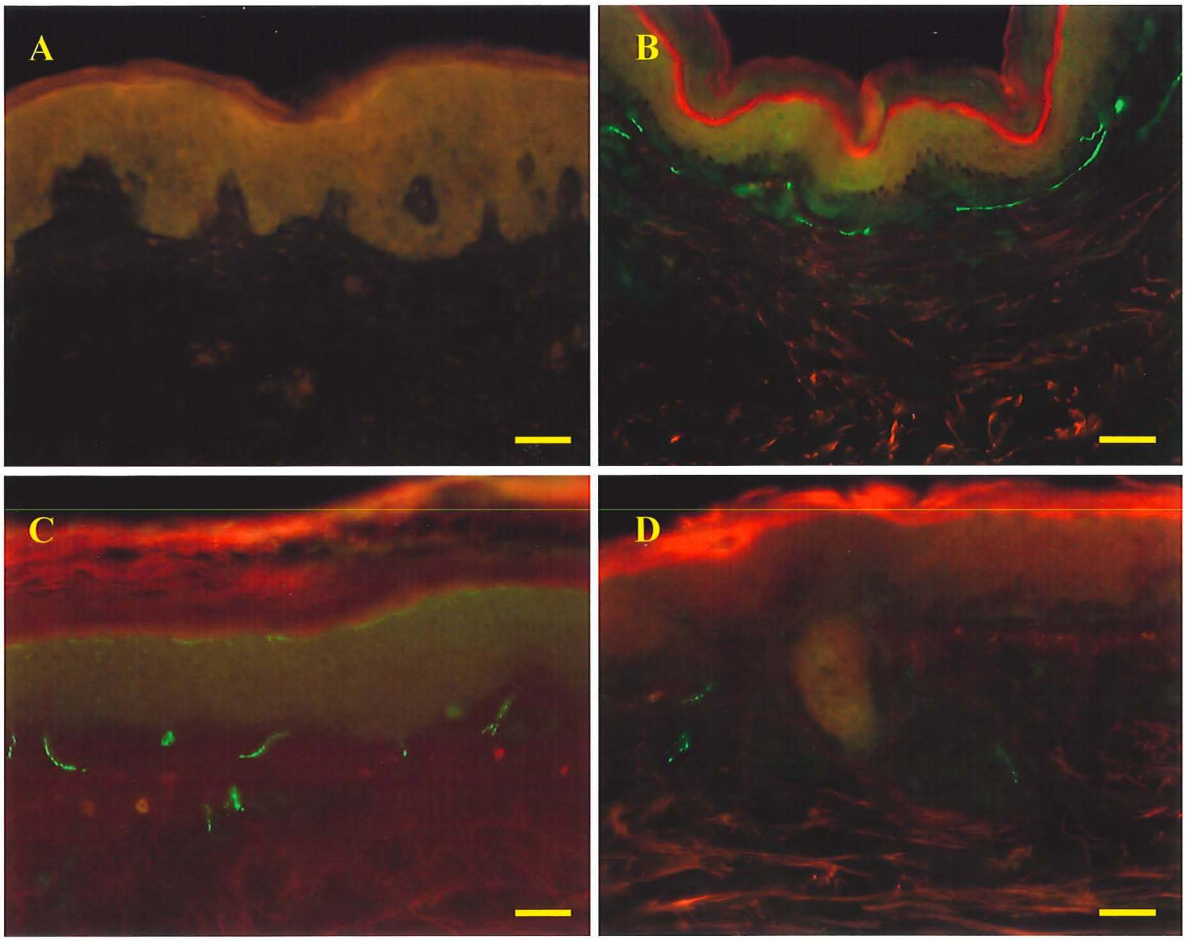

Photomicrographs of vertical sections through skin biopsies stained by indirect immunofluorescence using a primary antiserum to CGRP. Small sensory nerve fibres show as green fluorescence, against the red non-specific staining of Pontamine Sky Blue. Cutaneous fibres are almost entirely absent in established DSP [A], but after 6 months of LAC treatment (1500mg b.d.) [B] innervation by small sensory (C,Aδ) fibres increases to supranormal levels in the dermis, although epidermal innervation remains sparse compared to HIV negative, non-neuropathic controls [C]. Six months after stopping LAC treatment innervation is reduced [D]. Scale bar equals 40μm.

Figure 8.4: Effect of LAC Treatment Upon Sweat Gland Innervation by Cholinergic Sympathetic Fibres

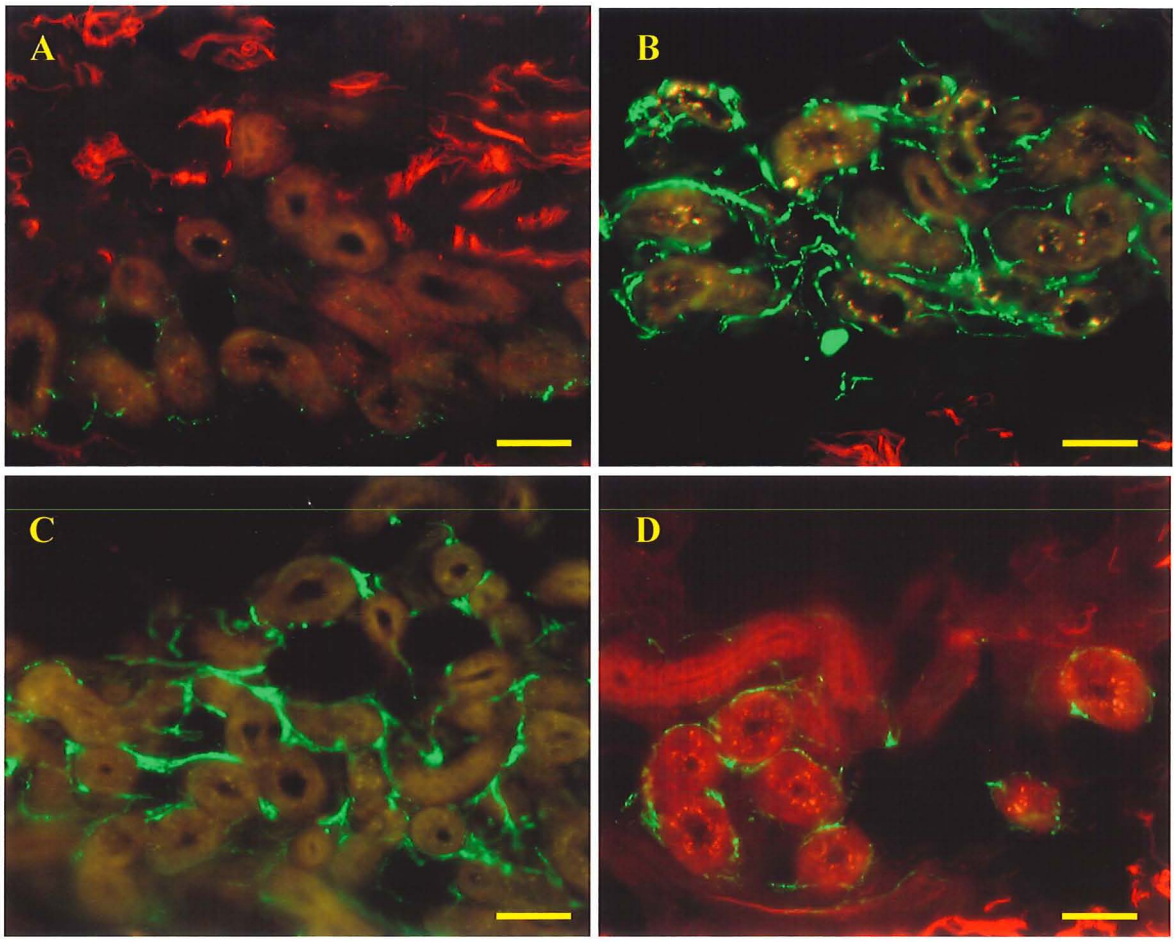

Photomicrographs of sections through dermal sweat glands stained by indirect immunofluorescence using a primary antiserum to VIP. Cholinergic sympathetic efferent nerve fibres show as green fluorescence, against the red of the non-specific stain Pontamine Sky Blue. Fibres are scarce, and atrophic in established DSP [A], but after 6 months of LAC treatment (1500mg b.d.) [B] innervation increases to normal levels [C]. Six months after stopping LAC treatment innervation is reduced [D]. Scale bar equals 40µm.

Table 8.1: Percentage Change in Fractional Area of Immunostaining After LAC Treatment

Anatomical Area:	Epidermis		Dermis		Sweat Glands	
Antiserum:	**PGP**	**CGRP**	**PGP**	**CGRP**	**PGP**	**VIP**
Patient 1	223%*	41%	5117%*	12401%*	212%*	133%*
Patient 2	69%	1363%	61%*	294%	328%*	71%
Patient 3	96%	359%	-21%*	111%	44%	67%
Patient 4	-65%	750332%	-42%	109%	737%*	5109%
Patient 5	222%*	1639%**	241%	1407%	373%*	272%*
Mean	**60%***	**599%****	**123%***	**445%****	**309%****	**295%****

Percentage change for each individual equals the difference between the pre- and post-treatment fractional areas of immunostaining, expressed as a percentage of the pre-treatment value (positive values reflect an increase in innervation, whilst negative values reflect a decrease).

* P value < 0.05, ** P value <0.001 post-treatment innervation compared to pre-treatment.

Table 8.2: Effect of LAC Treatment Upon Cutaneous Innervation in DSP Patients Compared to Non-Neuropathic HIV Negative Controls

	Antiserum:	Controls		Pre-Treatment		Post -Treatment	
		Total Area (µm2)	Fractional Area	Total Area (µm2)	Fractional Area	Total Area (µm2)	Fractional Area
Epidermis	PGP	89.91 (56.12)	0.00254 (0.00162)	55.17* (52.07)	0.00130** (0.00134)	80.66 (60.57)	0.00185 (0.00137)
	CGRP	33.46 (69.81)	0.00109 (0.00200)	3.83* (13.33)	0.0000557* (0.000199)	20.39 (27.25)	0.000539 (0.000689)
Dermis	PGP	690.87 (376.53)	0.00764 (0.00471)	344.43** (331.08)	0.00375** (0.00348)	692.14 (699.12)	0.00780 (0.00838)
	CGRP	142.21 (125.56)	0.00159 (0.00153)	56.49** (78.67)	0.000629* (0.000968)	303.67* (288.20)	0.00343* (0.00360)
Sweat Glands	PGP	2492.23 (2554.10)	0.0436 (0.0404)	768.90** (710.17)	0.0110** (0.00925)	3462.55* (2369.99)	0.0454 (0.00838)
	VIP	2236.73 (1983.50)	0.0358 (0.0157)	990.96** (1155.32)	0.0140** (0.0163)	2527.47 (2103.26)	0.0383 (0.0207)

Values stated are the mean (SD) total area of immunostaining (2 decimal places), and fractional area of immunostaining (3 significant figures) for each antibody in each anatomical area of interest (epidermis, dermis, or sweat glands) within the skin.

* P value < 0.05, ** P value <0.001 compared to control.

epidermal and dermal innervation, and Patient 3 showed a significant fall in dermal innervation (21%, p=0.025). Whilst epidermal innervation remained reduced after LAC treatment (73% of control), innervation of both the dermis (102% of control) and sweat glands (104%) normalised completely (Table 8.2).

8.3.4 Immunohistochemical Quantification - Small Sensory (C, Aδ) Fibres (CGRP)

Dermal innervation with CGRP positive fibres was significantly reduced (40% of control) in established DSP, whilst epidermal innervation was almost absent (5% of control). Highly significant increases occurred in both epidermal (mean 599%) and dermal (mean 445%) innervation after 6 months of LAC treatment (Table 8.2). Innervation increased in every patient (Table 8.1), such that the mean fractional area of immunostaining reached 49% of control in the epidermis, and 216% of control in the dermis.

LAC treatment was also found to increase the proportion of all nerves (PGP 9.5 positive) which displayed CGRP immunoreactivity in both the epidermis (pre-treatment 4%; post-treatment 29%; control 43%), and the dermis (pre-treatment 17%; post-treatment 44%; control 21%).

8.3.5 Immunohistochemical Quantification - Sympathetic Sudomotor Fibres (VIP)

The reduction in sympathetic efferent innervation of the sweat glands (VIP positive fibres, 39% of control) which was found in patients with established DSP was less than the reduction in their total innervation (PGP9.5 positive fibres, 25% of control) (Table 8.2). This was matched by atrophy of the sweat glands themselves, since the total area of sweat gland present within the sections examined was only 68% of control (p=0.039). Innervation increased in every patient after LAC treatment (Table 8.1), with the result that the mean fractional area of staining reached the same level as that found in controls (107% of control), as did the area of the sweat glands themselves (117% of control, p=0.322). The proportion of the total innervation (PGP9.5 positive) which was due to VIP immunoreactive fibres also returned to normal (pre-treatment 127%; post-treatment 84%; control 82%).

8.3.6 Effect of Withdrawing LAC Treatment

All patients continued to be followed in clinic after the second biopsy. Patients who discontinued LAC treatment after the initial 6 months have described a worsening of neuropathic symptoms or a reduction in their sense of well-being, in some cases beginning

within days of ceasing treatment. Those who have remained on LAC treatment have continued to show symptomatic improvement.

A third skin biopsy was obtained from Patient 1 six months after discontinuing LAC treatment, by which time he was suffering from Grade 4 neuropathic pain. Quantification of this biopsy revealed a decrease in the innervation of all areas of the skin examined, by all fibre types assessed (Table 8.3, *Figures 8.1D-8.4D*). Small sensory fibres showed the greatest overall reduction, and although innervation generally remained better than that found prior to commencing LAC treatment, CGRP immunoreactivity in the epidermis was less than in the initial baseline biopsy.

8.4 Discussion

8.4.1 Methodology

In the patient cohort NRTI induced DSP was diagnosed by a neurologist. All patients had stable DSP prior to recruitment, making spontaneous resolution unlikely to have accounted for the changes in symptoms and innervation that were found.

Immunohistochemical quantification (IC) of cutaneous innervation has previously been found to correlate with clinical tests of sensory function in leprosy [326], and in diabetic neuropathy [327], where during the course of the disease IC changes precede those of sensory testing [25]. The morphology of cutaneous innervation in DSP has previously been described qualitatively, and the density of epidermal fibres shown to be reduced along a proximal to distal gradient [320]. However fibre counts do not assess the health of surviving fibres, whose atrophy or regeneration can be quantified by determination of the area of immunostaining, as used in this study.

8.4.2 Cutaneous Innervation is Decreased in Established Distal Symmetrical Polyneuropathy (DSP)

Since PGP9.5 is a constitutive component of peripheral nerve fibres any decrease in immunoreactivity will reflect actual loss or atrophy of fibres rather than a reduction in function of surviving fibres, which is an additional cause of decreased immunoreactivity for fibre-type specific neuropeptide transmitters (e.g. CGRP, or VIP). It is therefore evident that in established DSP symptoms do reflect a reduction in the cutaneous innervation of the lower leg. Epidermal innervation is most affected, in keeping with the dieback hypothesis of sensory neuropathy [26], although there is also marked atrophy of the dermal and sweat gland plexi. This cutaneous denervation may explain the finding that neuropathic symptoms frequently do not begin to resolve for some weeks after starting

Table 8.3: Effect of Withdrawal of LAC Treatment Upon Cutaneous Innervation in a Patient with DSP

	Antiserum:	Pre-Treatment Fractional Area	Post-Treatment Fractional Area	Final Biopsy Fractional Area	% Reduction After Stopping Treatment
Epidermis	PGP	0.000481 (0.000544)	0.00156 (0.000583)	0.000886 (0.00143)	43%
	CGRP	0.000161 (0.000391)	0.000227 (0.000447)	0.000010 (0.000025)	96%*
Dermis	PGP	0.000355 (0.000313)	0.0185 (0.0111)	0.00155 (0.00114)	92%*
	CGRP	0.000045 (0.000050)	0.00563 (0.00321)	0.000398 (0.000408)	93%*
Sweat Glands	PGP	0.0149 (0.00557)	0.0464 (0.0112)	0.0252 (0.00557)	46%*
	VIP	0.0243 (0.00481)	0.0567 (0.0204)	0.0264 (0.0129)	53%

Values stated are the mean (SD) fractional area of immunostaining (3 significant figures) for each antibody in each anatomical area of interest (epidermis, dermis, or sweat glands) within the skin. Percentage reduction after stopping LAC treatment equals the fractional area of immunostaining found after 6 months of LAC treatment ("Post-Treatment") minus that found 6 months after ceasing LAC treatment ("Final Biopsy"), expressed as a percentage of the "post-treatment" value.

* P value < 0.05, ** P value <0.001 compared to control.

LAC treatment, and may then continue to improve for many months, since this timeframe matches the slow rate at which peripheral nerves regenerate.

As might be expected from the dysaesthetic algesic symptomatology of DSP, it is the small sensory (C, Aδ) fibres that are most affected, since this fibre type shows the greatest reduction in area of immunostaining when compared to normal controls. Furthermore, since the proportion of all fibre staining (PGP9.5) that was due to CGRP immunoreactivity was also markedly reduced in the epidermis (DSP 4%; control 43%), there is not only a loss of epidermal fibres, but also a reduction in function of the small sensory fibres that do survive. In contrast, the preservation of the CGRP:PGP9.5 ratio (DSP 17%; control 21%) in the dermis suggests that fibre loss or atrophy predominates, as also seems to be the case in the sweat glands where the VIP:PGP9.5 ratio remained unchanged (DSP 82%; control 84%).

8.4.3 L-acetyl-carnitine (LAC) Treatment Improves Cutaneous Innervation and Symptoms in Distal Symmetrical Polyneuropathy (DSP)

Six months of oral treatment with LAC resulted in significant increases in the innervation of the epidermis, dermis, and sweat glands. The PGP 9.5 results demonstrate that cutaneous nerve fibres did actually regenerate sufficiently that both dermal and sweat gland innervation reached the level found in normal skin. Intra-epidermal fibres also regenerated, although epidermal innervation did not reach a normal level either because epidermal innervation is reduced in non-neuropathic patients with HIV [320], or because reinnervation occurs more slowly in the epidermis than in other tissues [328], implying a need for greater than 6 months of LAC treatment. A study comparing the epidermal innervation of patients with DSP after prolonged LAC treatment (>12 months), to that of non-neuropathic HIV positive individuals is underway to address this question.

The increased ratio of CGRP and VIP to PGP9.5 immunostaining which was found after LAC treatment is a feature of regenerating nerve fibres, and also suggests that the reinnervating fibres were functional, although electrophysiological and sensory testing will be required to confirm this. The increase in dermal CGRP immunoreactivity to supranormal levels is likely to reflect the fact that regeneration into the epidermis was not complete, with the result that anterogradely transported CGRP accumulated in the dermal part of the fibres due to a distal "damming" effect, as has been described in early diabetic neuropathy [25].

Although LAC treatment resulted in a significant reduction in the grade of neuropathic pain experienced by subjects in this study, randomised controlled trial (RCT)

data utilising a validated visual analogue pain scale will be required to conclusively demonstrate a symptomatic benefit. A RCT is now underway which will provide this data, along with formal electrophysiology and thermal threshold testing to determine the functional effect of LAC treatment in DSP.

Whilst there was no placebo arm to this study, the natural history of untreated DSP, plus the return of symptoms and worsening of cutaneous innervation after cessation of LAC treatment in patient 1, suggests that the beneficial effects found in the patient cohort were a result of LAC treatment. Consideration of the mechanism by which LAC treatment may have effected such an improvement first requires an explanation of the pathogenesis of NRTI therapy associated DSP.

8.4.4 Mechanism of Action

Although the pathogenesis of DSP has not been entirely clarified, the DNA polymerase-γ hypothesis remains the most powerful explanation [202]. In eukaryote cells DNA is polymerised from individual deoxynucleotide triphosphates (dNTP) by DNA polymerase, the γ and β-isoforms of which are significantly inhibited by the dideoxynucleotide triphosphate (ddNTP) NRTI's [315]. Unlike nuclear DNA (nDNA) replication, mitochondrial DNA (mtDNA) replication is solely dependent upon the γ-isoform, inhibition of which is greatest in non-mitogenic cells where only mtDNA is replicated [202,315]. Due to its proximity to the free radical species generated by the respiratory chain complexes mtDNA is particularly liable to damage, and since there are no mtDNA repair mechanisms overall oxidative metabolic function must be maintained by replication [315]. Hence by impairing mtDNA replication, NRTI's reduce the cell's capacity for oxidative phosphorylation, which is the critical energy pathway in neurons. As a result neurons may apoptose [310], or fail to meet the metabolic requirements for maintaining long peripheral axons resulting in a die-back, glove and stocking neuropathy.

LAC treatment may therefore counteract ddNTP NRTI toxicity by several mechanisms. Firstly, it may reduce mtDNA damage by a direct antioxidant effect [295,296]. Secondly, LAC facilitates mitochondrial homeostasis of acetyl-CoA, promotes long-chain free fatty acid transport across mitochondrial membranes [247], and via regulation of malonyl-CoA promotes cytosolic FFA oxidation [294]. By promoting glucose utilisation and high-energy substrate oxidative metabolism, LAC thereby improves neuronal metabolic capacity [329]. In addition LAC may facilitate distal neurotrophic support, particularly of small myelinated and unmyelinated (C, Aδ) nociceptive neurons, since it increases NGF binding capacity [297], enhances the response to NGF [245], and promotes neurite extension in

response to NGF [244]. Furthermore, LAC promotes peripheral nerve regeneration [298] and function [249,304,330,331] independently of NRTI toxicity. Also, patients with NRTI associated peripheral neuropathy have reduced serum LAC levels, but asymptomatic HIV positive controls do not [332]. LAC penetrates the blood-brain barrier [302], and serum levels can be increased by oral or parenteral administration of LAC [303,333], which also reverses the depletion of LAC content that occurs in the peripheral nerves of diabetic rats [322].

8.4.5 Other Potential Benefits of L-acetyl-carnitine (LAC) Treatment

LAC may offer additional benefits in the management of HIV infection since the mitochondrial pathogenesis of DSP shares similarities with that of the lipodystrophy syndrome [334] that is associated with highly active antiretroviral therapy (HAART) [335]. Lipodystrophy may therefore be responsive to LAC treatment. Furthermore, the related compound L-carnitine (with which LAC equilibrates in-vivo) improves CD4 positive T-cell counts by limiting ceramide production and apoptosis [336-339] and by promoting mononuclear cell proliferation [336]; serum lipid profiles [337], and exercise capacity [340] may also improve. In this study an oral dose of 1500mg b.d. of LAC was safe, well tolerated, and unlike rhNGF treatment [324] no side effects occurred. LAC treatment was not associated with any progression of HIV infection; in fact the viral load fell, small increases in both absolute and percentage CD4 counts were found, and the CD4/CD8 ratio doubled ($p=0.008$).

8.4.6 Implications

Although nucleoside analogue antiretroviral agents have been partly superceded by other agents such as the protease inhibitors, they remain fundamental elements of combination therapy [26,318] and are likely to remain important components in the management of HIV for the foreseeable future [26]. Peripheral neuropathy has been the principal complication limiting the use of several of these agents [26,204], and LAC may now offer an effective, pathogenesis based approach to management, which can allow patients to remain on NRTI therapy. A full randomised controlled trial is now underway to attempt to validate the results of this study, and to determine the required duration of LAC treatment.

Chapter 9. Discussion

An estimated 300,000 peripheral nerve injuries occur each year in Europe alone, and yet even after optimal surgical repair sensory outcome remains disappointingly poor [5,6,9], such that "no adult with a major nerve transection has ever attained normal sensibility" [10]. That is the case even after primary repair of clean injuries, and it is accepted that outcome is even worse in the case of chronic nerve injuries, and those requiring nerve grafting [5,6]. Sensory outcome also impacts adversely upon motor outcome due to loss of normal proprioceptive feedback for motor control [15], and peripheral nerve injuries are therefore a major cause of morbidity, healthcare expenditure, and social disruption [6].

Quality of sensation depends upon the number of innervating neurons, so it is likely that the single most important determinant of poor sensory outcome after surgical repair of peripheral nerve injuries is the death of a large proportion of the sensory neuronal pool [19], although various other factors are also implicated [5,17,18]. Sensory neuronal death after peripheral nerve injury was first reported in the early 20th century, and subsequent studies have demonstrated that up to 50% neuronal loss occurs [55,96-98,102,107,108,111,118], that a similar magnitude of neuronal death does occur clinically [115], and that DNA fragmentation occurs [92,98,100,102]. Although sensory neuronal death was well recognised, it was not known how soon after nerve injury neuronal death begins, how long the period of neuronal death lasts for, and what effect peripheral nerve repair, and its timing after injury, had upon the magnitude of neuronal death. Administration of exogenous neurotrophic factors was known to reduce neuronal death in an experimental setting [47], but its immediate clinical applicability was questionable [7] (cf. *1.6*) and so a pressing need existed for alternative strategies with more immediate clinical potential.

The initial aim of this project was therefore to describe the timecourse of primary sensory neuronal death (cf. *Chapter 3*) in order to identify logical timepoints at which to test neuroprotective strategies, and to define a therapeutic window for the future clinical application of any successful strategies. Consideration of the pathogenetic events underlying neuronal death then led to the hypothesis that early surgical repair (cf. *Chapter 4*), and N-acetyl-cysteine (cf. *Chapter 5*) would reduce sensory neuronal death. Finally, the similarities between the effects of peripheral axotomy and the pathogenesis of distal symmetrical polyneuropathy neuropathy in HIV disease lead to the investigation of L-acetyl-carnitine (cf. *Chapters 6-8*) as a clinically applicable treatment which might

improve peripheral nerve regeneration and reduce sensory neuronal death after peripheral nerve injury.

Death of individual neurons was identified by TUNEL (cf. *1.4, 2.4.3, 2.5.1*), and the magnitude of neuronal loss was quantified from statistically unbiased stereological neuron counts obtained using the optical disector technique (cf. *1.4, 2.4.3, 2.5.2*). Sensory neuronal death within axotomised L4&5 dorsal root ganglia (DRG) began within 24 hours of injury, although this did not translate into actual neuron loss until 7 days after axotomy, reflecting the time taken for individual neurons to progress from DNA fragmentation to eventual involution and loss (cf. *3.4.4*). Neuronal death peaked 2 weeks after axotomy, as shown by TUNEL, and neuronal loss was virtually complete by 2 months after axotomy. Although neurons were still dying 6 months after injury, as shown by the presence of occasional TUNEL positive neurons, death occurred at a sufficiently low rate that the neuronal loss at 4 & 6 months after injury was not significantly different to that found at 2 months (cf. *3.4.4*). Around 40% of the entire sensory neuronal pool died by a process that did not exclusively involve apoptotic morphological features, and this was accompanied by a secondary wave of satellite cell death, which reached a peak 2 months after sciatic nerve transection (cf. *3.4.7*).

The experimental timepoints of 2 weeks and 2 months after injury were therefore adopted as reflecting the peaks of both neuronal death (TUNEL) and neuronal loss. Of more clinical relevance, it would appear that strategies to reduce neuronal death should ideally be implemented within 24 hours of injury, although intervention within 2 weeks of injury should still cause a significant reduction in neuronal death, and up to 2 months after injury some benefit may be accrued. However interventions later than this are unlikely to have any significant neuroprotective benefit. How precisely these results from a well-defined rat model can be applied to the more diverse clinical situation found in man is not certain, although it is likely that the overall pattern will be similar. Repeating this study in another animal model, such as the rabbit, and using lesions at different distances from the DRG may help to answer this question. Alternatively it may be possible to adapt in-vivo clinical techniques such as functional magnetic resonance imaging (fMRI) [341] and magnetic resonance neurography [342] for the estimation of sensory neuronal death, or to estimate DRG volume by high resolution MRI scanning, since changes in DRG volume were related to neuronal loss (cf. *3.4.6*).

Sensory neuronal death is reduced by exogenous growth factor administration after peripheral nerve injury [47,105,106,109,148,167,217] . Surgical nerve repair involves co-apting the axons in the proximal stump to the neurotrophic factory that is the distal nerve stump

[47,48,69], and may therefore be the simplest way to restore neurotrophic support and limit neuronal death. Despite prolonged debate over the optimal timing of surgical repair [6,11,13,42] the effect upon neuronal death has not been given due consideration, and although early repair is now generally recommended for most nerve injuries [5,6,11], nerve transections still do not have priority for access to theatre facilities. As a result they are frequently not repaired for some days, and closed injuries are generally left for a diagnostic period of several months prior to exploration [6].

Nerve repair has now been demonstrated to markedly reduce sensory neuronal death, and the principle that the neuroprotective benefit is greater the earlier repair is performed has been established (cf. *4.4.2*). It would therefore seem that where there is no contraindication, it is inadvisable to delay nerve repair even by 24 hours, and that early secondary nerve repairs [11] should be performed within two weeks of injury, and late secondary nerve repairs [11] within two months (cf. *4.4.3*). Since immediate repair will never be clinically feasible for the majority of injuries, further studies using larger experimental groups are now needed to determine the effect of short delays (6-48 hours) upon neuronal death. Alternatively, retrospective clinical studies could seek differences in sensory outcome between patients who underwent nerve repair at different times after injury, although it would be difficult to obtain sufficient numbers of patients with adequately standardised injuries to reliably detect any difference given the relative insensitivity of current clinical sensory tests.

Despite the reduction in sensory neuronal death that can be achieved by early peripheral nerve repair, there is still a clinical need for an adjuvant neuroprotective therapy. Neuronal death was not entirely eliminated even by immediate nerve repair (cf. *4.3*), and yet many patients are unlikely to undergo surgical repair within 8-12 hours of injury in even the best organised of trauma services. There is also a need to reduce the neuronal death that occurs after closed injuries, since these may not be explored until after several months of diagnostic delay [6] and may represent simple crush injuries (axonometsis). Nerve repair would not benefit these latter injuries, but significant sensory neuronal death may still occur [107]. Clinically applicable pharmaceutical agents were therefore sought which might reduce sensory neuronal death.

The mechanism by which axotomy effects neuronal death is thought to involve loss of distal neurotrophic support [17,47], increased generation of nitric oxide (NO) [196-198], mitochondrial dysruption (cf. *3.4.5*) and bio-energetic dysfunction [53,185,191], reactive oxygen species (ROS) [53,166], and possibly also abortive entry into the cell cycle [160,293] (cf. *1.5*). In neurons the principal means of defence against reactive oxygen species is

glutathione [242,270], but synthetic capacity is limited and intramitochondrial glutathione is rapidly depleted by oxidative stress, and the disruptive effects of ROS and nitric oxide (NO) upon energy metabolism are then potentiated [197,270,280,283] (cf. *5.4.3*).

N-acetyl-cysteine (NAC) has demonstrated antioxidant effects which are mediated via glutathione synthesis at low-doses, has anti-mitotic effects in neuronal cell lines, and has been shown to be neuroprotective in response to various neurotoxic stimuli in vitro (cf. *1.6 & 5.4.3*). NAC is already in clinical use as a glutathione precursor in the treatment of paracetamol overdose [241], and was therefore thought to offer potential as a neuroprotective agent after peripheral axotomy. After sciatic nerve transection NAC treatment resulted in a significant dose-related decrease in the number of TUNEL positive neurons found 2 weeks after injury ($p<0.05$), and in a significant decrease in the neuronal loss found 2 months later (control 35% loss; NAC treatment 3% loss, $p=0.002$) (cf. *5.4.2*). NAC did not entirely prevent sensory neuronal death, but over 10,000 neurons were protected by treatment. NAC therefore has considerable clinical potential for the adjuvant treatment of peripheral nerve trauma (cf. *5.4.4*), although further research will initially be required to establish what effect NAC has upon nerve regeneration.

The mechanism by which axotomy effects neuronal death is similar to that underlying the NRTI antiretroviral therapy associated neuropathy that affects around 20% of patients with HIV (cf. *8.1*), since both are postulated to involve mitochondrial dysfunction, failed oxidative metabolism, free radical generation, and loss of distal neurotrophic support (cf. *1.5 & 8.4.4*). L-acetyl-carnitine (LAC) has essential physiological roles in free fatty acid transport and mitochondrial energy metabolism [246,247,294]. It has antioxidant properties [295,296], facilitates the actions of NGF [244,245,297], and is neuroprotective in-vitro [244,245,248] (cf. *1.6 & 6.4.3*). LAC was known to stimulate peripheral nerve regeneration after sciatic nerve injury in the rat [298,299], and to improve symptoms in HIV infected patients with DSP after short-term therapy [301].

When LAC was administered to rats after sciatic nerve transection a significant dose-related decrease, of up to 91%, was found in the number of TUNEL positive neurons 2 weeks after axotomy ($p<0.01$) (cf. *6.4.2*). Sensory neuronal death was decreased to the extent that no neuron loss was found 2 months after injury (control 35% loss; LAC treatment –4% loss, $p<0.001$), and this represents the salvage of over 10,000 neurons, and the protection of almost the entire sensory neuronal pool of the sciatic nerve (cf. *6.4.2*). LAC treatment also a caused significant increase in the peripheral nerve regeneration found 6 weeks after late secondary repair, suggesting that not only is LAC neuroprotective, but that it also stimulates the regenerative capacity of individual neurons (cf. *7.4.2*). In

keeping with this, 6 months of oral LAC treatment (1500mg b.d.) not only improved symptoms in HIV infected patients with NRTI related DSP, but caused peripheral nerve regeneration back into target tissues (cf. *8.4.3*). Epidermal innervation increased, and both total dermal, and sudomotor innervation returned to normal control levels, with the NGF dependent small sensory C, Aδ fibres exhibiting the greatest response to treatment (cf. *8.4.3*).

The physiological peptide LAC has therefore been demonstrated to almost entirely eliminate sensory neuronal death after peripheral nerve transection (cf. *6.4.2*), and to promote peripheral nerve regeneration after nerve injury [298,299], even independently of its neuroprotective effect (cf. *7.4.2*). LAC has also now been demonstrated to cause peripheral nerve regeneration in a clinical setting of chronic nerve injury (cf. *8.4.3*), and to be safe and easy to administer clinically. LAC therefore has the potential not only to be the first pathogenesis based treatment for NRTI therapy associated DSP in HIV disease (cf. *8.4.6*), but also to be the first clinically applicable agent for the adjuvant pharmacotherapy of peripheral nerve injuries (cf. *6.4.4 & 7.4.4*). Further research is now required to determine the exact neuroprotective mechanism of LAC, and to establish how great a delay between injury and commencing LAC treatment is acceptable without losing the neuroprotective benefit of treatment. However, given the data presented to date, and the extensive clinical safety data available for LAC, clinical trials to establish the effect of LAC treatment upon the sensory outcome after major nerve injuries in the upper limb and brachial plexus are currently being scheduled.

Further studies are also needed to confirm whether or not the reduction in sensory neuronal death found after treatment with NAC & LAC will actually improve sensory function after nerve repair. This could either be determined experimentally by electrophysiological studies and by immunohistochemical quantification of cutaneous innervation at suitable timepoints after peripheral nerve repair, or by randomised prospective clinical trials of sensory outcome. It also remains to be determined whether these agents will show equal promise in preventing neuronal death after other forms of nervous system injury, and their effect upon motorneuron survival is currently under investigation in a model of brachial plexus injury. The applicability of LAC & NAC in limiting secondary neuronal death after traumatic brain and spinal cord injury should also be investigated. In the wider setting of neuronal death in general, mitochondrial bio-energetic, and oxidative stress mechanisms have been postulated for conditions as varied as ischaemia reperfusion injury, Alzheimers disease, Huntingdon's disease, Parkinson's disease, amyotrophic lateral sclerosis, and the neurodegeneration associated with ageing

[166,185,233-237,343]. Both LAC and NAC might therefore offer potential either as investigative tools in further eliciting the pathogenesis of these conditions, or possibly even as therapeutic agents.

In summary, this project has defined the timecourse of primary sensory neuronal death after peripheral nerve injury, thereby setting a logical timeframe for subsequent research and identifying a potential therapeutic window for interventions to reduce neuronal death. The principle that the timing of surgical nerve repair affects sensory neuronal death has been established, and this potentially has profound implications for the organisation of peripheral nerve surgery services. Two clinically safe pharmaceutical agents (NAC & LAC) have been demonstrated to almost eliminate sensory neuronal death after peripheral nerve injury, and L-acetyl-carnitine has also been demonstrated to enhance peripheral nerve regeneration in both an animal model of late secondary nerve repair, and in the clinical setting of HIV-associated distal symmetrical polyneuropathy (DSP). Further research into these drugs is underway, and the results of two randomised controlled clinical trials of LAC treatment in HIV-associated DSP, and in peripheral nerve injury are now awaited.

Appendices

Appendix 1 (Materials for Nerve Conduits & Caps):

Material	Source	Product Code
Polyhydroxybutyrate (PHB) Sheet	Astra, Astra Tech AB, Box 14, S-431 21 Mölndal, Sweden	18000
Low Vicosity, High Mannuronic Acid Content Ultrapure Sodium Alginate (LVM)	Pronova Biomedical, N-0371 Oslo, Norway	LVM
0.1% Fibronectin (Fn) Solution from Bovine Plasma	Sigma-Aldrich Ltd., Poole, Dorset, U.K.	F1141
Recombinant Murine Leukaemia Inhibitory Factor (LIF) (Specific Activity > $1x10^8$ U/mg)	Autogen Bioclear UK Ltd., Holly Ditch Farm, Mile Elm, Calne, Wiltshire, U.K.	ABC156
Recombinant Human Glial Growth Factor II (GGF)	Cambridge Neurosciences, U.S.A.	
High-Grade Silicone Rubber Tubing (1mm internal diameter)	Philip Harris International, Lichfield, Staffordshire, U.K.	T88-5420
White Air Inlet Needle	Avon Medicals, SIMS Portex Ltd., Redditch, Worcestershire, U.K.	A81
Monoject 1ml Syringe	Sherwood Davis & Geck, Northern Ireland	1100 601630
Dulbecco's Modified Eagle's Medium (DMEM)	Gibco Life Technologies, Glasgow, U.K.	21885
10% Foetal Calf Serum	Imperial Laboratories, London, U.K.	

Appendix 2 (N-Acetyl-Cysteine & L-Acetyl-Carnitine Treatment):

Material	Source	Product Code
L-acetyl-carnitine (anhydrous powder)	Sigma-Tau Farmaceutiche, 00144 Roma, Italia	5012300
L-acetyl-carnitine (capsules)	Sigma-Tau Farmaceutiche, 00144 Roma, Italia	
N-acetyl-cysteine ("Parvolex®")	Evans Medical Ltd., Leatherhead, U.K.	L1067BEVA
Sterile Normal Saline for Injection	Maco Pharma, Southampton House, London, U.K.	
Sterile 5% Glucose for Injection	Maco Pharma, Southampton House, London, U.K.	

Appendix 2 (Surgical Materials):

Material	Manufacturer	Product Code
18 Gauge Abbocath®-T	Venisystems, Abbott Ireland, Sligo, Ireland	G715 4535-18
Betadine 2% in alcohol	Royal Free Hospital Pharmacy, London	
9/0 Ethilon® Sutures	Ethicon Ltd., Bankhead Avenue, Edinburgh, U.K.	W2898
10/0 Ethilon® Sutures	Ethicon Ltd., Bankhead Avenue, Edinburgh, U.K.	W2850
Halothane BP	May & Baker Ltd., Dagenham, U.K.	
Halothane Regulator (Series 5 T.C.V.)	International Market Supply, Congleton, Cheshire, U.K.	
Hydrex® (Chlorhexidene Gluconate 0.5% w/v in 70% IMS)	Adams Healthcare, Lotherton Way, Leeds, U.K.	
25 Gauge Kendall Monoject® Hypodermic Needles	Sherwood Medical, Northern Ireland	1100-255312
Xylocaine (Lignocaine HCl) 2% with Adrenaline	Astra Pharmaceuticals Ltd., Kings Langley, England	PL 0017/5030R
Melolin	Smith & Nephew Medical Ltd., Hull, England	ART6696491
4/0 Polydioxanone (PDS®II) Sutures	Ethicon Ltd., Bankhead Avenue, Edinburgh, U.K.	W9734
3/0 Prolene® Sutures	Ethicon Ltd., Bankhead Avenue, Edinburgh, U.K.	W8878
6/0 Prolene® Sutures	Ethicon Ltd., Bankhead Avenue, Edinburgh, U.K.	W8718
Sagattal™ (sodium pentobarbitone 60mg/ml)	Rhône Mérieux Ltd., Harlow, Essex, U.K.	VPA 0040/21/1VSO
#15 Surgical Blade	Swan-Morton Ltd., Sheffield, U.K.	0205
Temgesic® (300μg buprenorphine/ml)	Schering-Plough, Shire Park, Hertfordshire, U.K.	108499
4/0 Vicryl® Sutures	Ethicon Ltd., Bankhead Avenue, Edinburgh, U.K.	W9825

Appendix 3 (Antibodies & Staining Reagents):

Antibody / Stain / Reagent	Abbreviation	Working Dilution	Source	Catalogue Number
Bovine Serum Albumin	BSA	1:1000	Sigma-Aldrich Ltd., Poole, Dorset, U.K.	A-2153
Rabbit Polyclonal Antibody to Calcitonin Gene Related Peptide	CGRP	1:3000	Affiniti Research Products Ltd., Mamhead, Exexter, U.K.	CA 1134
Fluorolink™ Cy™-3 Labelled Goat Anti-Mouse IgG (H+L)	Cy-3	1:100	Amersham Pharmacia Biotech UK Ltd., Little Chalfont, Buckinghamshire, U.K.	PA 43002
FITC Labelled Goat Anti-Rabbit	FITC	1:100	Vector Laboratories Inc., Burlingame, CA 94010, U.S.A.	J0813 FI-1000
Hoechst 33342	H33342	1:1000	Sigma-Aldrich Ltd., Poole, Dorset, U.K.	B-2261
Normal Goat Serum	NGS	1:100	Sigma-Aldrich Ltd., Poole, Dorset, U.K.	G-9023
Normal Horse Serum	NHS	1:100	Sigma-Aldrich Ltd., Poole, Dorset, U.K.	H-0146
Normal Rat Serum	NRS	1:100	DAKO, DK-2600 Glostrup, Denmark	X 0912
Mouse Monoclonal Antibody Cocktail to Phosphorylated Neurofilaments	PAMNF	1:1000	Affiniti Research Products Ltd., Mamhead, Exexter, U.K.	NA 1299
Rabbit Polyclonal Antiserum to Ubiquitin C-Terminal Hydroxylase (Protein Gene Product 9.5)	PGP9.5	1:1500	Affiniti Research Products Ltd., Mamhead, Exexter, U.K.	PG 9500
Propidium Iodide	PI	1:1000	Sigma-Aldrich Ltd., Poole, Dorset, U.K.	P-4170
Rabbit Anti-Cow S-100	S-100	1:1000	DAKO, DK-2600 Glostrup, Denmark	Z 0311
Promega Apoptosis Detection System Fluorescein	TUNEL Staining Kit		Promega Corporation, Madison, WI 53711-5399, U.S.A.	G3250
Polyclonal Rabbit Antiserum to Vasoactive Intestinal Polypeptide	VIP	1:2000	Hammersmith Hospital, London, U.K.	(VIP15)
Monoclonal Mouse Anti-Human Von Willebrand Factor	VWF	1:1000	DAKO, DK-2600 Glostrup, Denmark	M 0616

Appendix 4 (Miscellaneous Laboratory Materials & Equipment):

Item / Material	Manufacturer	Product Code
3.5X Magnification Surgical Loupes	Carl Zeiss, Postfach 1865, D-73408, Aalen, Germany	
50mm Glass Coverslips	Chance Propper Ltd., West Midlands, B66 1NZ, U.K.	
62mm Glass Coverslips	Chance Propper Ltd., West Midlands, B66 1NZ, U.K.	
BioRad H2500 Microwave Oven	Energy Beam Sciences Inc., Agawam, Massachusetts, U.S.A.	H2500
Boxer Autoclave	Borolabs, U.K.	
Cryostat	Bright Instruments Ltd., Huntingdon, U.K.	Model OTF
DAKO Pen for Immunohistochemistry	DAKO, DK-2600 Glostrup, Denmark	S 2002
Fluid Cooled Digital Spot Camera	Diagnostic Instruments, U.S.A.	Model 1.3.0
Fluorescent Lamp Burner Unit	Olympus Optical Co. Ltd., Japan	U-RFL-T
Gold Star Glass Slides (76x26mm)	Chance Propper Ltd., West Midlands, B66 1NZ, U.K.	
Optical Microscope	Olympus Optical Co. Ltd., Japan	BX60
Optical Microscope	Olympus Optical Co. Ltd., Japan	BX50
Paraformaldehyde (PFA)	Sigma-Aldrich Ltd., Poole, Dorset, U.K.	P-6148
Peristaltic Pump	Watson-Marlow Ltd., Falmouth, Cornwall, U.K.	505S/RL
Sodium Azide	Sigma-Aldrich Ltd., Poole, Dorset, U.K.	S-2002
Sodium Citrate	Sigma-Aldrich Ltd., Poole, Dorset, U.K.	S-4641
Sucrose	Sigma-Aldrich Ltd., Poole, Dorset, U.K.	S-9378
Triton X-100	BDH Laboratory Supplies, Poole, BH15 1TD, U.K.	306324N
Vectabond®	Vector Laboratories Inc., Burlingame, CA 94010, U.S.A.	SP-1800

Appendix 5 (Triple Staining Protocol):

1) **Fix** sections onto slides by drying on hotplate overnight & DAKO pen around edges.

2) **Stain** ganglia in runs of 3 animals (12 ganglia, 24 slides) at a time. Use a testes slide as a positive control, and a normal DRG slide as a -TdT control, giving a total of 26 slides per staining run.

3) **Rehydration**: PBS 10 minutes
   -at this point get out 4 phials of equilibration buffer, 4 of Nucleotide (FITC-dUTP) & 3 of TdT to thaw.

3) **Permeabilise**:
   -microwave in 250ml of 0.01M Na Citrate for 1.5 minutes, set at total time & control override, with a 1.5l water load (2 beakers of 750ml). Use 2 sets of slides together.
   -testing the power level of the microwave showed it to be 478W.

4) **Rapid Cooling:** immediately place slides into iced PBS for 5min.

5) **Equilibrate**: 100µl equilibration buffer per slide.
   Carefully cover with plastic coverslip (fold a corner up before applying it).
   Incubate for **8 min** at room temperature.

   Prepare Nucleotide mixture (protect from light):
   -require 50µl per slide.
   -Mix: 45µl equilibration buffer + 5µl nucleotide mix + 1µl TdT enzyme.
   -so require: 1170µl equilibration buffer + 130µl nucleotide mix + 26µl TdT enzyme.
   -negative control: 45µl equilibration buffer + 5µl nucleotide mix + 1µl distilled water.

6) **TdT Reaction** (protect from light):
   -carefully peel off coverslips, blot excess liquid & apply nucleotide mix (50µl per slide).
   -replace plastic coverslips.
   -incubate in humid chamber for 60 minutes at 37°C (protected from light).

7) **Terminate TdT reaction**:
   -dilute 20x SSC 10fold to give 2xSSC (use 60ml of 20xSSC into 600ml distilled water, into 2 staining jars. For second run top this up with remaining 10ml 20xSSC diluted to 100ml, and split between jars).
   -soak slides in jars for 15 minutes at room temperature in a humid chamber.

8) **Wash**: PBS 5 minutes.

9) **Apply 1µg/ml Propridium Iodide + 1µg/ml Hoechst 33342 in PBS**
   -apply onto slide (~300µl / slide), incubate for 10 minutes at room temperature.

10) **Wash**:
   -distilled water 8 minutes.
   -PBS 4 minutes.

13) **Mount Glass Coverslips (50mm / 64mm)**:
   -PBS/Glycerine mountant with glass coverslip. Seal with DPX.

Appendix 6 (Immunohistochemistry Protocol for Skin Biopsies):

1. **Fix** sections onto slides by drying on hotplate overnight & DAKO pen around edges.
2. **Permeabilise**: 0.2% Triton-X in PBS for 1hour.
3. **Wash**: PBS 3 min.
4. **Counterstain**: Pontamine Sky Blue 30min.
5. **Wash**: PBS 3min x 2.
6. **Primary Antibody Incubation**:

   -apply primary antibody & incubate overnight at 4°C in a humid chamber:

   -appropriate dilution of primary antisera diluted in antibody diluent + blocking antiserum (normal goat serum) 1:100:

   PGP 9.5 1:1500 CGRP 1:3000 VIP 1:2000
7. **Wash**: PBS 3min x 2.
8. **Secondary Antibody Incubation:**

   -Apply FITC-conjugated goat anti-rabbit antiserum (1:100 dilution in antibody diluent) & incubate for 1 hour at room temperature in humid chamber.
9. **Wash**: PBS 3min x 3.
10. **Mount Glass Coverslips (50mm / 64mm)**: mount with PBS/Glycerine, store slides at 4 °C.

Appendix 7 (Immunohistochemistry Protocol for Nerve Repairs):

1. **Fix** sections onto slides by drying on hotplate overnight & DAKO pen around edges.

2. **Permeabilise**: 1 hour in 0.1% Trition-X in PBS at room temperature.

3. **Wash**: 2 x 5 minute rinses in PBS.

4. **Block**: incubate for 1 hour at room temperature with 1:100 Normal Goat & Horse Serum in antibody diluent (~250µl per slide).

5. **Primary Antibody Incubation**:
   1 hour incubation at room temperature with primary Ab in antibody diluent: PAMNF (monoclonal) 1:1000 + S-100 (polyclonal) 1:1000

6. **Wash**: 2 x 5 minute rinses in PBS.

7. **Secondary Antibody Incubation**:
   2 hour incubation at room temperature with secondary Ab in antibody diluent:

   1:100 Cy-3 anti-mouse + 1:100 FITC anti-rabbit + 1:100 normal rat serum.

8. **Wash**: 2 x 5 minute rinses in PBS.

9. **Mount Glass Coverslips (50mm / 64mm)**: mount with PBS/Glycerine, store slides at 4 °C.

Appendix 8: Preparation & Storage of Reagents & Solutions

8.1 Phosphate Buffered Saline (PBS)

Phosphate buffered saline was prepared by dissolving 87.9g NaCl + 2.72g KH_2PO_4 + 11.35g Na_2HPO_4 into 5 litres of distilled water. A further 5 litres of distilled water was then added, and then at least 8.5 hours later the pH was tested, and adjusted to pH7.3 by addition of NaOh, or HCl as required.

8.2 Paraformaldehyde (PFA)

A stock 20% solution was prepared by dissolving 300g anhydrous PFA (Sigma-Aldrich, U.K.) in 1.5 litres of PBS, using a magnetic stirrer and a warming plate to maintain the solution at 35-45°C. The resulting solution was then aliquotted, and stored at –40°C. The day before use, an aliquot of 20% PFA was thawed and diluted to five times the volume with PBS, giving a final solution of 4% PFA in PBS. This solution was stored at 4°C prior to use within 24 hours.

8.3 Solution of Sucrose in Phosphate Buffered Saline (PBS Sucrose)

150g of sucrose and 1g of sodium azide (Sigma-Aldrich, U.K.) was dissolved into 1 litre of PBS.

8.4 Zamboni's Fluid (Tissue Fixative)

Zamboni's fluid was prepared in 1 litre aliquots by mixing 150ml of saturated picric acid solution with 850ml of a solution of 2% paraformaldehyde (PFA) in PBS (pH7.4). The fluid was stored at 4°C prior to use.

8.5 PBS - Glycerine Mountant

Glycerine slide mountant was prepared by dissolving 1g of antifade compound (1,4Dia20Bicyclo2.2.2Octane) in 4ml of PBS, and adding the resulting solution to 36ml of glycerine. The mountant was stored at 4°C prior to use.

8.6 Antibody Diluent Solution

All antibodies were diluted prior to application in a solution of 0.03% Triton-X + 0.1% Bovine Serum Albumin (BSA) + 0.1% Sodium Azide (Sigma-Aldrich, U.K.) in PBS. Aliquots of diluent solution were prepared by dissolving 0.1g sodium BSA, 0.1g sodium azide, and 30µl of Triton-X into 100ml of PBS. Diluent solution was stored at 4°C prior to use.

Appendix 9 (Frequently Used Abbreviations):

Abbreviation	Full Name	Abbreviation	Full Name
AIF's	Apoptosis Inducing Factors	IL-1β	Interleukin-1β
ASPA	Animals (Scientific Procedures) Act	iNOS	Inducible Nitric Oxide Synthase
BDNF	Brain Derived Neurotrophic Factor	ISEL	In-Situ End Labelling
C.A.S.T.	Computer Assisted Stereology Toolbox	JNK	c-Jun Kinase
CGRP	Calcitonin Gene Related Polypeptide	LAC	L-acetyl-carnitine (also termed cetyl-L-carnitine (ALCAR) by other authors)
CNTF	Ciliary Derived Neurotrophic Factor	LIF	Leukaemia Inhibitory Factor
Cy-3	Cyanine-3	NAC	N-acetyl-cysteine
D4T	Stavudine	NGF	Nerve Growth Factor
ddC	Zalcitabine	NGS	Normal Goat Serum
ddI	Didanosine	NHS	Normal Horse Serum
DRG	Dorsal Root Ganglion	NO	Nitric Oxide
DRG's	Dorsal Root Ganglia	NOS	Nitric Oxide Synthase
DNA	Deoxyribonucleotidyl Acid	nNOS	Neuronal (constitutive) Nitric Oxide Synthase
DSP	Distal Symmetrical Polyneuropathy	NRTI	Nucleoside-Analogue Reverse Transcriptase Inhibitor
FITC	Fluorescein Isothiocyanate	NT-3 / -4	Neurotrophin-3 / -4
GAP-43	Growth Associated Protein-43	NTF	Neurotrophic Factor
GGF	Glial Growth Factor	MAPK	Mitogen Activated Protein Kinase
GDNF	Glial Derived Neurotrophic Factor	MMP	Mitochondrial Membrane Potential
H33342	Hoechst 33342	mRNA	Messenger Ribonucleotidyal Acid
HIV	Human Immunodeficiency Virus	mtDNA	Mitochondrial Deoxyribonucleotidyl Acid
ICE	Interleukin Converting Enzyme		

Appendix 9 Continued (Frequently Used Abbreviations):

Abbreviation	Full Name	Abbreviation	Full Name
PAMNF	Pan-Axonal Marker of Neurofilament	ROS	Reactive Oxygen Species
PBS	Phosphate Buffered Saline	SD	Standard Deviation
PDS	Polydioxanone	SOD	Superoxide Dismutase
PFA	Paraformaldehyde	TdT	Terminal deoxyribonucleotidyl transferase
PGP9.5	Protein Gene Product 9.5	TNFα	Tumour Necrosis Factor α
PI	Propidium Iodide	TUNEL	Terminal deoxyribonucleotidyl transferase Uptake Nick-End Labelling
PTFE	polytetrafluoroethylene	VIP	Vasoactive Intestinal Polypeptide

Appendix 10 (Stereological Abbreviations):

Abbreviation	Full Name	Abbreviation	Full Name
a	Area	N_v	Numerical Volume
$\bar{a}$	Mean Area	N_{par}	Number of Particles
t	Thickness	s	Number of Sections
$\bar{t}$	Mean Thickness	V_{dis}	Disector Volume
N_{dis}	Number of Disectors	V_{ref}	Reference Volume

List of References

1. Lundborg G. *Nerve injury and repair.* Churchill Livingstone, Edinburgh, 1988.
2. Doolabi V.B., Hertl M.C., Mackinnon S.E. The role of nerve conduits in nerve repair: a review. *Reviews in the Neurosciences,* 1996, vol. 7, p. 47-84.
3. Millesi H. Nerve Grafting. *Clin Plast Surg,* 1964, vol. 11, no. 1, p. 105-113.
4. Terris D.J., Willard E.F. Current issues in nerve repair. *Arch Otolarygol Head Neck Surg,* 1993, vol. 119, p. 725-731.
5. Birch R., Bonney G., Wynn Parry C.B. *Surgical Disorders of the Peripheral Nerves.* 1st edition. Edinburgh, Churchill-Livingstone, 1998.
6. Dagum A.B. Peripheral nerve regeneration, repair, and grafting. *J Hand Ther,* 1998, vol. 11, no. 2, p. 111-117.
7. Terzis J.K., Sun D.D., Thanos P.K. Historical and basic science review: past, present, and future of nerve repair. *J Reconstr Microsurg,* 1997, vol. 13, no. 3, p. 215-225.
8. Wiberg M, Hazari A, Ljungberg C, Petterson K, Nordh E, Kvast-Rabben O et al. Sensory recovery after hand replantation: a clinical, morphological and neurophysiological study in man. *J Hand Surg [Br]*, [In Process Citation].
9. Glickman L.T., Mackinnon S.E. Sensory recovery following digital replantation. *Microsurgery,* 1990, vol. 11, no. 3, p. 236-242.
10. de Medinaceli L., Seaber A.V. Experimental nerve reconnection: importance of initial repair. *Microsurgery,* 1989, vol. 10, no. 1, p. 56-70.
11. Green B. Repair and grafting of the peripheral nerve. In: Green, editor. *Plastic Surgery*, 1998, p. 630-695.
12. Lundborg G. Neurotropism, frozen muscle grafts and other conduits. *J Hand Surg [Br],* 1991, vol. 16B, p. 473-476.
13. Gattuso J.M., Glasby M.A., Gschmeissner S.E., Norris R.W. A comparison of immediate and delayed repair of peripheral nerves using freeze thawed autologous muscle grafts- in the rat. *B J P S,* 1989, vol. 42, p. 306-313.
14. Mackinnon S.E. New directions in peripheral nerve surgery. *Ann Surg,* 1989, vol. 22, no. 257, p. 272.

15. Burstedt MKO, Schenker M, Wiberg M, Johansson R. Precision grip function in patients after hand replantation. [In Process Citation], 2001.

16. Westling G., Johansson R.S. Factors influencing the force control during precision grip. *Exp Brain Res,* 1984, vol. 53, no. 2, p. 277-284.

17. Fu S.Y., Gordon T. The cellular and molecular basis of peripheral nerve regeneration. *Mol Neurobiol,* 1997, vol. 14, no. 1-2, p. 67-116.

18. Lundborg G., Dahlin L., Danielsen N., Zhao Q. Trophism, tropism, and specificity in nerve regeneration. *J Reconstr Microsurg,* 1994, vol. 10, no. 5, p. 345-354.

19. Kuypers P.D.L., van Egeraat J.M., Godschalk M., Hovius S.E.R. Loss of Viable neuronal units in the proximal stump as possible cause for poor function recovery following nerve reconstructions. *Exp Neurol,* 1995, vol. 132, p. 77-81.

20. Seddon H.J. War injuries of the peripheral nerves in wounds of the extremities. *B J S (War Surg Suppl),* 1948, vol. 2, p. 325.

21. Seddon H.J. Peripheral nerve injuries. *Medical Research Council Special Report Series No. 282*, Seddon H.J., London, HMSO, 1954.

22. Dellon A.L. Evaluation of sensibility and re-education of sensation in the hand. Baltimore, Williams & Wilkins Company, 1981.

23. Bryan W.J., Schauder K., Tullos H.S. The axillary nerve and its relationship to common sports medicine shoulder procedures. *Am J Sports Med,* 1986, vol. 14, no. 2, p. 113-116.

24. Katzman B.M., Bozentka D.J. Peripheral nerve injuries secondary to missiles. *Hand Clin,* 1999, vol. 15, no. 2, p. 233-44, viii.

25. Properzi G., Francavilla S., Poccia G., Aloisi P., Gu X.H., Terenghi G. et al. Early increase precedes a depletion of VIP and PGP-9.5 in the skin of insulin-dependent diabetics--correlation between quantitative immunohistochemistry and clinical assessment of peripheral neuropathy. *J Pathol,* 1993, vol. 169, no. 2, p. 269-277.

26. Moyle G.J., Sadler M. Peripheral neuropathy with nucleoside antiretrovirals: risk factors, incidence and management. *Drug Saf,* 1998, vol. 19, no. 6, p. 481-494.

27. Miyamoto Y., Higaki T., Sugita T., Ikuta Y., Tsuge K. Morphological reaction of cellular elements and the endoneurium following nerve section. *Peripheral Nerve Repair & Regeneration,* 1986, vol. 3, p. 7-18.

28. Roytta M, Salonen V. Long-term endoneurial changes after nerve transection. *Acta Neuropathol,* 1988, vol. 76, p. 35-45.

29. Ma W., Bisby M.A. Increase of calcitonin gene-related peptide immunoreactivity in the axonal fibers of the gracile nuclei of adult and aged rats after complete and partial sciatic nerve injuries. *Exp Neurol,* 1998, vol. 152, no. 1, p. 137-149.

30. Sterman A.B., Delannoy M.R. Cell body responses to axonal injury: traumatic axotomy versus toxic neuropathy. *Exp Neurol,* 1985, vol. 89, no. 2, p. 408-419.

31. Wells M.R., Vaidya U. Morphological alterations in dorsal root ganglion neurons after peripheral axon injury: association with changes in metabolism. *Exp Neurol,* 1989, vol. 104, no. 1, p. 32-38.

32. Tonge D.A., Golding J.P., Edbladh M., Kroon M., Ekstrom P.E., Edstrom A. Effects of extracellular matrix components on axonal outgrowth from peripheral nerves of adult animals in vitro. *Exp Neurol,* 1997, vol. 146, no. 1, p. 81-90.

33. Tonge D.A., Aaronson O.S., Golding J.P., Jaggers D. Cellular migration and axonal outgrowth from adult mammalian peripheral nerves in vitro. *J Neurobiol,* 1996, vol. 29, no. 2, p. 151-164.

34. Sorenson E.J., Windebank A.J. Relative importance of basement membrane and soluble growth factors in delayed and immediate regeneration of rat sciatic nerve. *J Neuropathol Exp Neurol,* 1993, vol. 52, no. 3, p. 216-222.

35. Gold B.G., Spencer P.S. Neurotrophic Function in Normal Nerve and in Peripheral Neuropathies. In: Gorio A., editor. *Neuroregeneration.* New York, Raven Press Ltd., 1993, p. 101-122.

36. Burgess P.R., English K.B., Horsch K.W. Patterning in the regeneration of cutaneous receptors. *J Physiol,* 1974, vol. 236, p. 57.

37. Zelena J. Survival of Pacinian corpuscles after denervation in adult rats. *Cell Tissue Res,* 1982, vol. 224, no. 3, p. 673-683.

38. Millesi H. Interfascicular nerve grafting. *Ortho Clin North Am,* 1981, vol. 12, p. 287.

39. Richter H. Impairment of motor recovery after late nerve suture: experimental study in the rabbit. Parts I and II. *Neurosurgery,* 1998, vol. 10, p. 70.

40. Terenghi G., Calder J.S., Birch R., Hall S.M. A morphological study of Schwann cells and axonal regeneration in chronically transected human peripheral nerves. *J Hand Surg [Br],* 1998, vol. 4, no. 23B, p. 1-5.

41. Holmes W., Young J.Z. Nerve regeneration after immediate and delayed suture. *J Anat,* 1942, vol. 77, no. 1, p. 63-96.

42. Sunderland S. Nerves and nerve injuries. Edinburgh, E. & S. Livingstone, 1968.

43. Li H. Effects of delayed re-innervation on the expression of c-erbB receptors by chronically denervated rat Schwann cells in vivo. *Glia,* 1997, vol. 20, p. 333-347.

44. Millesi H. Progress in nerve reconstruction. *World J Surg,* 1990, vol. 14, p. 733-747.

45. Birch R. Peripheral nerve Injuries (Symposium). *J B J S,* 1986, vol. 68, p. 2.

46. Lemke G.E., Brockes J.P. Identification and purification of glial growth factor. *J Neurosci,* 1984, vol. 4, no. 1, p. 75-83.

47. Terenghi G. Peripheral nerve regeneration and neurotrophic factors. *J Anat,* 1999, vol. 194, no. 1, p. 1-14.

48. Reynolds M.L., Woolf C.J. Reciprocal Schwann cell-axon interactions. *Curr Opin Neurobiol,* 1993, vol. 3, p. 683-693.

49. de M.L., Merle M. Applying "cell surgery" to nerve repair: a preliminary report on the first ten human cases. *J Hand Surg [Br],* 1991, vol. 16B, no. 5, p. 499-504.

50. Howard M.J., David G., Barrett J.N. Resealing of transected myelinated mammalian axons in vivo: evidence for involvement of calpain. *Neuroscience,* 1999, vol. 93, no. 2, p. 807-815.

51. Griffin J.W., George R., Ho T. Macrophage systems in peripheral nerve repair. A review. *J Neuropathol Exp Neurol,* 1993, vol. 52, no. 6, p. 553-560.

52. Bowe C.M., Hildebrand C., Kocsis J.D., Waxman S.G. Morphological and physiological properties of neurons after long-term axonal regeneration: observations on chronic and delayed sequelae of peripheral nerve injury. *J Neurol Sci,* 1989, vol. 91, no. 3, p. 259-292.

53. Al-Abdulla N.A., Martin L.J. Apoptosis of retrogradely degenerating neurons occurs in association with the accumulation of perikaryal mitochondria and oxidative damage to the nucleus. *Am J Pathol,* 1998, vol. 153, no. 2, p. 447-456.

54. Liss A.G, af Ekenstam F.W., Wiberg M. Changes in the spinal terminal pattern of the superficial radial nerve after a peripheral nerve injury. *Scand J Plast Reconst Surg Hand Surg,* 1995, vol. 29, p. 000-000.

55. Vestergaard S., Tandrup T., Jakobsen J. Effect of permanent axotomy on number and volume of dorsal root ganglion cell bodies. *J Comp Neurol,* 1997, vol. 388, no. 2, p. 307-312.

56. Groves M.J., Giometto B., Scaravilli F. Axotomy-induced vacuolation of primary sensory neurons and effect of administered neurotrophic factors: a morphometric,

immunocytochemical and ultrastructural study. *Prim Sensory Neuron,* 1997, vol. 2, no. 2, p. 111-127.

57. Ranson S.W. Alterations in the spinal ganglion cells following neurotomy. *J Comp Neurol Psychol,* 1909, vol. 19, no. 1, p. 125-153.

58. Sun Y., Zigmond R.E. Leukaemia inhibitory factor induced in the sciatic nerve after axotomy is involved in the induction of galanin in sensory neurons. *Eur J Neurosci,* 1996, vol. 8, no. 10, p. 2213-2220.

59. Sebert M.E., Shooter E.M. Expression of mRNA for neurotrophic factors and their receptors in the rat dorsal root ganglion and sciatic nerve following nerve injury. *J Neurosci Res,* 1993, vol. 36, no. 4, p. 357-367.

60. Krekoski C.A., Parhad I.M., Clark A.W. Attenuation and recovery of nerve growth factor receptor mRNA in dorsal root ganglion neurons following axotomy. *J Neurosci Res,* 1996, vol. 43, no. 1, p. 1-11.

61. Tonra J.R., Curtis R., Wong V., Cliffer K.D., Park J.S., Timmes A. et al. Axotomy upregulates the anterograde transport and expression of brain- derived neurotrophic factor by sensory neurons. *J Neurosci,* 1998, vol. 18, no. 11, p. 4374-4383.

62. Jiang Y.Q., Pickett J., Oblinger M.M. Long-term effects of axotomy on beta-tubulin and NF gene expression in rat DRG neurons. *J Neural Transplant Plast,* 1994, vol. 5, no. 2, p. 103-114 [Abstract].

63. Noguchi K., Senba E., Morita Y., Sato M., Tohyama M. Prepro-VIP and preprotachykinin mRNAs in the rat dorsal root ganglion cells following peripheral axotomy. *Brain Res Mol Brain Res,* 1989, vol. 6, no. 4, p. 327-330 [Abstract].

64. Gillardon F., Klimaschewski L., Wickert H., Krajewski S., Reed J.C., Zimmermann M. Expression pattern of candidate cell death effector proteins Bax, Bcl- 2, Bcl-X, and c-Jun in sensory and motor neurons following sciatic nerve transection in the rat. *Brain Res,* 1996, vol. 739, no. 1-2, p. 244-250.

65. Ham J., Babij C., Whitfield J., Pfarr C.M., Lallemand D., Yaniv M. et al. A c-Jun dominant negative mutant protects sympathetic neurons against programmed cell death. *Neuron,* 1995, vol. 14, no. 5, p. 927-939.

66. Kenney A.M., Kocsis J.D. Temporal variability of jun family transcription factor levels in peripherally or centrally transected adult rat dorsal root ganglia. *Brain Res Mol Brain Res,* 1997, vol. 52, no. 1, p. 53-61.

67. Woolf C.J., Reynolds M.L., Molander C., O'Brien C., Lindsay R.M., Benowitz L.I. The growth-associated protein GAP-43 appears in dorsal root ganglion cells and in the dorsal horn of the rat spinal cord following peripheral nerve injury. *Neuroscience,* 1990, vol. 34, no. 2, p. 465-478.

68. Sommervaille T., Reynolds M.L., Woolf C.J. Time-dependent differences in the increase in GAP-43 expression in dorsal root ganglion cells after peripheral axotomy. *Neuroscience,* 1991, vol. 45, no. 1, p. 213-220.

69. Seniuk N.A. Neurotrophic factors: role in peripheral neuron survival and axonal repair. *J Reconstructive Microsurgery,* 1992, vol. 8, no. 5, p. 399-404.

70. Sterne G.D. Nt-3 modulates NPY expression in primary sensory neurons following peripheral nerve injury. *J Anat,* 1998, vol. 193, no. 2, p. 273-281.

71. Lee S.E., Shen H., Taglialatela G., Chung J.M., Chung K. Expression of nerve growth factor in the dorsal root ganglion after peripheral nerve injury. *Brain Res*, 1998,vol. 796, no. 1-2, p. 99-106.

72. Kashiba H., Hyon B., Senba E. Glial cell line-derived neurotrophic factor and nerve growth factor receptor mRNAs are expressed in distinct subgroups of dorsal root ganglion neurons and are differentially regulated by peripheral axotomy in the rat. *Neurosci Lett,* 1998, vol. 252, no. 2, p. 107-110.

73. Levi-Montalcini R., Dal T.R., della V.F., Skaper S.D., Leon A. Update of the NGF saga. *J Neurol Sci,* 1995, vol. 130, no. 2, p. 119-127.

74. Ji R.R., Zhang Q., Zhang X., Piehl F., Reilly T., Pettersson R.F. et al. Prominent expression of bFGF in dorsal root ganglia after axotomy. *Eur J Neurosci,* 1995, vol. 7, no. 12, p. 2458-2468.

75. Inaishi Y., Kashihara Y., Sakaguchi M., Nawa H., Kuno M. Cooperative regulation of calcitonin gene-related peptide levels in rat sensory neurons via their central and peripheral processes. *J Neurosci,* 1992, vol. 12, no. 2, p. 518-524.

76. Dijkhuizen P.A., Hermens W.T., Teunis M.A., Verhaagen J. Adenoviral vector-directed expression of neurotrophin-3 in rat dorsal root ganglion explants results in a robust neurite outgrowth response. *J Neurobiol,* 1997, vol. 33, no. 2, p. 172-184.

77. Xu Z.Q., Zhang X., Grillner S., Hokfelt T. Electrophysiological studies on rat dorsal root ganglion neurons after peripheral axotomy: changes in responses to neuropeptides. *Proc Natl Acad Sci U S A,* 1997, vol. 94, no. 24, p. 13262-13266.

78. Czeh G., Kudo N., Kuno M. Membrane properties and conduction velocity in sensory neurones following central or peripheral axotomy. *J Physiol (Lond),* 1977, vol. 270, no. 1, p. 165-180.

79. Oblinger M.M., Lasek R.J. Axotomy-induced alterations in the synthesis and transport of neurofilaments and microtubules in dorsal root ganglion cells. *J Neurosci,* 1988, vol. 8, no. 5, p. 1747-1758.

80. Redshaw J.D., Bisby M.A. Comparison of the effects of sciatic nerve crush or resection on the proteins of fast axonal transport in rat dorsal root ganglion cell axons. *Exp Neurol,* 1985, vol. 88, no. 2, p. 437-446.

81. Yin Q., Kemp G.J., Frostick S.P. Neurotrophins, neurones, and peripheral nerve regeneration. *J Hand Surg [Br],* 1998, vol. 23B, no. 4, p. 433-437.

82. Casaccia-Bonnefil P., Gu C., Chao M.V. Neurotrophins in cell survival/death decisions. *Adv Exp Med Biol,* 1999, vol. 468, p. 275-282.

83. Matheson C.R., Carnahan J., Urich J.L., Bocangel D., Zhang T.J., Yan Q. Glial cell line-derived neurotrophic factor (GDNF) is a neurotrophic factor for sensory neurons: comparison with the effects of the neurotrophins. *J Neurobiol,* 1997, vol. 32, no. 1, p. 22-32.

84. Di Stefano P.S., Currie A.R. Receptor mediated retrograde axonal transport of neurotrophic factors is increased after peripheral nerve injury. *Prog Brain Res,* 1994, vol. 103, p. 35-42.

85. Hendry I.A., Murphy M., Hilton D.J., Nicola N.A., Bartlett P.F. Binding and retrograde transport of leukemia inhibitory factor by the sensory nervous system. *J Neurosci,* 1992, vol. 12, no. 9, p. 3427-3434.

86. Thompson S.W., Vernallis A.B., Heath J.K., Priestley J.V. Leukaemia inhibitory factor is retrogradely transported by a distinct population of adult rat sensory neurons: co-localization with trkA and other neurochemical markers. *Eur J Neurosci,* 1997, vol. 9, no. 6, p. 1244-1251.

87. Curtis R., Scherer S.S., Somogyi R., Adryan K.M., Ip N.Y., Zhu Y. et al. Retrograde axonal transport of LIF is increased by peripheral nerve injury: correlation with increased LIF expression in distal nerve. *Neuron,* 1994, vol. 12, no. 1, p. 191-204.

88. Curtis R., Adryan K.M., Zhu Y., Harkness P.J., Lindsay R.M., DiStefano P.S. Retrograde axonal transport of ciliary neurotrophic factor is increased by peripheral nerve injury. *Nature,* 1993, vol. 365, no. 6443, p. 253-255.

89. Hammarberg H., Piehl F., Cullheim S., Fjell J., Hokfelt T., Fried K. GDNF mRNA in Schwann cells and DRG satellite cells after chronic sciatic nerve injury. *Neuroreport,* 1996, vol. 7, no. 4, p. 857-860.

90. Frostick S.P., Yin Q., Kemp G.J. Schwann cells, neurotrophic factors, and peripheral nerve regeneration. *Microsurgery,* 1998, vol. 18, no. 7, p. 397-405.

91. Hall S.M. The effect of inhibiting Schwann cell mitosis on the re-innervation of acellular autografts in the peripheral nervous system of the mouse. *Neuropathol Appl Neurobiol,* 1986, vol. 12, no. 4, p. 401-414.

92. Ekstrom P.A. Neurones and glial cells of the mouse sciatic nerve undergo apoptosis after injury in vivo and in vitro. *Neuroreport,* 1995, vol. 6, no. 7, p. 1029-1032.

93. Lu X., Richardson P.M. Responses of macrophages in rat dorsal root ganglia following peripheral nerve injury. *J Neurocytol,* 1993, vol. 22, no. 5, p. 334-341.

94. Lu X., Richardson P.M. Inflammation near the nerve cell body enhances axonal regeneration. *J Neurosci,* 1991, vol. 11, no. 4, p. 972-978.

95. Hikawa N., Horie H., Takenaka T. Macrophage-enhanced neurite regeneration of adult dorsal root ganglia neurones in culture. *Neuroreport,* 1993, vol. 5, no. 1, p. 41-44.

96. Cajal S.R.Y. Degeneration & Regeneration of the Nerve Centres. In: May R.M., editor. *Degeneration & Regeneration of the Nervous System*. London, Oxford University Press, 1928, p. 397-463.

97. Ranson S.W. Retrograde degeneration in the spinal nerves. *J Comp Neurol,* 1906, vol. 16, p. 265-293.

98. Groves M.J., Christopherson T., Giometto B., Scaravilli F. Axotomy-induced apoptosis in adult rat primary sensory neurons. *J Neurocytol,* 1997, vol. 26, no. 9, p. 615-624.

99. Oliveira A.L., Risling M., Deckner M., Lindholm T., Langone F., Cullheim S. Neonatal sciatic nerve transection induces TUNEL labeling of neurons in the rat spinal cord and DRG. *Neuroreport,* 1997, vol. 8, no. 13, p. 2837-2840.

100. Whiteside G., Doyle C.A., Hunt S.P., Munglani R. Differential time course of neuronal and glial apoptosis in neonatal rat dorsal root ganglia after sciatic nerve axotomy. *Suppl Eur J Neurosci,* 1998, vol. 10, no. 11, p. 3400-3408.

101. Hou X.E., Lundmark K., Dahlstrom A.B. Cellular reactions to axotomy in rat superior cervical ganglia includes apoptotic cell death. *J Neurocytol,* 1998, vol. 27, no. 6, p. 441-451.

102. Hart A.M., Brannstrom T., Wiberg M., Terenghi G. Primary sensory neurons and satellite cells after peripheral axotomy in the adult rat: timecourse of cell death and elimination. *Exp Brain Res,* 2001, [In Process Citation].

103. Ambron R.T., Walters E.T. Priming events and retrograde injury signals. A new perspective on the cellular and molecular biology of nerve regeneration. *Mol Neurobiol,* 1996, vol. 13, no. 1, p. 61-79.

104. Ekstrom P.A., Hedlund G., Karlsson J., Andersson G. The immune modulator Linomide prevents neuronal death in injured peripheral nerves of the mouse. *Neuroreport,* 1998, vol. 9, no. 7, p. 1337-1341.

105. Rich K.M., Luszczynski J.R., Osborne P.A., Johnson E.M.J. Nerve growth factor protects adult sensory neurons from cell death and atrophy caused by nerve injury. *J.Neurocytol.,* 1987, vol. 16, no. 2, p. 261-268.

106. Cheema S.S., Richards L., Murphy M., Bartlett P.F. Leukemia inhibitory factor prevents the death of axotomised sensory neurons in the dorsal root ganglia of the neonatal rat. *J Neurosci Res,* 1994, vol. 37, no. 2, p. 213-218.

107. Rich K.M., Disch S.P., Eichler M.E. The influence of regeneration and nerve growth factor on the neuronal cell body reaction to injury. *J Neurocytol,* 1989, vol. 18, p. 569-576.

108. Himes B.T., Tessler A. Death of some dorsal root ganglion neurons and plasticity of others following sciatic nerve section in adult and neonatal rats. *J Comp Neurol,* 1989, vol. 284, p. 215-230.

109. Ljungberg C., Novikov L., Kellerth J-O., Wiberg M. The neurotrophins NGF and NT-3 reduce sensory neuronal loss in adult rat after peripheral nerve lesion. *Neurosci Lett,* 1999, vol. 262, p. 29-32.

110. Arvidsson J., Ygge J., Grant G. Cell loss in lumbar dorsal root ganglia and transganglionic degeneration after sciatic nerve resection in the rat. *Brain Res,* 1986, vol. 373, no. 1-2, p. 15-21.

111. Risling M., Aldskogius H., Hildebrand C., Remahl S. Effects of sciatic nerve resection on L7 spinal roots and dorsal root ganglia in adult cats. *Exp Neurol,* 1983, vol. 82, no. 3, p. 568-580.

112. Tessler A., Himes B.T., Krieger N.R., Murray M., Goldberger M.E. Sciatic nerve transection produces death of dorsal root ganglion cells and reversible loss of substance P in spinal cord. *Brain Res,* 1985, vol. 332, no. 2, p. 209-218.

113. Liss A.G, af Ekenstam F.W., Wiberg M. Cell loss in sensory ganglia after peripheral nerve injury: an anatomical tracer study using lectin-coupled horse-radish peroxidase in cats. *Scand J Plast Reconst Surg Hand Surg,* 1994, vol. 28, p. 177-187.

114. Liss A.G, af Ekenstam F.W., Wiberg M. Loss of neurons in the dorsal root ganglia after transection of a peripheral sensory nerve: an anatomical study in monkeys. *Scand J Plast Reconst Surg Hand Surg,* 1996, vol. 30, p. 1-6.

115. Suzuki H., Oyanagi K., Takahashi H., Kono M., Yokoyama M., Ikuta F. A quantitative pathological investigation of the cervical cord, roots and ganglia after long-term amputation of the unilateral upper arm. *Acta Neuropathol,* 1993, vol. 85, p. 666-673.

116. Swett J.E., Hong C.Z., Miller P.G. Most dorsal root ganglion neurons of the adult rat survive nerve crush injury. *Somatosens Motor Res,* 1995, vol. 12, no. 3-4, p. 177-189.

117. Peyronnard J.M., Charron L., Lavoie J., Messier J.P., Bergouignan F.X. A comparative study of the effects of chronic axotomy, crush lesion and re-anastomosis of the rat sural nerve on horseradish peroxidase labelling of primary sensory neurons. *Brain Res,* 1988, vol. 443, no. 1-2, p. 295-309.

118. Ygge J. Neuronal loss in lumbar dorsal root ganglia after proximal compared to distal sciatic nerve resection: a quantitative study in the rat. *Brain Res,* 1989, vol. 478, no. 1, p. 193-195.

119. Schmalbruch H. The number of neurons in dorsal root ganglia L4-L6 of the rat. *Anat Rec,* 1987, vol. 219, no. 3, p. 315-322.

120. Greenlund L.J., Deckwerth T.L., Johnson E.M.J. Superoxide dismutase delays neuronal apoptosis: a role for reactive oxygen species in programmed neuronal death. *Neuron,* 1995, vol. 14, no. 2, p. 303-315.

121. Barres B.A., Jacobson M.D., Schmid R., Sendtner M., Raff M.C. Does oligodendrocyte survival depend upon axons? *Curr Biol,* 1993, vol. 3, no. 489, p. 497.

122. Wyllie A.H. Glucocorticoid-induced thymocyte apoptosis is associated with endogenous endonuclease activition. *Nature,* 2000, vol. 284, p. 555.

123. Bilbao F.De., Dubois-Dauphin M. Time-course of axotomy-induced apoptotic cell death in facial motorneurons of neonatal wild type and *bcl*-2 transgenic mice. *Neuroscience,* 1996, vol. 71, no. 4, p. 1111-1119.

124. West M.J. New stereological methods for counting neurons. *Neurobiol Ageing,* 1993, vol. 14, p. 275-285.

125. Coggleshall R.E. A consideration of neural counting methods. *T I N S,* 1992, vol. 15, no. 1, p. 9-13.

126. Coggleshall R.E., Pover C.M., Fitxgerald M. Dorsal root ganglion cell death and surviving cell numbers in relation to the development of sensory innervation in the rat hindlimb. *Dev Brain Res,* 1994, vol. 82, p. 193-212.

127. Abercrombie M. Estimation of nuclear populations from microtome sections. *Anat Rec,* 1948, vol. 94, p. 239-247.

128. Königsmark B.W. Methods for the counting of neurons. In: Nauta W.J., Ebbesson S.O.E., editors. *Contemporary research methods for the counting of neurons*. New York, Springer-Verlag, 1970, p. 315-340.

129. West M.J. Stereological methods for estimating the total number of neurons and synapses: issues of precision and bias. *Trends Neurosci,* 1999, vol. 22, p. 51-61.

130. Gundersen J.G., Bendtsen T.F., Korbo L., Marcussen N., Moller A., Nielsen K. et al. Some new, simple and efficient stereological methods and their use in pathological research and diagnosis. *A P M I S,* 1988, vol. 96, p. 379-394.

131. Pover C.M., Coggeshall R.E. Verification of the disector method for counting neurons, with comments on the empirical method. *Anat Rec,* 1991, vol. 231, p. 573-578.

132. Tandrup T. A method for producing unbiased and efficient estimation of number and mean volume of specified neuron subtypes in rat dorsal root ganglion. *J Comp Neurol,* 1993, vol. 329, p. 269-276.

133. Benes F.M., Lange N. Two-dimensional versus three-dimensional cell counting: a practical perspective. *Trends Neurosci,* 2001, vol. 24, no. 1, p. 11-17.

134. Coggeshall R.E., La F.R., Klein C.M. Calibration of methods for determining numbers of dorsal root ganglion cells [published erratum appears in J Neurosci Methods 1991 Dec;40(2- 3):87-90]. *J Neurosci Methods,* 1990, vol. 35, no. 3, p. 187-194.

135. Harding A.J., Halliday G.M., Cullen K. Practical considerations for the use of the optical disector in estimating neuronal number. *J Neurosci Methods,* 1994, vol. 51, p. 83-89.

136. Gundersen H.J.G., Bagger P., Bendtsen T.F., Evans S.M., Korbo L., Marcussen N. et al. The new stereological tools: Disector, fractionator, nucleator and point sampled intercepts and their use in pathological research and diagnosis. *A P M I S,* 1988, vol. 96, p. 857-881.

137. Whiteside G., Munglani R. TUNEL, hoechst and immunohistochemistry triple-labelling: an improved method for detection of apoptosis in tissue sections-an update. *Brain Res Brain Res Protoc,* 1998, vol. 3, no. 1, p. 52-53.

138. Crowe M.J., Bresnahan J.C., Shuman S.L., Masters J.N., Beattie M.S. Apoptosis and delayed degeneration after spinal cord in jury in rats and monkeys. *Nature Med,* 1997, vol. 3, no. 1, p. 73-76.

139. Negoescu A, Lorimier P., Labat-Moleur F., Azoti L., Robert C., Guillermet C. et al. TUNEL: Improvement and Evaluation of the Method for *in situ* apoptotic cell identification. *Biochemica,* 1997, vol. 2, p. 12-17.

140. Gavrieli Y., Sherman Y., Ben-Sasson S.A. Identification of programmed cell death in situ via specific labeling of nuclear DNA fragmentation. *J Cell Biol,* 1992, vol. 119, no. 3, p. 493-501.

141. Charriaut-Marlangue C., Ben-Ari Y. A cautionary note on the use of the TUNEL stain to determine apoptosis. *Neuroreport,* 1995, vol. 7, no. 1, p. 61-64.

142. Gold R., Schmied M., Giegerich G., Breitschoff H., Hartung H.P., Toyka K.V. et al. Differentiation between cellular apoptosis and necrosis by the combined use of *in situ* and nick translation techniques. *Lab Invest,* 1994, vol. 71, no. 2, p. 219-225.

143. Sanders E.J., Wride M.A. Ultrastructural identification of apoptotic nuclei using the TUNEL technique. *Histochem J,* 1996, vol. 28, no. 4, p. 275-281.

144. Kerr J.F.R., Wyllie A.H., Currie A.R. Apoptosis: a basic biological phenomenon with wide-ranging implications in tissue kinetics. *Br J Cancer,* 1972, p. 26-239.

145. Bredesen D.E. Keeping neurons alive: the molecular control of apoptosis (Part I). *The Neuroscientist,* 1996, vol. 2, no. 3, p. 181-190.

146. Clarke P.G.H. Apoptosis versus necrosis: How valid a dichotomy for neurons. In: Koliatsos V.E., Ratan R.R., editors. *Cell Death and Diseases of the Nervous System.* Totowa, New Jersey, Humana Press Inc., 1999, p. 3-28.

147. Stewart B. Mechanisms of apoptosis: Integration of Genetic, Biochemical, and Cellular Indicators. *Journal of the National Cancer Institute,* 1994, vol. 86, no. 17, p. 1286-1295.

148. Groves M.J., An S.F., Giometto B., Scaravilli F. Inhibition of sensory neuron apoptosis and prevention of loss by NT-3 administration following axotomy. *Exp Neurol,* 1999, vol. 155, no. 2, p. 284-294.

149. Ratan R.R., Murphy T.H., Baraban J.M. Macromolecular synthesis inhibitors prevent oxidative stress-induced apoptosis in embryonic cortical neurons by shunting cysteine from protein synthesis to glutathione. *J Neurosci,* 1994, vol. 14, no. 7, p. 4385-4392.

150. Liu X.Z., Xu X.M., Hu R., Du C., Zhang S.X., McDonald J.W. et al. Neuronal and glial apoptosis after traumatic spinal cord injury. *J Neurosci,* 1997, vol. 17, no. 14, p. 5395-5406.

151. Wetts R., Vaughn J.E. Peripheral and central target requirements for survival of embryonic rat dorsal root ganglion neurons in slice cultures. *J Neurosci,* 1998, vol. 18, no. 17, p. 6905-6913.

152. Figueirido H.F. Skin-derived NGF modulates message levels of apoptosis-related genes in developing terminal ganglia. *Soc Neurosci,* 1998, vol. 24.

153. Cheema S.S., Barrett G.L., Bartlett P.F. Reducing p75 nerve growth factor receptor levels using antisense oligonucleotides prevents the loss of axotomized sensory neurons in the dorsal root ganglia of newborn rats. *J Neurosci Res,* 1996, vol. 46, no. 2, p. 239-245.

154. Farlie P.G., Dringen R., Rees S.M., Kannourakis G., Bernard O. bcl-2 transgene expression can protect neurons against developmental and induced cell death. *Proc Natl Acad Sci U S A,* 1995, vol. 92, no. 10, p. 4397-4401.

155. Migheli A., Attanasio A., Schiffer D. Ultrastructural detection of DNA strand breaks in apoptotic neural cells by in situ end-labelling techniques. *J Pathol,* 1995, vol. 176, no. 1, p. 27-35.

156. Kouroku Y., Urase K., Fujita E., Isahara K., Ohsawa Y., Uchiyama Y. et al. Detection of activated Caspase-3 by a cleavage site-directed antiserum during naturally occurring DRG neurons apoptosis. *Biochem Biophys Res Commun,* 1998, et al. vol. 247, no. 3, p. 780-784.

157. Tong J.X., Eichler M.E., Rich K.M. Intracellular calcium levels influence apoptosis in mature sensory neurons after trophic factor deprivation. *Exp Neurol,* 1996, vol. 138, no. 1, p. 45-52.

158. Lo A.C., Li L., Oppenheim R.W., Prevette D., Houenou L.J. Ciliary neurotrophic factor promotes the survival of spinal sensory neurons following axotomy but not during the period of programmed cell death. *Exp Neurol,* 1995, vol. 134, no. 1, p. 49-55.

159. Martin D.P., Schmidt R.E., DiStefano P.S., Lowry O.H., Carter J.G., Johnson E.M.J. Inhibitors of protein synthesis and RNA synthesis prevent neuronal death caused by nerve growth factor deprivation. *J Cell Biol,* 1988, vol. 106, no. 3, p. 829-844.

160. Ferrari G., Yan C.Y., Greene L.A. N-acetylcysteine (D- and L-stereoisomers) prevents apoptotic death of neuronal cells. *J Neurosci,* 1995, vol. 15, no. 4, p. 2857-2866.

161. Hockenbery D.M. bcl-2, a novel regulator of cell death. *Bioessays,* 1995, vol. 17, no. 7, p. 631-638.

162. Gagliardini V., Fernandez P.A., Lee R.K., Drexler H.C., Rotello R.J., Fishman M.C. et al. Prevention of vertebrate neuronal death by the crmA gene [see comments] [published erratum appears in Science 1994 Jun 3;264(5164):1388]. *Science,* 1994, vol. 263, no. 5148, p. 826-828.

163. Bergeron L., Yuan J. Sealing one's fate: control of cell death in neurons. *Curr Opin Neurobiol,* 1998, vol. 8, no. 1, p. 55-63.

164. Edstrom A., Ekstrom P.A., Tonge D. Axonal outgrowth and neuronal apoptosis in cultured adult mouse dorsal root ganglion preparations: effects of neurotrophins, of inhibition of neurotrophin actions and of prior axotomy. *Neuroscience,* 1996, vol. 75, no. 4, p. 1165-1174.

165. Tolosano E., Cutufia M.A., Hirsch E., Stefanuto G., Voyron S., Fasolo A. et al. Ciliary neurotrophic factor constitutively expressed in the nervous system of transgenic mice protects embryonic dorsal root ganglion neurons from apoptosis. *Eur J Neurosci,* 1996, vol. 8, no. 3, p. 521-529.

166. Koliatsos V.E., Ratan R.R, Cell Death and Diseases of the Nervous System. Totowa, New Jersey, Humana Press, 1999.

167. Otto D., Unsicker K., Grothe C. Pharmacological effects of nerve growth factor and fibroblast growth factor applied to the transectioned sciatic nerve on neuron death in adult rat dorsal root ganglia. *Neurosci Lett,* 1987, vol. 83, no. 1-2, p. 156-160.

168. Wiberg M., Ljungberg C., O'Byrne A., Brown R., Whitworth I., Liss A. et al. Primary sensory neuron survival following targeted administration of NGF to an injured nerve. *Scand J Plast Reconst Surg Hand Surg,* 1999, vol. 33, no. 4, p. 387-392.

169. Bennett D.L., Michael G.J., Ramachandran N., Munson J.B., Averill S., Yan Q. et al. A distinct subgroup of small DRG cells express GDNF receptor components and GDNF is protective for these neurons after nerve injury. *J Neurosci,* 1998, vol. 18, no. 8, p. 3059-3072.

170. Nunez G., del Peso L. Linking extracellular survival signals and the apoptotic machinery. *Curr Opin Neurobiol,* 1998, vol. 8, p. 613-618.

171. Vogelbaum M.A., Tong J.X., Rich K.M. Developmental regulation of apoptosis in dorsal root ganglion neurons. *J Neurosci,* 1998, vol. 18, no. 21, p. 8928-8935.

172. Estus S., Zaks W.J., Freeman R.S., Gruda M., Bravo R., Johnson E.M.J. Altered gene expression in neurons during programmed cell death: identification of c-jun as necessary for neuronal apoptosis. *J Cell Biol,* 1994, vol. 127, no. 6 Pt 1, p. 1717-1727.

173. De Felipe C., Hunt S.P. The differential control of c-jun expression in regenerating sensory neurons and their associated glial cells. *J Neurosci,* 1994, vol. 14, no. 5 Pt 1, p. 2911-2923.

174. Kenney A.M., Kocsis J.D. Peripheral axotomy induces long-term c-Jun amino-terminal kinase-1 activation and activator protein-1 binding activity by c-Jun and junD in adult rat dorsal root ganglia In vivo. *J Neurosci,* 1998, vol. 18, no. 4, p. 1318-1328.

175. Park D.S., Stefanis L., Yan C.Y.I., Farinelli S.E., Greene L.A. Ordering the cell death pathway. Differential effects of BCL2, an interleukin-1-converting enzyme family protease inhibitor, and other survival agents on JNK activation in serum/nerve growth factor-deprived PC12 cells. *J Biol Chem,* 1996, vol. 271, no. 36, p. 21898-21905.

176. Jenkins R., McMahon S.B., Bond A.B., Hunt S.P. Expression of c-Jun as a response to dorsal root and peripheral nerve section in damaged and adjacent intact primary sensory neurons in the rat. *Eur J Neurosci,* 1993, vol. 5, no. 6, p. 751-759.

177. Deckwerth T.L., Easton R.M., Knudson C.M., Korsmeyer S.J., Johnson E.M.J. Placement of the BCL2 family member BAX in the death pathway of sympathetic neurons activated by trophic factor deprivation. *Exp Neurol,* 1998, vol. 152, no. 1, p. 150-162.

178. Gold B.G., Storm-Dickerson T., Austin D.R. Regulation of the transcription factor c-JUN by nerve growth factor in adult sensory neurons. *Neurosci Lett,* 1993, vol. 154, no. 1-2, p. 129-133.

179. Davies A.M. The Bcl-2 family of proteins, and the regulation of neuronal survival. *Trends Neurosci,* 1995, vol. 18, no. 8, p. 355-358.

180. Merry D.E., Korsmeyer S.J. Bcl-2 gene family in the nervous system. *Annu Rev Neurosci,* 1997, vol. 20:245-67, p. 245-267.

181. Parsadanian A.S., Cheng Y., Keller-Peck C.R., Holtzman D.M., Snider W.D. Bcl-xL is an antiapoptotic regulator for postnatal CNS neurons. *J Neurosci,* 1998, vol. 18, no. 3, p. 1009-1019.

182. Allsopp T.E., Wyatt S., Paterson H.F., Davies A.M. The proto-oncogene bcl-2 can selectively rescue neurotrophic factor- dependent neurons from apoptosis. *Cell,* 1993, vol. 73, no. 2, p. 295-307.

183. Batistatou A., Merry D.E., Korsmeyer S.J., Greene L.A. Bcl-2 affects survival but not neuronal differentiation of PC12 cells. *J Neurosci,* 1993, vol. 13, no. 10, p. 4422-4428.

184. Borner C. Diminished cell proliferation associated with the death-protective activity of Bcl-2. *J Biol Chem,* 1996, vol. 271, no. 22, p. 12695-12698.

185. Budd S.L., Nicholls D.G. Mitochondria in the life and death of neurons. *Essays Biochem,* 1998, vol. 33:43-52, p. 43-52.

186. Gillardon F., Wickert H., Zimmermann M. Differential expression of bcl-2 and bax mRNA in axotomized dorsal root ganglia of young and adult rats. *Eur J Neurosci,* 1994, vol. 6, no. 10, p. 1641-1644.

187. Middleton G., Nunez G., Davies A.M. Bax promotes neuronal survival and antagonises the survival effects of neurotrophic factors. *Development,* 1996, vol. 122, no. 2, p. 695-701.

188. Kruman I.I., Mattson M.P. Pivotal role of mitochondrial calcium uptake in neural cell apoptosis and necrosis. *J Neurochem,* 1999, vol. 72, no. 2, p. 529-540.

189. Friedlander R.M., Gagliardini V., Rotello R.J., Yuan J. Functional role of interleukin 1 beta (IL-1 beta) in IL-1 beta- converting enzyme-mediated apoptosis. *J Exp Med,* 1996, vol. 184, no. 2, p. 717-724.

190. Freeman R.S. The cell cycle and neuronal death. In: Koliatsos V.E., Ratan R.R., editors. *Cell Death and Diseases of the Nervous System.* Totowa, New Jersey, Humana Press Inc., 1999, p. 103-122.

191. Nicholls D.G., Budd S.L. Mitochondria and neuronal survival. *Physiol Rev,* 2000, vol. 80, no. 1, p. 315-360.

192. Beal M.F. Energetics in the pathogenesis of neurodegenerative diseases. *Trends Neurosci,* 2000, vol. 23, p. 298-304.

193. Martin L.J., Kaiser A., Price A.C. Motor neuron degeneration after sciatic nerve avulsion in adult rat evolves with oxidative stress and is apoptosis. *J Neurobiol,* 1999, vol. 40, no. 2, p. 185-201.

194. Novikov L., Novikova L., Kellerth J.-O. Brain-derived neurotrophic factor promotes survival and blocks nitric oxide synthase expression in adult rat spinal motoneurons after ventral avulsion. *Neurosci Lett,* 1995, vol. 200, p. 45-48.

195. He J., Hirata K., Kuraoka A., Kawabuchi M. An improved method for avulsion of lumbar nerve roots as an experimental model of nitric oxide-mediated neuronal degeneration. *Brain Res Brain Res Protoc,* 2000, vol. 5, no. 3, p. 223-230.

196. Brorson J.R., Schumacker P.T., Zhang H. Nitric oxide acutely inhibits neuronal energy production. The Committees on Neurobiology and Cell Physiology. *J Neurosci,* 1999, vol. 19, no. 1, p. 147-158.

197. Heales S.J., Bolanos J.P., Stewart V.C., Brookes P.S., Land J.M., Clark J.B. Nitric oxide, mitochondria and neurological disease. *Biochim Biophys Acta,* 1999, vol. 1410, no. 2, p. 215-228.

198. Estevez A.G., Spear N., Manuel S.M., Radi R., Henderson C.E., Barbeito L. et al. Nitric oxide and superoxide contribute to motor neuron apoptosis induced by trophic factor deprivation. *J Neurosci,* 1998, vol. 18, no. 3, p. 923-931.

199. Moncada S. Nitric oxide and cell respiration: physiology and pathology. *Verh K Acad Geneeskd Belg,* 2000, vol. 62, no. 3, p. 171-179.

200. Keller J.N., Kindy M.S., Holtsberg F.W., St C.D., Yen H.C., Germeyer A. et al. Mitochondrial manganese superoxide dismutase prevents neural apoptosis and reduces ischemic brain injury: suppression of peroxynitrite production, lipid peroxidation, and mitochondrial dysfunction. *J Neurosci,* 1998, vol. 18, no. 2, p. 687-697.

201. Castilho R.F., Ward M.W., Nicholls D.G. Oxidative stress, mitochondrial function, and acute glutamate excitotoxicity in cultured cerebellar granule cells. *J Neurochem,* 1999, vol. 72, no. 4, p. 1394-1401.

202. Lewis W., Dalakas M.C. Mitochondrial toxicity of antiviral drugs. *Nature Med,* 1995, vol. 1, no. 5, p. 417-422.

203. Chen C.H., Vazquez-Padua M., Cheng Y.C. Effect of anti-human immunodeficiency virus nucleoside analogs on mitochondrial DNA and its implication for delayed toxicity. *Mol Pharmacol,* 1991, vol. 39, no. 5, p. 625-628.

204. Simpson D.M., Tagliati M. Nucleoside analogue-associated peripheral neuropathy in human immunodeficiency virus infection. *J Acquir Immune Defic Syndr Hum Retrovirol,* 1995, vol. 9, no. 2, p. 153-161.

205. Rosenfeld J., Cook S., James R. Expression of superoxide dismutase following axotomy. *Exp Neurol,* 1997, vol. 147, no. 1, p. 37-47.

206. Mayer M., Noble M. N-acetyl-L-cysteine is a pluripotent protector against cell death and enhancer of trophic factor-mediated cell survival in vitro. *Proc Natl Acad Sci USA,* 1994, vol. 91, no. 16, p. 7496-7500.

207. ElShamy W.M., Fridvall L.K., Ernfors P. Growth arrest failure, G1 restriction point override, and S phase death of sensory precursor cells in the absence of neurotrophin-3. *Neuron,* 1998, vol. 21, no. 5, p. 1003-1015.

208. Boonman Z., Isacson O. Apoptosis in neuronal development and transplantation: role of caspases and trophic factors. *Exp Neurol,* 1999, vol. 156, no. 1, p. 1-15.

209. Nicholson D.W., Thornberry N.A. Caspases: killer proteases. *Trends Biochem Sci,* 1997, vol. 22, no. 8, p. 299-306.

210. Cregan S.P., MacLaurin J.G., Craig C.G., Robertson G.S., Nicholson D.W., Park D.S. et al. Bax-dependent caspase-3 activation is a key determinant in p53-induced apoptosis in neurons. *J Neurosci,* 1999, vol. 19, no. 18, p. 7860-7869.

211. Krajewski S., Krajewska M., Ellerby L.M., Welsh K., Xie Z., Deveraux Q.L. et al. Release of caspase-9 from mitochondria during neuronal apoptosis and cerebral ischemia. *Proc Natl Acad Sci USA,* 1999, vol. 96, no. 10, p. 5752-5757.

212. Yakovlev A.G., Knoblach S.M., Fan L., Fox G.B., Goodnight R., Faden A.I. Activation of CPP32-like caspases contributes to neuronal apoptosis and neurological dysfunction after traumatic brain injury. *J Neurosci,* 1997, vol. 17, no. 19, p. 7415-7424.

213. Yuan J. Transducing signals of life and death. *Curr Op Cell Biol,* 1997, vol. 9, p. 247-251.

214. Ljungberg C., Novikov L., Kellerth J.O., Ebendal T., Wiberg M. The neurotrophins NGF and NT-3 reduce sensory neuronal loss in adult rat after peripheral nerve lesion. *Neurosci Lett,* 1999, vol. 262, no. 1, p. 29-32.

215. Novikova L., Novikov L., Kellerth J.-O. Brain derived neurotrophic factor reduces necrotic zone and supports neuronal survival after spinal cord hemisection in adult rats. *Neurosci Lett,* 1996, vol. 220, p. 203-206.

216. Whitworth I., Brown R.A., Dore C.J., Anand P., Green C.J., Terenghi G. Nerve growth factor enhances nerve regeneration through fibronectin mats. *J Hand Surg [Br],* 1996, vol. 21B, no. 4, p. 514-522.

217. Leclere P., Ekstrom P., Edstrom A., Priestley J., Averill S., Tonge D.A. Effects of glial cell line-derived neurotrophic factor on axonal growth and apoptosis in adult mammalian sensory neurons in vitro. *Neuroscience,* 1998, vol. 82, no. 2, p. 545-558.

218. Gold B.G., Mobley W.C., Matheson S.F. Regulation of axonal caliber, neurofilament content, and nuclear localization in mature sensory neurons by nerve growth factor. *J Neurosci,* 1991, vol. 11, no. 4, p. 943-955.

219. Mohiuddin L., Fernandez K., Tomlinson D.R., Fernyhough P. Nerve growth factor and neurotrophin-3 enhance neurite outgrowth and up- regulate the levels of messenger RNA for growth-associated protein GAP- 43 and T alpha 1 alpha-tubulin in cultured adult rat sensory neurones. *Neurosci Lett,* 1995, vol. 185, no. 1, p. 20-23.

220. Mohiuddin L., Fernyhough P., Tomlinson D.R. Acidic fibroblast growth factor enhances neurite outgrowth and stimulates expression of GAP-43 and T alpha 1 alpha-tubulin in cultured neurones from adult rat dorsal root ganglia. *Neurosci Lett,* 1996, vol. 215, no. 2, p. 111-114.

221. Thompson S.W., Majithia A.A. Leukemia inhibitory factor induces sympathetic sprouting in intact dorsal root ganglia in the adult rat in vivo. *J Physiol (Lond),* 1998, vol. 506, no. Pt 3, p. 809-816.

222. Kopp D.M., Trachtenberg J.T., Thompson W.J. Glial Growth Factor rescues schwann cells of mechanoreceptors from denervation-induced apoptosis. *J Neurosci,* 1997, vol. 17, no. 17, p. 6697-6706.

223. Bryan D.J., Holway A.H., Wang K.K., Silva A.E., Trantolo D.J., Wise D. et al. Influence of glial growth factor and Schwann cells in a bioresorbable guidance channel on peripheral nerve regeneration. *Tissue Eng,* 2000, vol. 6, no. 2, p. 129-138.

224. Cohen S., Levi-Montalcini R. A nerve growth-stimulating factor isolated from snake venom. *Proc Nat Acad Sci USA,* 1956, vol. 42, p. 571-574.

225. Novikova L.N., Novikov L.N., Kellerth J-O. BDNF abolishes the survival effect of NT-3 in axotomised Clarke's nucleus of adult rats. *J Comp Neurol,* 2000, vol. 428, p. 671-680.

226. Gold B.G. Axonal regeneration of sensory nerves is delayed by continuous intrathecal infusion of nerve growth factor. *Neuroscience,* 1997, vol. 76, no. 4, p. 1153-1158.

227. Novikova L.N., Novikov L.N., Kellerth J.-O. Survival effects of BDNF and NT-3 on axotomized rubrospinal neurons depend on the temporal pattern of neurotrophin administration. *Eur J Neurosci,* 2000, vol. 12, p. 776-780.

228. Soilu-Hanninen M., Ekert P., Bucci T., Syroid D., Bartlett P.F., Kilpatrick T.J. Nerve growth factor signaling through p75 induces apoptosis in Schwann cells via a Bcl-2-independent pathway. *J Neurosci,* 1999, vol. 19, no. 12, p. 4828-4838.

229. McArthur J.C., Yiannoutsos C., Simpson D., Adornato B.T., Singer E.J., Hollander H. et al. A phase II trial of nerve growth factor for sensory neuropathy associated with HIV infection. *Neurology,* 2000, vol. 54, no. 1of2, p. 1080-1088.

230. Metcalf D., Gearing D.P. Fatal syndrome in mice engrafted with cells producing high levels of the leukemia inhibitory factor. *Proc Natl Acad Sci USA,* 1989, vol. 86, no. 15, p. 5948-5952.

231. Martin D., Merkel E., Tucker K.K., McManaman J.L., Albert D., Relton J. et al. Cachectic effect of ciliary neurotrophic factor on innervated skeletal muscle. *Am J Physiol,* 1996, vol. 271, no. 5 Pt 2, p. R1422-R1428.

232. Eriksdotter J.M., Nordberg A., Amberla K., Backman L., Ebendal T., Meyerson B. et al. Intracerebroventricular infusion of nerve growth factor in three patients with Alzheimer's disease. *Dement Geriatr Cogn Disord,* 1998, vol. 9, no. 5, p. 246-257.

233. Gadaleta M.N., Cormio A., Pesce V., Lezza A.M., Cantatore P. Aging and mitochondria. *Biochimie,* 1998, vol. 80, no. 10, p. 863-870.

234. Borthwick G.M., Johnson M.A., Ince P.G., Shaw P.J., Turnbull D.M. Mitochondrial enzyme activity in amyotrophic lateral sclerosis: implications for the role of mitochondria in neuronal cell death. *Ann Neurol,* 1999, vol. 46, no. 5, p. 787-790.

235. Fiskum G., Murphy A.N., Beal M.F. Mitochondria in neurodegeneration: acute ischemia and chronic neurodegenerative diseases. *J Cereb Blood Flow Metab,* 1999, vol. 19, no. 4, p. 351-369.

236. Budd S.L. Mechanisms of neuronal damage in brain hypoxia/ischemia: focus on the role of mitochondrial calcium accumulation. *Pharmacol Ther,* 1998, vol. 80, no. 2, p. 203-229.

237. Kong J., Xu Z. Massive mitochondrial degeneration in motor neurons triggers the onset of amyotrophic lateral sclerosis in mice expressing a mutant SOD1. *J Neurosci,* 1998, vol. 18, no. 9, p. 3241-3250.

238. Wu Y., Li Y., Liu H., Wu W. Induction of nitric oxide synthase and motoneuron death in newborn and early postnatal rats following spinal root avulsion. *Neurosci Lett,* 1995, vol. 194, no. 1-2, p. 109-112.

239. Deckwerth T.L., Johnson E.M.J. Temporal analysis of events associated with programmed cell death (apoptosis) of sympathetic neurons deprived of nerve growth factor. *J Cell Biol,* 1993, vol. 123, no. 5, p. 1207-1222.

240. Dringen R., Hamprecht B. N-acetylcysteine, but not methionine or 2-oxothiazolidine-4- carboxylate, serves as cysteine donor for the synthesis of glutathione in cultured neurons derived from embryonal rat brain. *Neurosci Lett,* 1999, vol. 259, no. 2, p. 79-82.

241. Meredith T.J. N-Acetylcysteine. 1st edition. Cambridge University Press, 1995.

242. Ratan R.R., Murphy T.H., Baraban J.M. Oxidative stress induces apoptosis in embryonic cortical neurons. *J Neurochem,* 1994, vol. 62, no. 1, p. 376-379.

243. Ratan R.R., Baraban J.M. Apoptotic death in an in vitro model of neuronal oxidative stress. *Clin Exp Pharmacol Physiol,* 1995, vol. 22, no. 4, p. 309-310.

244. Manfridi A., Forloni G.L., Arrigoni-Martelli E., Mancia M. Culture of dorsal root ganglion neurons from aged rats: effects of acetyl-L-carnitine and NGF. *Int J Dev Neurosci,* 1992, vol. 10, no. 4, p. 321-329.

245. Taglialatela G., Angelucci L., Ramacci M.T., Werrbach-Perez K., Jackson G.R., Perez-Polo J.R. Acetyl-L-carnitine enhances the response of PC12 cells to nerve growth factor. *Brain Res Dev Brain Res,* 1991, vol. 59, p. 221-230.

246. Colucci W.J., Gandour R.D. Carnitine acyltransferase: a review of its biology, enzymology and bioorganic chemistry. *Bioorg Chem,* 1988, vol. 16, p. 307-334.

247. Bremer J. The role of carnitine in intracellular metabolism. *J Clin Chem Clin Biochem,* 1990, vol. 28, no. 5, p. 297-301.

248. Virmani M.A., Biselli R., Spadoni A., Rossi S., Corsico N., Calvani M. et al. Protective actions of L-carnitine and acetyl-L-carnitine on the neurotoxicity evoked by mitochondrial uncoupling or inhibitors. *Pharmacol Res,* 1995, vol. 32, no. 6, p. 383-389.

249. De Grandis D., Santoro L., Di Benedetto P. L-Acetylcarnitine in the treatment of patients with peripheral neuropathies. *Clin Drug Invest,* 1995, vol. 10, no. 6, p. 317-322.

250. Greene EC, editor. Anatomy of the rat. New York, Hafner Publishing Co., 1955.

251. Promega©. Apoptosis Detection System, Fluorescein. Technical Bulletin No. 235. Instructions for use of product G3250. 1999.

252. Whiteside G., Cougnon N., Hunt S.P., Munglani R. An improved method for detection of apoptosis in tissue sections and cell culture, using the TUNEL technique combined with Hoechst stain. *Brain Res Brain Res Protoc,* 1998, vol. 2, no. 2, p. 160-164.

253. Swett J.E., Torigoe Y., Elie V.R., Bourassa C.M., Miller P.G. Sensory neurons of the rat sciatic nerve. *Exp Neurol,* 1991, vol. 114, p. 82-103.

254. Kato H., Kanellopoulos G.K., Matsuo S., Wu Y.J., Jacquin M.F., Hsu C.Y. et al. Neuronal apoptosis and necrosis following spinal cord ischemia in the rat. *Exp Neurol,* 1997, vol. 148, no. 2, p. 464-474.

255. Tan S., Wood M., Maher P. Oxidative stress induces a form of programmed cell death with characteristics of both apoptosis and necrosis in neuronal cells. *J Neurochem,* 1998, vol. 71, no. 1, p. 95-105.

256. Kerezoudi E., King R.H., Muddle J.R., O'Neill J.A., Thomas P.K. Influence of age on the late retrograde effects of sciatic nerve section in the rat. *J Anat,* 1995, vol. 187, no. Pt 1, p. 27-35.

257. Snider W.D., Elliott J.L., Yan Q. Axotomy induced neuronal death during development. *J Neurobiol,* 1992, vol. 23, no. 9, p. 1231-1246.

258. Hedreen J.C. What was wrong with the Abercrombie and empirical cell counting methods? A review. *Anat Rec,* 1998, vol. 250, no. 3, p. 373-380.

259. Hedreen J.C. Lost caps in histological counting methods. *Anat Rec,* 1998, vol. 250, no. 3, p. 366-372.

260. Bergman E., Ulfhake B. Loss of primary sensory neurons in the very old rat: neuron number estimates using the disector method and confocal optical sectioning. *J Comp Neurol,* 1998, vol. 396, p. 211-222.

261. Tandrup T. Are the neurons in the dorsal root ganglion pseudounipolar? A comparison of the number of neurons and number of myelinated and unmyelinated fibres in the dorsal root. *J Comp Neurol,* 1995, vol. 357, no. 3, p. 341-347.

262. Devor M., Govrin-Lippmann R., Frank I., Raber P. Proliferation of primary sensory neurons in adult rat dorsal root ganglion and the kinetics of retrograde cell loss after sciatic nerve section. *Somatosens Res,* 1985, vol. 3, no. 2, p. 139-167.

263. Chun J., Blaschkie A.J. Identification of neural programmed cell death throught the detection of DNA fragmentation in situ and by PCR. *Current protocols in neuroscience.* London, John Wiley & Sons, 1997, p. 3.8.1-3.8.19.

264. Carlson J., Lais A.C., Dyck P.J. Axonal atrophy from permanent peripheral axotomy in adult cat. *J Neuropathol Exp Neurol,* 1979, vol. 38, no. 6, p. 579-585.

265. Bien A., Seidenbecher C.I., Bockers T.M., Sabel B.A., Kreutz M.R. Apoptotic versus necrotic characteristics of retinal ganglion cell death after partial optic nerve injury. *J Neurotrauma,* 1999, vol. 16, no. 2, p. 153-163.

266. Colbourne F., Sutherland G.R., Auer R.N. Electron microscopic evidence against apoptosis as the mechanism of neuronal death in global ischemia. *J Neurosci,* 1999, vol. 19, no. 11, p. 4200-4210.

267. Liabotis S., Schreyer D.J. Magnitude of GAP-43 induction following peripheral axotomy of adult rat dorsal root ganglion neurons is independent of lesion distance. *Exp Neurol,* 1995, vol. 135, no. 1, p. 28-35.

268. Ratan R.R. Antioxidants and the treatment of neurological disease. In: Koliatsos V.E., Ratan R.R., editors. *Cell Death and Diseases of the Nervous System*. Totowa, New Jersey, Humana Press Inc., 1999, p. 649-666.

269. Chabrier P.E., Auguet M., Spinnewyn B., Auvin S., Cornet S., Demerle-Pallardy C. et al. BN 80933, a dual inhibitor of neuronal nitric oxide synthase and lipid peroxidation: a promising neuroprotective strategy [see comments]. *Proc Natl Acad Sci USA,* 1999, vol. 96, no. 19, p. 10824-10829.

270. Cooper A.J., Kristal B.S. Multiple roles of glutathione in the central nervous system. *Biol Chem,* 1997, vol. 378, no. 8, p. 793-802.

271. Seaton T.A., Cooper J.M., Schapira A.H. Free radical scavengers protect dopaminergic cell lines from apoptosis induced by complex I inhibitors. *Brain Res,* 1997, vol. 777, no. 1-2, p. 110-118.

272. Yan C.Y., Ferrari G., Greene L.A. N-acetylcysteine-promoted survival of PC12 cells is glutathione- independent but transcription-dependent. *J Biol Chem,* 1995, vol. 270, no. 45, p. 26827-26832.

273. Lucas J.H., Wheeler D.G., Emery D.G., Mallery S.R. The endogenous antioxidant glutathione as a factor in the survival of physically injured mammalian spinal cord neurons. *J Neuropathol Exp Neurol,* 1998, vol. 57, no. 10, p. 937-954.

274. Goss J.R., Taffe K.M., Kochanek P.M., DeKosky S.T. The antioxidant enzymes glutathione peroxidase and catalase increase following traumatic brain injury in the rat. *Exp Neurol,* 1997, vol. 146, no. 1, p. 291-294.

275. Cruz-Aguado R., Fernandez-Verdecia C.I., Diaz-Suarez C.M., Gonzalez-Monzon O., Antunez-Potashkina I., Bergado-Rosado J. Effects of nerve growth factor on brain glutathione-related enzymes from aged rats. *Fundam Clin Pharmacol,* 1998, vol. 12, no. 5, p. 538-545.

276. Pan Z., Perez-Polo R. Increased uptake of L-cysteine and L-cystine by nerve growth factor in rat pheochromocytoma cells. *Brain Res,* 1996, vol. 740, no. 1-2, p. 21-26.

277. Mattson M.P., Barger S.W., Begley J.G., Mark R.J. Calcium, free radicals, and excitotoxic neuronal death in primary cell culture. *Methods Cell Biol,* 1995, vol. 46:187-216, p. 187-216.

278. Pettmann B., Henderson C.E. Neuronal cell death. *Neuron,* 1998, vol. 20, no. 4, p. 633-647.

279. Kamata H., Tanaka C., Yagisawa H., Matsuda S., Gotoh Y., Nishida E. et al. Suppression of nerve growth factor-induced neuronal differentiation of PC12 cells. N-acetylcysteine uncouples the signal transduction from ras to the mitogen-activated protein kinase cascade. *J Biol Chem,* 1996, vol. 271, no. 51, p. 33018-33025.

280. Lizasoain I., Moro M.A., Knowles R.G., Darley-Usmar V., Moncada S. Nitric oxide and peroxynitrite exert distinct effects on mitochondrial respiration which are differentially blocked by glutathione or glucose. *Biochem J,* 1996, vol. 314 (Pt 3), p. 877-880.

281. Deng G., Su J.H., Ivins K.J., Van H.B., Cotman C.W. Bcl-2 facilitates recovery from DNA damage after oxidative stress. *Exp Neurol,* 1999, vol. 159, no. 1, p. 309-318.

282. Myers K.M., Fiskum G., Liu Y., Simmens S.J., Bredesen D.E., Murphy A.N. Bcl-2 protects neural cells from cyanide/aglycemia-induced lipid oxidation, mitochondrial injury, and loss of viability. *J Neurochem,* 1995, vol. 65, no. 6, p. 2432-2440.

283. Wullner U., Seyfried J., Groscurth P., Beinroth S., Winter S., Gleichmann M. et al. Glutathione depletion and neuronal cell death: the role of reactive oxygen intermediates and mitochondrial function. *Brain Res,* 1999, vol. 826, no. 1, p. 53-62.

284. Drukarch B., Schepens E., Jongenelen C.A., Stoof J.C., Langeveld C.H. Astrocyte-mediated enhancement of neuronal survival is abolished by glutathione deficiency. *Brain Res,* 1997, vol. 770, no. 1-2, p. 123-130.

285. Noack H., Possel H., Rethfeldt C., Keilhoff G., Wolf G. Peroxynitrite mediated damage and lowered superoxide tolerance in primary cortical glial cultures after induction of the inducible isoform of NOS. *Glia,* 1999, vol. 28, no. 1, p. 13-24.

286. Barker J.E., Bolanos J.P., Land J.M., Clark J.B., Heales S.J. Glutathione protects astrocytes from peroxynitrite-mediated mitochondrial damage: implications for neuronal/astrocytic trafficking and neurodegeneration. *Dev Neurosci,* 1996, vol. 18, no. 5-6, p. 391-396.

287. Wang X.F., Cynader M.S. Astrocytes provide cysteine to neurons by releasing glutathione. *J Neurochem,* 2000, vol. 74, no. 4, p. 1434-1442.

288. Sagara J.I., Miura K., Bannai S. Maintenance of neuronal glutathione by glial cells. *J Neurochem,* 1993, vol. 61, no. 5, p. 1672-1676.

289. Wagner R., Heckman H.M., Myers R.R. Wallerian degeneration and hyperalgesia after peripheral nerve injury are glutathione-dependent. *Pain,* 1998, vol. 77, no. 2, p. 173-179.

290. Han D., Sen C.K., Roy S., Kobayashi M.S., Tritschler H.J., Packer L. Protection against glutamate-induced cytotoxicity in C6 glial cells by thiol antioxidants. *Am J Physiol,* 1997, vol. 273, no. 5 Pt 2, p. R1771-R1778.

291. Dringen R., Pfeiffer B., Hamprecht B. Synthesis of the antioxidant glutathione in neurons: supply by astrocytes of CysGly as precursor for neuronal glutathione. *J Neurosci,* 1999, vol. 19, no. 2, p. 562-569.

292. Castagne V., Lefevre K., Natero R., Clarke P.G., Bedker D.A. An optimal redox status for the survival of axotomized ganglion cells in the developing retina. *Neuroscience,* 1999, vol. 93, no. 1, p. 313-320.

293. Yan C.I., Greene L.A. Prevention of PC12 cell death by N-acetylcysteine requires activation of the Ras pathway. *J Neurosci,* 1998, vol. 18, no. 11, p. 4042-4049.

294. Calvani M., Nicolai R., Barbarisi A., Reda E., Benatti P., Peluso G. Carnitine system and cancer. In, *Advances in nutrition and cancer*. Plenum Publishing Corporation, 2000.

295. Calvani M., Arrigoni-Martelli E. Attenuation by acetyl-L-carnitine of neurological damage and biochemical derangement following brain ischemia and reperfusion. *Int J Tissue React,* 1999, vol. 21, no. 1, p. 1-6.

296. Tesco G., Latorraca S., Piersanti P., Piacentini S., Amaducci L., Sorbi S. Protection from oxygen radical damage in human diploid fibroblasts by acetyl-L-carnitine. *Dementia,* 1992, vol. 3, p. 58-60.

297. Angelucci L., Ramacci M.T., Taglialatela G., Hulsebosch C., Morgan B., Werrbach-Perez K. et al. Nerve growth factor binding in aged rat central nervous system: effect of acetyl-L-carnitine. *J Neurosci Res,* 1988, vol. 20, p. 491-496.

298. Fernandez E., Pallini P.R., Gangitano C., Aurora DF., Sangiacomo C.O., Sbriccoli A. et al. Effects of L-carnitine, L-acetylcarnitine and gangliosides on the regeneration of the transected sciatic nerve in rats. *Neurol Res,* 1989, vol. 11, p. 57-62.

299. Fernandez E., Pallini R., Gangitano C., Del F.A., Olivieri-Sangiacomo C., Sbriccoli A. et al. Studies on the degenerative and regenerative phenomena occurring after transection and repair of the sciatic nerve in rats: effects of acetyl- L-carnitine. *Int J Clin Pharmacol Res,* 1990, vol. 10, no. 1-2, p. 85-99.

300. Larkin M. Nerve growth factor promising in diabetic neuropathy...and in HIV-1-related neuropathy [news] [see comments]. *Lancet,* 1998, vol. 352, no. 9133, p. 1039.

301. Scarpini E., Sacilotto G., Baron P., Cusini M., Scarlato G. Effect of Acetyl-L-Carnitine in the treatment of painful peripheral neuropathies in HIV+ Patients. *J Periph Nerv Sys,* 1997, vol. 2, no. 3, p. 250-252.

302. Parnetti L., Gaiti A., Mecocci P., Cadini D., Senin U. Pharmacokinetics of IV and oral acetyl-L-carnitine in a multiple dose regimen in patients with senile dementia of Alzheimer type [published erratum appears in Eur J Clin Pharmacol 1993;44(6):604]. *Eur J Clin Pharmacol,* 1992, vol. 42, no. 1, p. 89-93.

303. Marzo A., Arrigoni M.E., Urso R., Rocchetti M., Rizza V., Kelly J.G. Metabolism and disposition of intravenously administered acetyl-L- carnitine in healthy volunteers. *Eur J Clin Pharmacol,* 1989, vol. 37, no. 1, p. 59-63.

304. Stevens M.J., Lattimer S.A., Feldman E.L., Helton E.D., Millington D.S., Sima A.A. et al. Acetyl-L-carnitine deficiency as a cause of altered nerve myo-inositol content, Na,K-ATPase activity, and motor conduction velocity in the streptozotocin-diabetic rat. *Metabolism,* 1996, vol. 45, no. 7, p. 865-872.

305. Singer P., Mehler S. Glucose and leucine uptake in the hypoglossal nucleus after hypoglossal nerve transection with and without prevented regeneration in the Sprague-Dawley rat. *Neurosci Lett,* 1986, vol. 67, no. 1, p. 73-77.

306. Tham S.K., Dowsing B., Finkelstein D., Donato R., Cheema S.S., Bartlett P.F. et al. Leukaemia Inhibitory Factor enhances the regeneration of transected rat sciatic nerve and the function of reinnervated muscle. *J Neurosci Res,* 1997, vol. 47, p. 208-215.

307. Fernandez E., Pallini P.R., Gangitano C., Del Fa A., Olivieri-Sangiacomo C., Sbriccoli A. et al. Studies on the degenerative and regenerative phenomena occurring after transection and repair of the sciatic nerve in rats: effects of acetyl-L-carnitne. *Int J Clin Pharm Res,* 1990, vol. 10, p. 85-99.

308. Hart A.M., Terenghi G., Johnson M.A., Youle M. L-acetyl-carnitine: a pathogenesis based treatment for HIV-Associated distal symmetrical polyneuropathy. *J Neuropathol Exp Neurol,* 2001, [In Process Citation].

309. Dyck P.G., O'Brien P.C. Diagnosis, staging and classification of diabetic neuropathy and association with other complications. In, Dyck P.J., Thomas P.K., Asbury A.K., Winegrad A.I., Porte D., editors. *Diabetic Neuropathy.* Philadelphia, W.B. Saunders, 1987.

310. Adle-Biassette H., Bell J.E., Creange A., Sazdovitch V., Authier F.J., Gray F. et al. DNA breaks detected by in situ end-labelling in dorsal root ganglia of patients with AIDS. *Neuropathol Appl Neurobiol,* 1998, vol. 24, no. 5, p. 373-380.

311. Russell J.W., Sullivan K.A., Windebank A.J., Herrmann D.N., Feldman E.L. Neurons undergo apoptosis in animal and cell culture models of diabetes. *Neurobiol Dis,* 1999, vol. 6, no. 5, p. 347-363.

312. Kieburtz K., Simpson D., Yiannoutsos C., Max M.B., Hall C.D., Ellis R.J. et al. A randomized trial of amitriptyline and mexiletine for painful neuropathy in HIV infection. AIDS Clinical Trial Group 242 Protocol Team. *Neurology,* 1998, vol. 51, no. 6, p. 1682-1688.

313. Hall C.D., Snyder C.R., Messenheimer J.A., Wilkins J.W., Robertson W.T., Whaley R.A. et al. Peripheral neuropathy in a cohort of human immunodeficiency virus-infected patients. Incidence and relationship to other nervous system dysfunction. *Arch Neurol,* 1991, vol. 48, no. 12, p. 1273-1274.

314. Moore R.D., Wong W.M., Keruly J.C., McArthur J.C. Incidence of neuropathy in HIV-infected patients on monotherapy versus those on combination therapy with didanosine, stavudine and hydroxyurea. *AIDS,* 2000, vol. 14, no. 3, p. 273-278.

315. Brinkman K., ter Hofstede H.J., Burger D.M., Smeitink J.A., Koopmans P.P. Adverse effects of reverse transcriptase inhibitors: mitochondrial toxicity as common pathway [editorial]. *AIDS,* 1998, vol. 12, no. 14, p. 1735-1744.

316. Kieburtz K., Simpson D., Yiannoutsos C., Max M.B., Hall C.D., Ellis R.J. et al. A randomized trial of amitriptyline and mexiletine for painful neuropathy in HIV infection. AIDS Clinical Trial Group 242 Protocol Team. *Neurology,* 1998, vol. 51, no. 6, p. 1682-1688.

317. Simpson D.M., Dorfman D., Olney R.K., McKinley G., Dobkin J., So Y. et al. Peptide T in the treatment of painful distal neuropathy associated with AIDS: results of a placebo-controlled trial. The Peptide T Neuropathy Study Group. *Neurology,* 1996, vol. 47, no. 5, p. 1254-1259.

318. Pozniak A., Gazzard B.G., Churchill D., Johnson M.A., Williams I., Deutsch J.C. et al. British HIV Association (BHIVA) guidelines for the treatment of HIV-infected adults with antiretroviral therapy. *British HIV Association,* 2000, <http://www.aidsmap.com/bhiva/bhivagd1299.htm>.

319. Keilbaugh S.A., Prusoff W.H., Simpson M.V. The PC12 cell as a model for studies of the mechanism of induction of peripheral neuropathy by anti-HIV-1 dideoxynucleoside analogs. *Biochem Pharmacol,* 1991, vol. 42, no. 1, p. R5-R8.

320. McCarthy B.G., Hsieh S.T., Stocks A., Hauer P., Macko C., Cornblath D.R. et al. Cutaneous innervation in sensory neuropathies: evaluation by skin biopsy. *Neurology,* 1995, vol. 45, no. 10, p. 1848-1855.

321. Cunningham W.E., Shapiro M.F., Hays R.D., Dixon W.J., Visscher B.R., George W.L. et al. Constitutional symptoms and health-related quality of life in patients with symptomatic HIV disease. *Am J Med,* 1998, vol. 104, no. 2, p. 129-136.

322. Sima A.A.F., Ristic H., Merry A., Kamijo M., Lattimer S.A., Stevens M.J. et al. Primary preventive and secondary interventionary effects of acetyl-L-carnitine on diabetic neuropathy in the bio-breeding Worcester rat. *J Clin Invest,* 1996, vol. 97, p. 1900-1907.

323. Onofrj M., Fulgente T., Melchionda D. L-acetylcarnitine as a new therapeutic approach for peripheral neuropathies with pain. *Int J Clin Pharmacol Res,* 1995, vol. 15, p. 9-15.

324. Famularo G., De Simone C., Cifone G. Carnitine stands on its own in HIV infection. *Arch Int Med,* 1999, vol. 159, p. 1143-1144.

325. Baddeley A.J., Gundersen H.J., Cruz-Orive L.M. Estimation of surface area from vertical sections. *J Microsc,* 1986, vol. 142 (Pt 3), p. 259-276.

326. Facer P., Mathur R., Pandya S.S., Ladiwala U., Singhal B.S., Anand P. Correlation of quantitative tests of nerve and target organ dysfunction with skin immunohistology in leprosy. *Brain,* 1998, vol. 121 (Pt 12), p. 2239-2247.

327. Levy D.M., Terenghi G., Gu X., Abraham R.R., Springall D.R., Polak J.M. Immunohistochemical measurements of nerves and neuropeptides in diabetic skin: relationship to tests of neurological function. *Diabetologia,* 1992, vol. 35, p. 889-897.

328. Navarro X., Verdu E., Wendelschafer-Crabb G., Kennedy W.R. Immunohistochemical study of skin reinnervation by regenerative axons. *J Comp Neurol,* 1997, vol. 380, no. 2, p. 164-174.

329. Peluso G., Benatti P., Nicolai R., Reda E., Calvani M., Carnitine system and insulin resistance. In, Crepaldi G, Tiengo A, Del Prato S, editors, *Carnitine system and insulin resistance.* Amsterdam, Elsevier, 1998.

330. Kano M., Kawakami T., Hori H., Hashimoto Y., Tao Y., Ishikawa Y. et al. Effects of ALCAR on the fast axoplasmic transport in cultured sensory neurons of streptozotocin-induced diabetic rats. *Neurosci Res,* 1999, vol. 33, no. 3, p. 207-213.

331. Giammusso B., Morgia G., Spampinato A., Motta M. Improved pallesthetic sensitivity of pedendal nerve in impotent diabetic patients treated with acetyl-L-carnitine. *Acta Urol Ital,* 1996, vol. 10, no. 3, p. 185-187.

332. Famularo G., Moretti S., Marcellini S., Trinchieri V., Tzantzoglou S., Santini G. et al. Acetyl-carnitine deficiency in AIDS patients with neurotoxicity on treatment with retroviral nucleoside analogues. *AIDS,* 1997, vol. 11, p. 185-190.

333. Chasseau L.F., Hawkins D.R., Mayo B.C., Baldock G.A. Pharmacokinetics and metabolism of ^{14}C-labelled L-acetylcarnitine and related compounds in the rat. Huntingdon Research Centre, Department of Printing, Huntingdon Research Centre. 1984, vol. SGM4/5/8176, p. 1-181.

334. Brinkman K., Smeitink J.A., Romijn J.A., Reiss P. Mitochondrial toxicity induced by nucleoside-analogue reverse- transcriptase inhibitors is a key factor in the pathogenesis of antiretroviral-therapy-related lipodystrophy [comment] [see comments]. *Lancet,* 1999, vol. 354, no. 9184, p. 1112-1115.

335. Behrens G.M., Stoll M., Schmidt R.E. Lipodystrophy syndrome in HIV infection: what is it, what causes it and how can it be managed?. *Drug Saf,* 2000, vol. 23, no. 1, p. 57-76.

336. De Simone C., Famularo G., Tzantzoglou S., Trinchieri V., Moretti S., Sorice F. Carnitine depletion in peripheral blood mononuclear cells from patients with AIDS: effect of oral L-carnitine. *AIDS,* 1994, vol. 8, no. 5, p. 655-660.

337. De Simone C., Tzantzoglou S., Famularo G., Moretti S., Paoletti F., Vullo V. et al. High dose L-carnitine improves immunologic and metabolic parameters in AIDS patients. *Immunopharmacol Immunotoxicol,* 1993, vol. 15, no. 1, p. 1-12.

338. Di Marzio L., Alesse E., Roncaioli P., Muzi P., Moretti S., Marcellini S. et al. Influence of L-carnitine on CD95 cross-lining-induced apoptosis and ceramide generation in human cell lines: correlation with its effects on purified acidic and neutral sphingomyelinases in vitro. *Proc Assoc Am Physicians,* 1997, vol. 109, no. 2, p. 154-163.

339. De Simone C., Famularo G., Cifone G., Mitsuya H. HIV-I infection and cellular metabolism. *Immunol Today,* 1996, vol. 17, no. 6, p. 256-258.

340. Vecchiet L., Di Lisa F., Pieralisi G., Ripari P., Menabo R., Giamberardino M.A. et al. Influence of L-carnitine administration on maximal physical exercise [see comments]. *Eur J Appl Physiol,* 1990, vol. 61, no. 5-6, p. 486-490.

341. Barinaga M. fMRI Provides new view of monkey brains. *Science,* 1998, vol. 282, p. 139-139.

342. Filler A.G., Kliot, Howe F.A., Hayes C.E., Saunders D.E., Goodkin R. et al. Applications of magnetic resonance neurography in the evaluation of patients with peripheral nerve pathology. *J Neurosurg,* 1996, vol. 85, p. 299-309.

343. France-Lanord V., Brugg B., Michel P.P., Agid Y., Ruberg M. Mitochondrial free radical signal in ceramide-dependent apoptosis: a putative mechanism for neuronal death in Parkinson's disease. *J Neurochem,* 1997, vol. 69, no. 4, p. 1612-1621.